



Universität für Bodenkultur Wien
University of Natural Resources
and Life Sciences, Vienna

Master Thesis

An analysis of frequency, mean rain rate, and seasonality of daily, hourly, and event-based heavy precipitation in the Greater Vienna region

Submitted by

Vanessa SCHEUNGRABER, BSc

in the framework of the international Master programme

Natural Resources Management and Ecological Engineering

in partial fulfilment of the requirements for the academic degree

Master of Science

Vienna, January 2022

Co-Supervisor:

Assoc.Prof. Peter Almond, PhD
Dept. of Soil and Physical Sciences
Lincoln University New Zealand

Main Supervisor:

Univ.Prof. Dr. Harald Rieder
Institute of Meteorology and Climatology
Dept. of Water, Atmosphere and Environm.
Univ. of Natural Resources and Life Sciences,
Vienna

Affidavit

I hereby declare that I have authored this master thesis independently, and that I have not used any assistance other than that which is permitted. The work contained herein is my own except where explicitly stated otherwise. All ideas taken in wording or in basic content from unpublished sources or from published literature are duly identified and cited, and the precise references included.

I further declare that this master thesis has not been submitted, in whole or in part, in the same or a similar form, to any other educational institution as part of the requirements for an academic degree.

I hereby confirm that I am familiar with the standards of Scientific Integrity and with the guidelines of Good Scientific Practice, and that this work fully complies with these standards and guidelines.

Vienna, 17.01.2022

Vanessa SCHEUNGRABER (*manu propria*)

*Twenty-five years ago, people could be excused for not knowing
much, or doing much, about climate change.*

Today we have no excuse.

Desmond Tutu, 2014

Acknowledgements

First, I would like to thank Professor Harald Rieder for the chance to gain knowledge and experience in a field that was new to me, for his warm support and advice.

Thanks goes also to Professor Peter Almond for his support from the other side of the world and his suggestions for the optimisation of this work.

Furthermore, I want to thank Vinzent Klaus for his ideas on which angles of this topic could be further explored and Christoph Stähle who helped me when I got stuck with my code.

I would also like to thank ZAMG for collecting and providing the high-quality rainfall data that formed the basis of this work.

Big gratitude goes to Frank Spithoven for his endless support and an open ear when I wanted to discuss my results or worries, and to my friends who enriched my studies and my time in Vienna so much.

The deepest appreciation goes to my parents, who set the course for my academic career and without their support, studying would have been far more difficult.

Abstract

Heavy precipitation has the potential to cause great damage and endanger human lives. Climate change can increase the intensity and frequency of heavy precipitation; however, changes vary regionally. The aim of this work is therefore to identify changes in heavy precipitation at the local /regional level for Vienna and its surroundings. The main research question addressed in this thesis is: How has the frequency and intensity of heavy precipitation changed in the Greater Vienna region during recent decades? To answer this question, 10-minute and daily precipitation measurements of the last 30 to 40 years at ten selected stations were analysed. Both 24h-precipitation as well as 1h- and event-precipitation were examined. The results show an increase in frequency and mean rain rate of heavy precipitation in the last 15 years, although results vary for different temporal frameworks for which heavy precipitation has been computed. The analysis shows the largest increase in the frequency of heavy precipitation days, while the smallest increase can be observed in the categorisation of heavy precipitation as events. In contrast to frequency, the intensity of heavy precipitation has increased only slightly, here however, most strongly for events with a 12 % increase. The calculations show that it is important to include different time units of heavy precipitation as well as both frequency and intensity in analyses seeking to understand the changing nature of heavy precipitation, as the results differ depending on the definition applied.

Kurzfassung

Starkniederschläge haben das Potenzial große Schäden zu verursachen und Menschenleben zu gefährden. Der Klimawandel kann die Intensität und Häufigkeit von Starkniederschlag zudem verstärken, allerdings sind Veränderungen regional unterschiedlich. Das Ziel dieser Arbeit ist daher Veränderungen des Starkniederschlags auf lokaler/regionaler Ebene für Wien und seine Umgebung zu identifizieren. Die Hauptforschungsfrage, die in dieser Arbeit behandelt wird, lautet: Wie hat sich die Häufigkeit und Intensität von Starkniederschlägen im Wiener Raum in den letzten Jahrzehnten verändert? Um diese Frage zu beantworten, wurden 10-Minütige und tägliche Niederschlagsmessungen der letzten 30 bis 40 Jahre an zehn ausgewählten Stationen analysiert. Untersucht wurden sowohl 24h-Starkniederschläge als auch 1h- und Eventniederschläge. Die Ergebnisse zeigen eine Zunahme der Häufigkeit und der mittleren Regenraten von Starkniederschlägen in den letzten 15 Jahren, obwohl sich die Ergebnisse für die verschiedenen berechneten zeitlichen Rahmen der Starkniederschläge unterscheiden. Die Analyse zeigt den größten Anstieg der Häufigkeit bei Starkniederschlagstagen, während der geringste Anstieg bei der Kategorisierung von Starkniederschlägen als Events zu beobachten ist. Im Gegensatz zur Häufigkeit hat die Intensität des Starkniederschlags nur geringfügig zugenommen, jedoch am stärksten für Events mit einer Zunahme von 12 %. Die Berechnungen zeigen die Wichtigkeit verschiedene Zeiteinheiten des Starkniederschlags sowie sowohl Frequenz als auch Intensität in Analysen einzubeziehen, wenn man Veränderungen des Starkniederschlags umfassend verstehen möchte, da die Ergebnisse je nach Definition unterschiedlich ausfallen.

Table of content

1	Introduction and Motivation.....	1
2	State of Knowledge	4
2.1	Formation of (heavy) precipitation.....	4
2.1.1	Classification of heavy precipitation.....	8
2.1.2	Global and regional changes of (heavy) precipitation	9
2.1.3	Impacts of heavy precipitation	10
2.1.4	Mitigation of heavy precipitation impacts	12
2.2	Precipitation measurement	14
2.2.1	Manual, mechanical, and electrical rain gauges	14
2.2.2	Uncertainties and errors in the measurement of precipitation	17
2.2.3	Precipitation measurements with radar.....	18
2.2.4	Precipitation measurements with satellites	19
2.2.5	Snow measurement	22
2.3	Study area	23
3	Methods	25
3.1	Data collection	25
3.2	Data processing.....	25
3.3	Data management	25
4	Empirical analysis.....	27
4.1	Data.....	27
4.2	Implementation in R	28
4.3	Data analysis	28
4.3.1	Determining daily, hourly and event heavy precipitation	29
4.3.2	Theory of extreme value statistics	29
5	Results and discussion.....	32
5.1	Reproduction of previous studies.....	32
5.1.1	Thresholds to identify heavy precipitation days	32
5.1.2	Seasonality of precipitation in study area.....	33
5.2	Daily precipitation analysis.....	34
5.2.1	Frequency of daily heavy precipitation.....	36
5.2.2	Mean rain rate of daily heavy precipitation.....	37
5.2.3	Seasonality of daily heavy precipitation	41
5.2.4	Correlation analysis of seasonal and annual heavy precipitation	42
5.3	Hourly precipitation analysis	48
5.3.1	Frequency of hourly heavy precipitation	50
5.3.2	Mean rain rate of hourly heavy precipitation	52
5.3.3	Seasonality of hourly heavy precipitation.....	56
5.4	Event analysis.....	58

5.4.1	Frequency of heavy precipitation events	60
5.4.2	Mean rain rate of heavy precipitation events	61
5.4.3	Seasonality of heavy precipitation events	64
5.5	Return periods of daily heavy precipitation maxima	67
6	Summary and Conclusions.....	74
	References.....	78
	Table of Figures	86
	List of Tables	88
	List of Abbreviations	90
	Appendix	91

1 Introduction and Motivation

Extreme weather events such as heat waves, heavy precipitation and droughts are very likely to become more frequent and intense as global warming progresses (IPCC, 2021). In fact, record-breaking precipitation events have increased globally since 1980 (Lehmann, et al., 2015). Also in Austria an increase of daily heavy precipitation has been observed, although changes differ regionally and seasonally (Chimani, et al., 2016). While precipitation is an important part of the hydrological cycle, distributing fresh water across the Earth's surface (WMO, 2018a), heavy precipitation can have potentially detrimental impacts (Beniston, et al., 2007). The summer of 2021 serves as an illustrative example, showing Europe and the world the destructive power of heavy precipitation, with some floods more extreme than at any time in perhaps a thousand years (Eddy, et al., 2021). Multiple days of heavy precipitation in July, caused by a slow-moving upper-level low, resulted in widespread destructive flooding in Western Europe, especially in Belgium and North-western Germany (Puca, et al., 2021), while Southern Germany and Austria faced catastrophic flooding only a few days later (Copernicus, 2021). While the occurrence of heavy precipitation events (frequently defined as events exceeding the 90th percentile (IPCC, 2013)) is by definition rare (Beniston, et al., 2007), global warming increases the frequency of extreme precipitation (Lehmann, et al., 2015) as well as the intensity of extreme events (IPCC, 2021). As a warmer atmosphere can hold more water vapour (Trenberth, 1999) more water is present to form precipitation clouds and thus heavy precipitation (Westra, et al., 2013). This is described by the Clausius-Clapeyron relation according to which each degree of warming can increase the saturation water vapour pressure in the atmosphere by 6-7 % (Allen & Ingram, 2002). And indeed, the IPCC report of 2013 stated with medium confidence that extreme precipitation increases at a rate of 5-10 % per degree of warming. Eight years later in the sixth assessment report confidence has been revised to high, and the report states that for every degree of warming extreme daily precipitation intensifies by 7 % on a global scale (IPCC, 2021). Regionally, however, the change is not uniform. Even within Europe in some regions heavy precipitation is increasing while in others decreasing trends are observed (Lehmann, et al., 2015; IPCC, 2021). One explanation for opposing trends could be that temperature and the accompanying increase in humidity are not the only factors leading to a change in heavy precipitation (Westra, et al., 2013). Altered atmospheric circulation patterns might also play a role regarding precipitation change in Europe (IPCC, 2013). The principle of precipitation formation is that evaporating water rises in the atmosphere and condenses in colder layers. The resulting clouds may be transported through the atmosphere, while condensed raindrops that are too heavy rain down (Mason, et al., n.d.; Strangeways, 2006; IPCC, 2013; WMO, 2018a). If these precipitating clouds concentrate regionally, they might cause heavy precipitation and floods. For instance, the upper-level low in July that brought heavy precipitation to Western Europe, stayed in one place for a particularly long time because it was blocked by two areas of high pressure (Puca, et al., 2021). However, so far it is not clear if the slow movement was caused by changed circulation patterns as individual events cannot be directly associated with climate change (Junghädel, et al., 2021). Also, to date, scientific studies could not detect robustly changes in blocking weather patterns due to climate change (Woollings, et al., 2018). And although the Alpine region is experiencing an even higher temperature increase (Blöschl, et al., 2017) than the global average temperature rise of 1.2°C (IPCC, 2021), previous studies about Austria could not detect a clear climate change signal regarding extreme precipitation. This might be related to the rareness of extreme events (Villarini, et al., 2011) or Austria's great regional variability and orographic structure where the Alpine region receives higher amounts of precipitation than the relatively dry Eastern region (Hofstätter & Matulla, 2010; Hiebl & Frei, 2018). Moreover, in the West of Austria other weather conditions are causing heavier precipitation than in the East (Seibert, et

al., 2007). The continental East receives the largest precipitation amounts through Vb-weather conditions (Formayer & Kromp-Kolb, 2009) although this type of weather pattern is only responsible for a fraction of heavy precipitation in all of Austria. And although the East is one of the driest regions in Austria, it has the potential for very intense precipitation (Seibert, et al., 2007). As mentioned above, Chimani et al. (2016) found an increase in heavy precipitation days for Austria, while changes in the intensity of heavy precipitation in Eastern Austria were found to be non-significant (Zeder & Fischer, 2020). However, for sub-daily heavy precipitation Formayer & Fritz (2017) found for a station in Vienna an increase of hourly heavy precipitation rates. Nevertheless, according to Blöschl et al. (2017) there is no gradual change or trend regarding convective precipitation in all of Austria.

Although extreme events are rare, they have the potential to cause colossal damage to private and public property and threaten human life (Hofstätter & Matulla, 2010). The July flood alone caused €29 billion in damage (Tagesschau, 2021), injured 766 people and killed 133 in Germany alone (ZDF, 2021). The river Danube was also affected by the heavy July precipitation in its catchment area near the city of Vienna and therefore carried high water (Stadt Wien, 2021a). However, the city of Vienna has excellent flood protection measures such as the New Danube and the Danube Island, which is why the city itself is well protected even from centennial floods (Stadt Wien, s.a. a). However, before these flood protection measures were built, Vienna was frequently affected by flooding due to heavy rainfall events (Stadt Wien, 2021b). Moreover, even if heavy precipitation events do not lead to river flooding, buildings, roads, and critical infrastructure can be obstructed or destroyed through the precipitation itself, negatively impacting the population (Groenemeijer, et al., 2015; Gandini, et al., 2020). Therefore, it is in the public and private interest to better understand the course of future extreme events under changing climate conditions (Hofstätter & Matulla, 2010).

While there is a limited number of studies investigating daily, and sometimes even sub-daily heavy precipitation in Austria, small-scale analyses of heavy precipitation in North-Eastern Austria are missing. The objective of this thesis is to close this gap and to analyse precipitation data in and around Vienna for heavy precipitation changes in the last 15 years. Special attention is given to the analysis of heavy precipitation at different time intervals, i.e., daily, hourly and event precipitation. The following research question is to be answered by the quantitative analysis of the precipitation data: How has the frequency and intensity of heavy precipitation changed in the Greater Vienna region during the period 2006-2020?

To answer the research question daily and 10-minute precipitation data of ten stations in and around Vienna provided by the Austrian National Weather Service (ZAMG) were analysed with the statistical program "R" (The R foundation, s.a.). To determine any changes in frequency or mean rain rate, the study period 2006-2020 is compared with a reference period. For daily analyses, the years 1979-1993 were chosen as the reference period, as this time span has already been used in previous studies and thus allows a comparison of the present study results with existing work. Since 10-minute data have mainly been recorded since the 1990s (along with the advent of automatic weather stations), the period 1991-2005 was chosen as the reference period for hourly and event analyses which are based on 10-minute data. Thresholds were calculated based on the reference periods and then used for the main study period to identify heavy precipitation and calculate any changes. Changes in frequency, mean rain rate as well as seasonal changes were analysed. Moreover, a correlation analysis of seasonal and annual heavy precipitation is conducted using daily precipitation data. Additionally, return periods of daily heavy precipitation periods are calculated using two different approaches. In a first step, the averaged threshold for daily heavy precipitation in the study area is used as a threshold for the extreme value analysis. In a second step individual thresholds are calculated for each station and the extreme value analysis is repeated.

The thesis is structured as follows: first, in Chapter 2 a theoretical overview is given of the formation of precipitation including the characterization of various synoptic regions of Austria.

In addition, important weather conditions for the study area are discussed. Furthermore, missing international standards and different classification possibilities of heavy precipitation are addressed, followed by global and regional changes of precipitation and heavy precipitation, impacts of heavy precipitation and possibilities to mitigate them. The theory chapter concludes with an introduction to the different possibilities of precipitation measurement and the presentation of the study area. Chapter 3 describes the collection and quality control of precipitation data by the Austrian National Weather Service as well as the distribution of precipitation data to the end-user. Chapter 4 contains detailed descriptions of the data used, their analysis with R, and the procedure for determining thresholds for extreme precipitation on a daily, hourly and event basis. In addition, an introduction to extreme value statistics is given and the approach used in this thesis is described. This is followed by the presentation of the results in Chapter 5 and discussion and conclusions in Chapter 6.

2 State of Knowledge

The following subchapters describe how precipitation and heavy precipitation develop globally and in Austria. Furthermore, it is described how heavy precipitation is classified, how global and regional (heavy) precipitation has changed, what the impacts of heavy precipitation are and how adverse effects of heavy precipitation can be mitigated. Furthermore, the different methods of precipitation measurement are explained and last, but not least an overview of the study area is presented.

2.1 Formation of (heavy) precipitation

Precipitation can either be liquid (e.g., rain, drizzle) or solid (e.g., hail, snow) and is an important process within the hydrological cycle, distributing fresh water from water surfaces through the atmosphere back to the Earth's surface (Mason, et al., n.d.; WMO, 2018a). Not included into the definition of precipitation is condensation such as dew, fog, frost, or rime (Strangeways, 2006; WMO, 2018a). Precipitation is based on cloud formation through rising damp air, which cools in higher levels of the atmosphere. When the air becomes saturated with water vapour, condensation occurs on aerosol particles suspended in the air. When the air is supersaturated, cloud droplets form. While cloud droplets grow and become too heavy to be supported by the up streaming warm air, they fall through the cloud, eventually collide and fuse with other smaller droplets before reaching the ground as rain or drizzle. Where the cloud reaches elevations with air temperatures below or well below 0°C snowflakes or ice crystals can form (Mason, et al., n.d.; Strangeways, 2006; IPCC, 2013; WMO, 2018a).

There are several types of clouds, which all bring different amounts of precipitation. For detailed descriptions of different cloud types as well as the basic physical processes underlying cloud formation the reader is referred to e.g., Strangeways (2006). In this thesis the attention is focused on clouds relevant in Europe, especially those important for forming heavy precipitation. The process responsible for forming most precipitation clouds is convection, which refers to the organized (predominantly) vertical movement of heat through the atmosphere. The World Meteorological Organization (WMO) defines convective clouds as cumuliform clouds that form in an atmospheric layer made unstable by heating at the base or cooling at the top (WMO, 2017). Convective clouds of a certain size, such as cumulonimbus cloud, can produce hail and thunderstorms and even tornadoes. The smallest cumulonimbus cloud, the so-called single-cell storm, lasts only 30 minutes to two hours after formation. However, if several convective cells cluster together, they become a multicell storm that can last several hours and spread out up to 10 km horizontally (Strangeways, 2006; Pehsl, 2021). Supercell storms contain a rotating upward wind and can be part of a multi-cell storm or exist on their own (Pehsl, 2021).

An exception to the principle of cloud formation through cooling of ascending moist air is the stratus cloud. It is usually formed through sideways motion of air, or advection, and is created when damp air is carried by light wind over cold land masses or the sea. As stratus clouds are thin, they usually produce little precipitation compared to cumulonimbus clouds.

Aside from convection and advection, clouds can form through the collision of cold and warm air masses. Extratropical cyclones, also referred to as frontal depressions, can develop when cold air flows beneath warm air masses lifting them up, or when warm air masses cool through rising over cold air, forming an extensive zone of low pressure. In the mid-latitudes, frontal depressions are responsible for most of the precipitation received, mainly through nimbostratus cloud, which can last for several hours (Strangeways, 2006). Moreover, extratropical cyclones are responsible for extreme wind speeds and heavy precipitation

especially in winter (IPCC, 2013). Last, clouds can form orographically when winds meet a topographic barrier. These clouds are of the same type as usually formed clouds and differ only in the circumstance of their formation (Strangeways, 2006).

Precipitation is subject to annual fluctuation due to climate oscillations, which are driven by changes in pressure related to sea surface temperature variation. Well-known is for example the El Niño Southern Oscillation (ENSO). The term El Niño was coined by fishermen in South America when every few years around Christmas a warm current replaced the very cold northward current. Usually, moderate trade winds are pushing the warm surface waters of the Pacific westwards towards Australia allowing the colder layers of the water to reach the surface at the coast of Peru. The differences in sea surface temperatures result in high barometric pressure in the East and low pressure in the West causing heavy convective precipitation over Australia and Indonesia. The inverse phenomenon of stronger trade winds is called La Niña. La Niña brings similar, but slightly more intense precipitation. Oppositely, during El Niño trade winds are weak allowing warm surface waters extend to the East, leading to high pressure over Australia as well as South America which causes low pressure over Tahiti and the central Pacific resulting in heavy precipitation there (Strangeways, 2006). Although ENSO influences precipitation variability mainly over the tropics, its teleconnection with regional climate extends globally (Strangeways, 2006; IPCC, 2013).

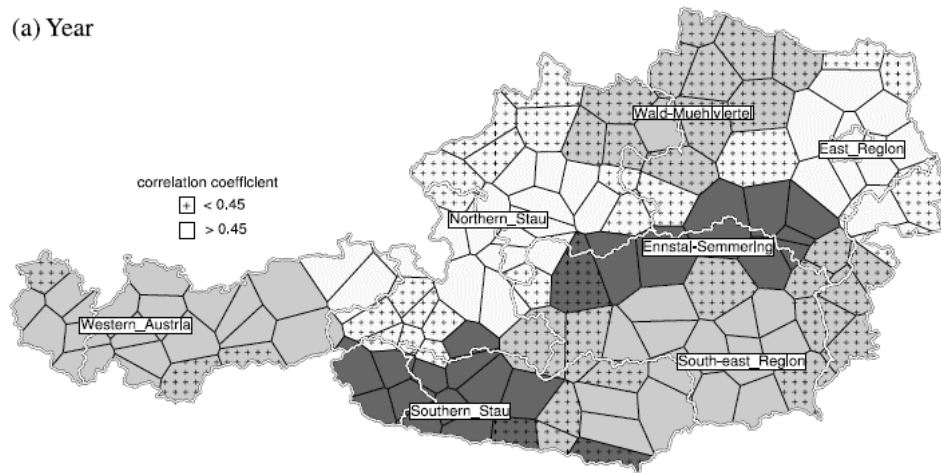
An important oscillation in the North Atlantic region, affecting precipitation variability from North America to Europe and Northern Asia, is the North Atlantic Oscillation (NAO). The NAO is frequently characterized by an index calculated as the anomaly of the pressure differences between the Azores, where pressures are usually high, and the Icelandic low. When the pressure gradient increases due to a stronger high and stronger low, more intense winter depressions form and cause warm and wet winters in Europe. In this configuration the phenomenon is referred to as the NAO in its positive phase. A negative gradient caused by a weaker high and low leads to weaker depressions (Strangeways, 2006), referred to as the NAO in its negative phase. It is expected that in a warmer climate the NAO becomes on average somewhat more positive (IPCC, 2013).

In Austria, the NAO is associated with more frequent extreme daily rainfall in the mountainous west of the country, while the East seems to be less affected (Villarini, et al., 2011). This is one example of the regional variability of precipitation in Austria. On the one hand, precipitation is influenced by the complex orographic structure of Austria; on the other, by different, large-scale weather conditions. Over the course of the year, different regions in Austria therefore receive precipitation in different amounts and intensities (Hofstätter & Matulla, 2010). In total, seven regional precipitation patterns were identified for Austria by Seibert et al. (2007) illustrated in Figure 1. The most relevant region for this thesis is the East-Region which includes Vienna, parts of Lower Austria and a northern part of Burgenland. Contrary to popular belief, the Vienna Woods, which are part of the eastern foothills of the Alps, do not seem to divide the East-Region climatically, the study by Seibert et al. (2007) finds. The different regions show slightly different patterns for the summer and winter half-year, i.e., while the East-region spreads far north-west to the borders of Lower Austria including the Waldviertel in the winter half-year, in the summer half-year the East-Region is the smallest. Otherwise, the regions in summer are similar to the ones for the whole year (Seibert, et al., 2007).

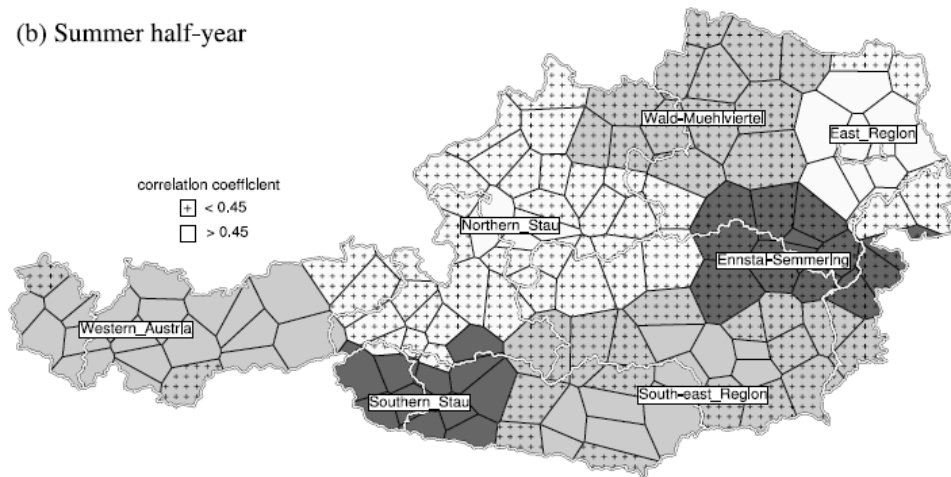
Austria shows a West-East gradient in precipitation amounts. Since the East has a stronger continental influence, it generally receives less precipitation than the West. Nevertheless, if Vb-weather conditions are present the highest precipitation intensities can be found in the South and the East. Such weather conditions are characterized by cold air forcing into the Gulf of Genoa which triggers the development of low-pressure. The core of the low-pressure area then travels over Italy, Slovenia, and Hungary to Poland, leading to multiple days of rain over all of Austria, often causing large-scale flood events (Formayer & Kromp-Kolb, 2009). But Vb

cyclones are rare events, which occur on average only 2.3 (Messmer, et al., 2015) to 3.5 times per year, mostly in spring and autumn (Hoftätter & Chimani, 2012).

(a) Year



(b) Summer half-year



(c) Winter half-year

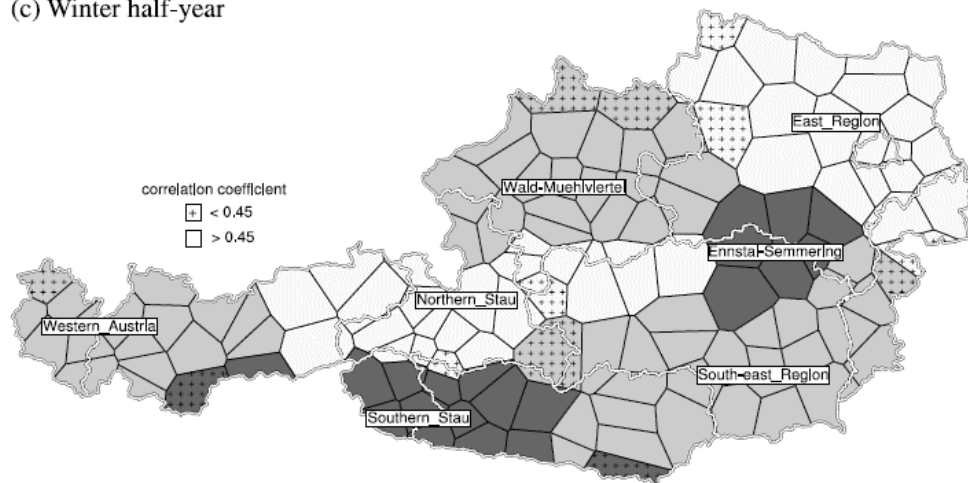


Figure 1: Regions in Austria with similar daily precipitation identified through clustering by Seibert et al. (2007) for a) the whole year, b) the summer half-year and c) the winter half-year. Different precipitation regions indicated by grey shading; white lines mark the federal states of Austria. Correlation of stations with others of their clusters is represented by crosses.

In a warming climate Vb-weather conditions are projected to become less frequent, however, if they occur, they are also projected to bring even more intense precipitation, especially in summer (Formayer & Kromp-Kolb, 2009). And particularly the summer season is - due to higher water content in the atmosphere - associated with greater flooding risk in connection with Vb cyclones (Hoftätter & Chimani, 2012). Although Vb is the weather pattern that causes the highest precipitation amounts in eastern Austria, Seibert et al. (2007) found that only 12 % of heavy precipitation in all of Austria is caused by it.

The synoptic pattern responsible for almost half of all heavy precipitation in Austria is one with very slow movement near the ground and a weak pressure gradient. It is mainly convective, with pre-frontal storms and summer cold-front passages, thus, it displays a pronounced seasonal cycle with most events happening in summer and the least in winter. It is the most frequent reason for heavy precipitation in absolute terms, as it occurs predominantly in the summer season, when precipitation amounts are generally higher. However, in the East its intensity is the weakest (Seibert, et al., 2007).

Another pattern identified as having an effect on the East-Region was referred to by Seibert et al. (2007, p. 149) as “cut-off low to the east”. This pattern is characterized by a “well-developed low-pressure system at higher levels in the (north-) east of Austria caus[ing] cold-air advection at its back” (Seibert, et al., 2007, p. 148) leading to northerly flows and destabilisation of air, hence, promoting precipitation. Other synoptic patterns were identified by Seibert et al. (2007), but those are mostly relevant for the Alpine region in the West and South of the country and less for the East and, thus, this thesis.

Although climate change cannot be linked directly to the forming of individual extreme events, progressing warming is projected to increase the frequency and intensity of heavy precipitation events. This is very likely for most land masses in the mid-latitudes (IPCC, 2013). It should be noted that the Alpine region and Austria have been affected more by global warming than other parts of the northern hemisphere. The average temperature in Austria increased by +2°C since 1970 opposed to 1.5°C increase in the northern hemisphere (Blöschl, et al., 2018). As warm air can hold more moisture, rising temperatures increase the water holding capacity of the atmosphere as well as evaporation, provided that sufficient surface moisture is available (Trenberth, 1999), thus, increasing the water vapour content in the atmosphere (IPCC, 2013). This is described by the Clausius-Clapeyron relation, according to which the saturation water vapour pressure increases by 6-7 % per degree of surface warming (Allen & Ingram, 2002). Aside from being a potent greenhouse gas, leading to further warming, water vapour is also linked to more intense precipitation events (IPCC, 2013). However, this is counterbalanced, when aerosol pollution partially shields the surface from direct solar radiation, leading to less evapotranspiration, thus, potentially shortening the frequency and duration of events (IPCC, 2007). Nevertheless, daily extreme precipitation rates are expected to increase by 7 % per °C of warming, which exceeds the rate of mean precipitation (IPCC, 2021). This matches the findings by Formayer and Fritz (2017) who investigated the increase of hourly extreme precipitation in relation to surface and cloud layer temperature in Vienna and found increases of 8.5 % per degree warming. For central Europe, increased atmospheric moisture, increased moisture convergence and intensification of extratropical cyclone activity are projected to increase mean precipitation in the winter half-year (October to March), but lead to only small changes in the summer half-year (IPCC, 2013). Over Austria, however, it was impossible to make conclusive statements on effects of climate change on extreme precipitation in previous studies due to the rare characteristic of such events and therefore possibly weak climate change signal (Villarini, et al., 2011). Inconclusive results could also be related to the fact that other factors and processes besides atmospheric moisture content seem to be involved in the formation of heavy precipitation at the local level (Breugem, et al., 2020). Moreover, previous observations have shown that precipitation is subject to strong interannual and decadal variability and is also influenced by internal variability, volcanic forcing, and anthropogenic aerosol loads. This contributes to the difficulty in identifying clear trends (IPCC, 2013).

2.1.1 Classification of heavy precipitation

Heavy precipitation events are classified - like heat waves, droughts, winter storms and sea surges - as extreme climatic events. Those events are often characterized as rare, intense, and severe (Beniston, et al., 2007). However, regarding precipitation there is no internationally agreed definition for a rain intensity constituting a heavy event. Some use rain rates of 4 mm/h for heavy rain and 10 mm/h for heavy showers. Yet, those rain intensities might be heavy in one region while even higher rain intensities might be typical for another region (WMO, 2020; Breugem, et al., 2020). The use of percentiles can account for regional differences in precipitation. According to the IPCC (2013, p. 134) “an extreme weather event would normally be as rare as or rarer than the 10th or 90th percentile”. Precipitation in particular can be classified as extreme when the mean rainfall for a specific period exceeds the 90th to 98th percentile (Kuleshov, et al., 2020).

As precipitation falls intermittently and involves rainless periods, usually rainfall is viewed in terms of ‘events’ (Dunkerley, 2008a). Events can be defined by multiple criteria which often vary between studies making it difficult to compare them meaningfully (Dunkerley, 2008b). One criterion is the minimum inter-event time (MIT) which is an arbitrary rainless period before and after an event, defining the beginning and end of that event. Often the MIT is 6-8h, but it can range between 3 minutes to 24h (Dunkerley, 2008a). Consequently, the MIT includes shorter rainless periods into the rain event. Such rainless periods within an event can be described by the intra-event rainfall intermittency (IERI) which is the percentage of the event duration with no rain. IERI can give a hint on the intensity of rainfall, as a greater intermittency for an event means that it rained in shorter periods of time within the event (Dunkerley, 2015). According to Dunkerley (2008a), different MITs are adopted to ensure independence of events in order to reduce the impacts of previous events on e.g., soil wetness or canopy interception and therefore better interpret the event’s contribution to runoff formation. If studying urban runoff other MITs might be adopted according to e.g., surface depression storage capacity. In short, the length of the MIT is determined by conditions of the subject that is studied. Aside from the subject of the study, the MIT is dependent on the study area as for example arid regions might require different MITs than e.g., the tropics. The MIT is often supplemented by other criteria such as minimum rain depth, minimum rain event duration and minimum rain rate. Minimum rain depth varies across studies from 0.2 mm to 12.5 mm while minimum rain event durations range from 30 minutes to 4h. Minimum rain rate can either mean a minimum rain rate for a period within an event, for which it varies across literature from 1 mm h⁻¹ to ≥2.8 mm h⁻¹ or a minimum rain rate can be used to identify the start of an event and another one to identify the end (Dunkerley, 2008a). According to Dunkerley (2008b), it is important to distinguish between two different types of rain rates: the instantaneous rainfall rate (I), which should be the only rain rate to be referred to as rainfall intensity, having integration times of 10s or less, and the mean rainfall rate (R), which is the extrapolated instantaneous rainfall rate over a period of time. Nevertheless, according to the WMO (2018a), rainfall intensity can be derived over a one-minute period as well. The mean rainfall rate can be calculated as the total event depth (D_e) divided by the event duration (T_e) or as the total rain depth of a time interval (D_t) divided by the time interval (T_t), thus:

$$R_e = D_e / T_e$$

or

$$R_t = D_t / T_t \tag{1}$$

However, such averaging over time affects extreme values because of the strong temporal and spatial inhomogeneity of precipitation. Therefore, when choosing temporal and spatial intervals for analysis it is necessary to take into account the strong, short-lived and localized nature of convective events opposed to stratiform events that cover larger areas and include fewer bursts (Eggert, et al., 2015). Moreover, aside from considering regional differences of rainfall, it is also important to take into account the true range of rain rates when categorizing them as weak or heavy (Dunkerley, 2008b).

Naturally, depending on the chosen parameters the number of events can vary even within the same dataset. Additionally, to the MIT, the 'inter-event time' (IET) describes the actual length of rainless periods between events (Dunkerley, 2008a). However, often events are described through the depth of rain delivered in 24h and are then classified accordingly as e.g., 'light', 'moderate' or 'heavy', when reaching a certain threshold (Dunkerley, 2008b). Seibert et al. (2007) analysed heavy precipitation in Austria, identifying heavy events as the 98th percentile of a 15-year long data set and found that for Austria a day with 20 mm rain can be classified as a heavy precipitation day. More specifically, for the region of the study area, days with 13 mm/d can be considered as heavy as this region is drier than other regions in Austria. In other studies, heavy precipitation is classified as the 90th – 95th percentile of wet days (Chimani, et al., 2016). Although the use of percentiles of wet days is common in climate change studies, Ban et al. (2015) do not recommend it as changes in wet or dry days might lead to an over- or underestimation of heavy events, respectively. Therefore, rather the use of percentiles established over all days, including dry days, is recommended. Moreover, aside from daily rainfall depth, the less common rainfall or event depth (D_e), which is the amount of rainfall in a rain event, should be considered according to Breugem et al. (2020).

2.1.2 Global and regional changes of (heavy) precipitation

Global precipitation over land increased slightly over the course of the 20th century, but there is no significant trend detectable that matches the trend of global warming. Moreover, changes are not linear but rather showing multidecadal fluctuations above and below the mean. Similar patterns of precipitation change emerge for the Northern and Southern hemisphere. A slightly larger upward trend could be observed for the Southern hemisphere; however, the biggest relative increases were detected in the middle- and high latitudes of the Northern hemisphere (Strangeways, 2006). For Europe, precipitation changes are not uniform. Simulations show that by the end of the 21st century, precipitation will decrease in southern Europe, and increase in northern Europe, especially in winter. In the intermediate regions, the projected changes are only small, while the main difference is more in the seasons. An increase in precipitation is predicted in winter and spring, while summers and to some extent also autumns get drier (Dankers & Hiederer, 2008). Austria, located in central Europe, is an example for such an intermediate region with no clear annual trend, but a strong shift in seasonal precipitation (Formayer & Kromp-Kolb, 2009). However, currently a different trend is observed in Austria than predicted for Europe. In Austria, summer precipitation increased over the last decades, Blöschl et al. (2017) found in their analysis of hydrological baseline data and other research results. Further results show that mean annual precipitation in Austria had a pronounced minimum in 1977, but since 2005 returned to a similarly high level as in the 1960s. Halmova et al. (2015) found similar results for Vienna when looking at 30-year moving averages of precipitation, except that precipitation in the summer half-year is today even larger than in the 1960s. In fact, their study revealed that the Danubian lowland region experienced the wettest decade during 1891-1900. The driest decade occurred only recently between 1981 and 1990, although before 1870 the climate was most likely even drier. However, broad and sufficient data are lacking to be certain. This shows, opposed to temperature, that precipitation does not show any distinct long-term trends, but is subject to multidecadal fluctuations. There is a slight

increase in annual precipitation in Austria, which is attributed to an increase in summer precipitation. On the other hand, two significantly dry summers in 2013 and 2015 occurred (Blöschl, et al., 2017).

Regarding heavy precipitation it is not possible to measure global means as the definition of extremes varies widely depending on the studied region (Strangeways, 2006). However, it is possible to analyse precipitation maxima of different regions and any changes in them. Lehmann et al. (2015), for instance, found that the frequency of record-breaking precipitation events has increased globally. The authors demonstrated that this increase is linked to rising temperatures and that one in ten record-breaking events between 1981 and 2010 can be attributed to climate change. Also, an analysis of annual maxima of daily precipitation showed global increasing trends for two thirds of the examined stations. However, the authors note that they could not detect systematic trends within a region, rather the distribution of stations with increasing or decreasing trends seems random in some areas (Westra, et al., 2013). This finding seems to be consistent with the IPCC's (2014) statements that there has most likely been an increase in the frequency and intensity of heavy precipitation events in Europe since 1950, with some seasonal and regional variations. The changes are favoured by an increase in atmospheric water vapour and altered atmospheric circulation (IPCC, 2013). Similar to the overall precipitation change, Frei et al. (2006) also found that different models show increases of heavy precipitation predominantly over land masses of the middle and high latitudes. This is confirmed by Zeder and Fischer (2020) who find that daily heavy precipitation becomes more intense over most of Central Europe. The increase of extreme precipitation in Europe reported by the IPCC (2013) was observed mostly in winter, although some regions show decreasing trends. These results are similar to the study of Lehmann et al. (2015), whereby an increase in extreme precipitation in summer and even more pronounced increase during winter has been found for the northern extratropics while, e.g., in the Mediterranean region also decreasing trends were observed, especially in winter. Within Austria, the western Alps show increasing trends in the intensity of annual daily maxima, especially in winter, while trends in the East are not significant (Zeder & Fischer, 2020).

Depending on the season the duration of heavy rainfall can have various impacts. While in winter, it is mainly episodes that last for several days that have negative effects, in summer even short rainfalls can have a large impact (Frei, et al., 2006; Beniston, et al., 2007). Simulations by Ban et al. (2015) showed that a decrease in mean summer precipitation over central and southern Europe is projected due to less frequent small and intermediated events, however, heavy daily and hourly events are projected to become more frequent and intense. Specifically, the frequency of events above 10 mm/h increased strongly in the study. In Austria, an increase in summer precipitation was observed, with summer having a higher frequency of extreme rainfall and July being the month with most extreme precipitation days throughout the year (Villarini, et al., 2011). In Eastern Austria, summer receives twice as much heavy precipitation than winter although total rain depth in this area is generally lower than in the rest of the country (Isotta, et al., 2014). However, no gradual or significant change regarding convective heavy precipitation events is observed, but two phases of high convective activity (1989-1994 and 2006-2014) were identified by Blöschl et al. (2017). Nevertheless, the authors note that due to the complexity of small-scale and short-lived heavy precipitation events, statements about changes are very uncertain and can vary depending on the studied region.

2.1.3 Impacts of heavy precipitation

Extreme precipitation can impact human health as well as have negative effects on agriculture, forestry, buildings, infrastructure, and ecosystems (Beniston, et al., 2007), mainly because it has the potential to cause runoff and flooding (Lenderink & van Meijgaard, 2010; Breugem, et al., 2020). While floods are already one of the most common natural disasters affecting human

health and the economy in Europe (Hajat, et al., 2003), an increased frequency and intensity of heavy precipitation additionally increases the risk of flooding at regional scale (IPCC, 2014). Moreover, other factors such as land use changes and settlements in flood-prone areas also contribute to flooding risks and increase vulnerabilities towards floods (Trenberth, 1999; Breugem, et al., 2020). In the Alpine region, flood risk will increase due to two factors: on the one hand, increased precipitation in winter due to changed precipitation patterns and on the other hand, with rising temperatures, precipitation increasingly will fall as rain rather than snow, thus, not being retained but directly running off. This development, in addition to a rising snow line, leads to significantly increased flood risk in the lowlands and Alpine foothills. Areas that will be affected the most by changed snow patterns lie between 500 and 2000 metres in altitude, as lower lying regions already receive more than half of their winter heavy precipitation in form of rain. Moreover, elevated temperature and changed precipitation patterns might have a negative effect on the Alpine vegetation, thus, increasing the amount of precipitation that directly runs off instead of being intercepted and infiltrated. Although the East is more affected by drier conditions, changes in weather patterns can lead to floods in every river in Austria, including the Danubian region (Formayer & Kromp-Kolb, 2009).

Additionally, negative impacts on vegetation might not only increase flood risk but also could have negative effects on Austria's economy as forestry plays an important role in it. About half of the Austrian national territory is covered by forests (WKO, 2021), and especially spruces were planted frequently due to their economic importance, even in climatically non-optimal locations. With global warming, growing conditions are worsening for spruce, and especially Eastern Austria is becoming increasingly unsuitable for spruce stands (Formayer & Kromp-Kolb, 2009). While drought stress is a serious problem in forestry, too much rain on the other hand can lead to water stress and thus have negative effects also on tree populations (Beniston, et al., 2007).

Another economically important sector for Austria is tourism. As most tourists come to Austria for outdoor activities such as skiing and hiking, changed precipitation and temperature patterns might have negative effects on the number of visitors. Naturally, Vienna as the capital is characterised by shorter city and business trips, but also there hotter or wetter weather might impact tourism. Large-scale heavy precipitation that lasts several days as well as locally and temporally confined heavy precipitation events both have the potential to damage infrastructure and interrupt traffic, as well as pose a risk at outdoor activities. Large-scale extreme precipitation can cause floods, landslides, and damage to buildings, and prevent tourists from coming at all. Local heavy precipitation on the other hand can cause debris flows and impact food prices due to necessary imports. Lastly, extreme weather can threaten the life of tourists due to storms, lightning, hail, or avalanches (Pröbstl-Haider, et al., 2020).

In addition to external injuries caused by extreme weather, it has been observed that flooding can also have negative impacts on the mental health of the exposed population (Weilnhammer, et al., 2021). Also, the risk of infection, e.g., through contamination of drinking water sources, can be increased through flooding. However, the risk is low and can be minimized further if it is responded to accordingly. Additionally, flooding increases the risk of contracting water-borne diseases (World Health Organization, n.d.) when heavy rains create large areas with standing water. Also, extreme precipitation might lead to contamination of water bodies with livestock faeces and thereby pose another health risk (O'Dwyer, et al., 2016). On the other hand, if contaminated water is transported with the flood to agricultural land, the risk of transmission of foodborne diseases increases, especially if such produce is eaten raw (Lake & Barker, 2018).

Flora and fauna might also be affected negatively by changing precipitation patterns. Increased heavy precipitation, i.e., not the amount of rain but only the duration of the events changes (stronger but fewer events) can promote exotic species to invade and alter existing terrestrial ecosystems as well as cause soil water stress. However, not all terrestrial ecosystems are affected negatively (Knapp, et al., 2008). Depending on the type of ecosystem, Knapp et al.

(2008) argue that changed precipitation patterns might even have a positive impact. Nevertheless, negative effects of prolonged or heavier rainfall have been observed in the survival rate of nestlings of certain bird species, as rain affects thermoregulation, food supply and predation risk (Schöll & Hille, 2020). Moreover, changed precipitation patterns will not only affect biodiversity and survival of plant and animal species but the human food chain as well. Assuming future rain scenarios for central Europe, i.e., precipitation will be stronger but less frequent, Tataw et al. (2016) found that wheat production – an important source of carbohydrates for the global population - will see a significant yield reduction due to drought stress. Similar results were obtained in a previous study with field pea (Tataw, et al., 2014). Aside from yield reduction through drought stress, excess soil moisture also leads to reduced yields and is already causing billions of dollars in damage today. An increase in the amount of rain or the frequency of heavy precipitation, thus, clearly increases the probability of agricultural damage, apart from potential physical damage of plants through heavy precipitation or hail (Rosenzweig, et al., 2002). Additionally, food production is also threatened by pests. However, studies investigating how pests are affected by heavy precipitation are very limited and more research is necessary to assess potential damage to agricultural production in that regard (Seidel, 2014).

Heavy precipitation has the potential to damage buildings and critical infrastructure. The vulnerability of buildings to heavy precipitation varies and depends on several factors. For instance, existing damage to the roof or façade allows water to penetrate the building envelope and cause further damage in the occurrence of a heavy rain event. The presence of a basement and openings on the ground floor also increase vulnerability in the case of flooding. With flat roofs, rapidly accumulating rain may drain more poorly, and infiltration may occur. In addition, the façade can be damaged by heavy precipitation. This ranges from soiling, infiltration and corrosion to cracks, detachments, or deformation. The material of the building also plays a role in how much water is absorbed and infiltrated in the case of flooding. Wood, for example, is most easily damaged, whereas stone material has the greatest resistance. In the event of the building being affected by heavy rainfall, the use of the building determines how strong the negative impact on society is. Certain buildings can be out of service indefinitely, as they are not essential, such as car parks and cultural centres. Others need to be available all the time, such as hospitals and pharmacies. Residential buildings can only be inaccessible for a limited amount of time, as well as facilities that are important for the economy such as offices, restaurants, and shops (Gandini, et al., 2020). Critical infrastructure such as roads, railways, electrical power grids and telecommunication networks are affected the most by windstorms, heavy precipitation, and river floods. Furthermore, snow and freezing precipitation might also have negative consequences. However, different types of critical infrastructure are affected by the various weather phenomena to different extents. Transportation infrastructure and emergency services, for example, are particularly affected by heavy precipitation. It can cause erosion of streets and rail embankments, flooding of tunnels, streets, highways, and railroads, and poses a risk of aquaplaning. Additionally, heavy precipitation can lead to secondary effects such as river flooding and landslides/mudslides. The latter can block and damage streets and railroads while the former can erode and damage bridges as well as flood streets and railways (Groenemeijer, et al., 2015).

2.1.4 Mitigation of heavy precipitation impacts

The impact of an event on a system depends on the system's state and is determined by different economic and social factors. Therefore, different levels of adaptation and adaptation capacity influence the severity of the impact of an extreme weather event (Beniston, et al., 2007). This also means that developing countries are the most vulnerable to extreme events due to fewer resources at their disposal (UNFCCC, 2007). But even within wealthier countries,

inequalities lead to different extents of vulnerabilities to climate change. This becomes evident as the poor are systematically pushed into areas that are more vulnerable to flooding, water contamination and mud slides because they lack the resources to settle in safer areas (UN, 2016).

If resources are available, there are different approaches to reduce the damage of extreme events. For instance, shield panels or sealants can protect buildings temporary in the event of a flood. Drainage systems that can channel water out of the building can further reduce vulnerability to heavy rainfall and flooding (Gandini, et al., 2020). In Europe, drainage systems are also in place for roads and railways to protect critical infrastructure. However, changing heavy precipitation patterns might make current drainage systems inadequate in the future and research is necessary to assess the state of such systems, update them, and potentially design new ones (Groenemeijer, et al., 2015). Other measures to reduce damages are early warning systems, river management, flood retention basins, emergency drainage channels, inlet structures upstream of stream culverts to protect piped watercourses in localities from clogging, more efficient drainage systems in outlying areas, flood-reduced land management and small-scale retention in agricultural areas, renaturation, flood-adapted planning, construction, and renovation as well as flood protection measures by individuals. But even if all measures are implemented, it is no guarantee that the flood risk from heavy rainfall events will be averted. Rather, the use of flood-prone areas must be adapted to flooding to reduce the extent of damage (Hässler-Kiefhaber & Lorig, 2018). For example, areas prone to flooding should be identified, marked in a land use plan, and kept free of buildings. Moreover, areas should also be planned multifunctionally, i.e., in addition to their original use, they can be flooded in the event of heavy rainfall and then serve as temporary storage for precipitation water. Suitable for such secondary use in flood prevention are usually all public areas on which no (expensive) water-sensitive objects are located like open spaces, sports fields, or playgrounds (Piroth, 2018).

Most of the aforementioned measures are a direct response to existing or emerging flooding. Others, however, can help to prevent flooding from occurring in the first place. A key factor here is the way in which agricultural land is cultivated. Increasing water infiltration and reducing silting which impedes infiltration is essential. Conservation tillage, i.e., not using the plough, and direct seeding are measures that can contribute to increase the infiltration capacity. Further agronomic measures include, among others, minimizing the time interval without soil cover through crop rotation as well as the permanent planting of particularly endangered arable land or slope depressions and channels (Müller, et al., 2018). In urban areas, urban planning, road and traffic planning, open space planning as well as the often very individual house and property design play a role in flood prevention additionally to urban water management. For example, roads and traffic areas can be used for drainage or temporary storage of water in the event of rare or exceptionally heavy precipitation, if already considered during construction (Piroth, 2018). Moreover, building cities as so-called sponge cities can make them more resilient to heavy precipitation. Such efforts have been pursued, e.g., in China for almost a decade (Zevenberger, et al., 2018), and the sponge city concept is also becoming increasingly popular in Europe. For example, the City of Vienna is using the sponge city approach in certain urban development areas like Seestadt Aspern to combat urban heat islands, reduce drought stress of city trees and decrease or even avoid impacts from heavy precipitation. This is achieved through expanding the available root space under roads, car parks and pavements with water retaining materials (Stadt Wien, s.a. b). Vienna additionally has a dual system implemented where contaminated water not suitable for plants is directed to the sewer network and the remaining surface runoff is directed to water trees and vegetation at the roadside and eventually infiltrates into the groundwater (Stadt Wien, s.a. c). A sponge city is thus able to collect, store and purify precipitation (Zevenberger, et al., 2018) and hence contributes to the natural water cycle (Stadt Wien, s.a. c).

2.2 Precipitation measurement

In order to counteract the negative effects of precipitation, it is necessary to have knowledge about local precipitation patterns. For this, precipitation must be measured at representative locations over a sufficiently long period of time. While precipitation measurements were already carried out for a short period in India in the fourth century BC as well as in Palestine from the second century BC for agricultural use, quantitative measurements of precipitation were done for the first time in China in 1247 and in Korea in 1441. However, in Europe first attempts to measure precipitation were not carried out until 200 years later. Moreover, regular measurements were available only since the early nineteenth century in many European cities (Strangeways, 2006). In Vienna for example, station Hohe Warte started recording daily precipitation measurements in 1872. In Kremsmünster and Stift Zwettel measurements are available since 1762 and 1833, respectively (ZAMG, 2019). The measurement of precipitation presents some difficulties, as it is sensitive to exposure, wind, and topography. This must be considered when selecting the location and instruments to obtain representative measurements. Due to the high sensitivity, metadata about the measurement circumstances should be available for users of the data (WMO, 2018a). The different types of precipitation measurements used today will be explained in the following sub-chapters.

2.2.1 Manual, mechanical, and electrical rain gauges

Rain can be measured with so-called rain gauges - devices that collect the rain in a funnel and then quantify it. They function either manually, mechanically, or electronically and can be of recording or non-recording type. There are over 50 different types of manual rain gauges used globally. Typically, these consist of a funnel with a precisely turned, bevelled rim that sits on a base set on the floor. Inside the base is a removable container holding a bottle. It is usually installed on short-cut grass or gravel with the rim above the ground (Strangeways, 2006) to avoid potential splashes from the ground which could distort the measurement. Mostly used installation heights are between 0.5 m and 1.5 m, but like sizes and shapes, gauge heights also vary from country to country (WMO, 2018a). The outer container can collect additional precipitation in case the bottle overflows. The collected precipitation is usually measured daily with a graduated glass cylinder which is marked in steps of 0.1 mm and additionally at 0.05 mm; alternatively, it can be weighed. For weekly or monthly measurements or in areas with large rainfall amounts bigger containers are necessary (Strangeways, 2006). See Figure 2 for a schematic representation of a manual non-recording rain gauge.

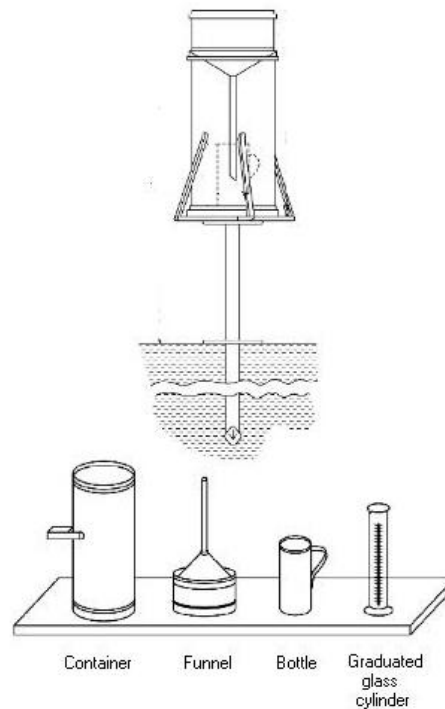


Figure 2: Schematic representation of a typical manual non-recording rain gauge and its components (Český hydrometeorologický ústav, 2003, modified).

Mechanically operated rain gauges usually serve as a supplement to manual gauges to record the beginning and end of rainfall. The basic principle of mechanical rain gauges is to record precipitation with a pen on a paper chart with float- or weight-operated recorders. Float-operated recorders use a float in the cylinder that rises as water enters through the funnel, causing a pin on the paper to move upward. Once at the top, the float causes the cylinder to empty through a natural siphon or through tilting the cylinder to the side and thus starting the siphoning process. Figure 3 shows the measuring principle of a mechanical float-operated rain gauge. Weight-operated rain gauges work similarly to float-operated gauges. Rain is collected in a vessel that is placed either directly on a spring or on a spring that is connected to a balancing arm. The weight of the collected rain moves the vessel downwards and thus the pen that records the rain measurement (see Figure 4). To be able to operate continuously and for accuracy of measurements, weighing gauges need to be emptied periodically, either by hand or through siphoning or tilting. (Strangeways, 2006). To record the amount and timing of liquid precipitation, a recording tape on a clock-operated drum is used (Český hydrometeorologický ústav, 2003). Weighing gauges can also be electrical when the pen is replaced with a potentiometer which produces an electrical output that can be logged (Strangeways, 2006). The weighing gauge is the only recording precipitation gauge type that can also be used for snowfall measurements (WMO, 2018a).

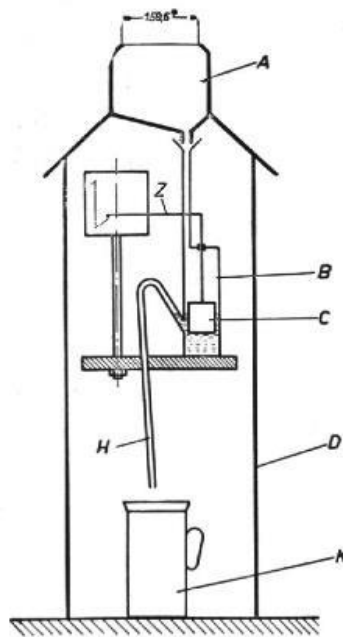


Figure 3: Schematic representation of a float-operating mechanical recording rain gauge. (A) aperture ring, (B) float vessel, (C) float, (D) container, (H) siphon, (K) collecting vessel, (Z) pen arm (Dr. Alfred Müller Meteorologische Instrumente KG, 2020).

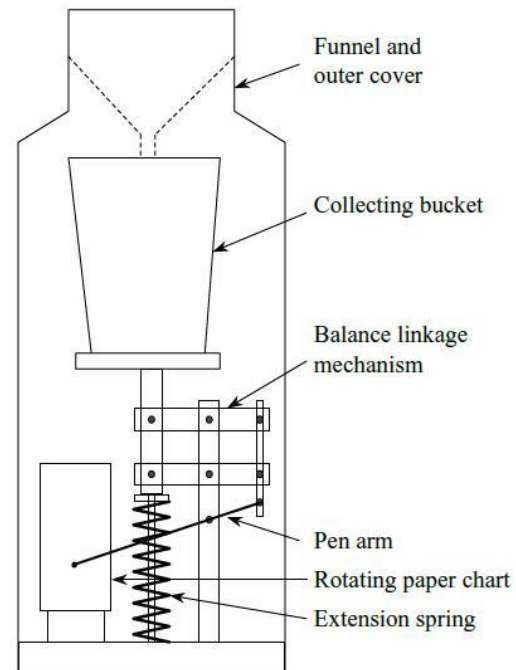


Figure 4: Schematic representation of a weight-operated mechanical recording rain gauge (Strangeways, 2006).

The third type of a recording rain gauge is the tipping-bucket rain gauge. It is an electronic gauge and the most used automatic rain gauge today (Strangeways, 2006). It operates with two symmetrical metallic or plastic buckets that are balanced to measure rain in portions of equal weight. When one bucket is full, it tips and empties itself out while the other bucket is brought into position to collect the next portion of rain (WMO, 2018a). When tipping, a magnet is moved past a magnetic reed switch creating an electrical impulse. That output is recorded by a data logger either as total amount of tips within a period or as date and time of the tip happening. Figure 5 shows the layout of a tipping bucket rain gauge. The shape and size of buckets vary across gauge models, but they should be able to hold at least ten millimetres of rain. Further, gauges differ in tip intervals from 0.1 mm to 1 mm. Some tipping buckets are additionally combined with a weighing device, having the advantage to collect rain that otherwise might be lost as excess when it accumulates in the tipping bucket that is still being emptied, thus unable to measure any continuing rain for that period (Strangeways, 2006).

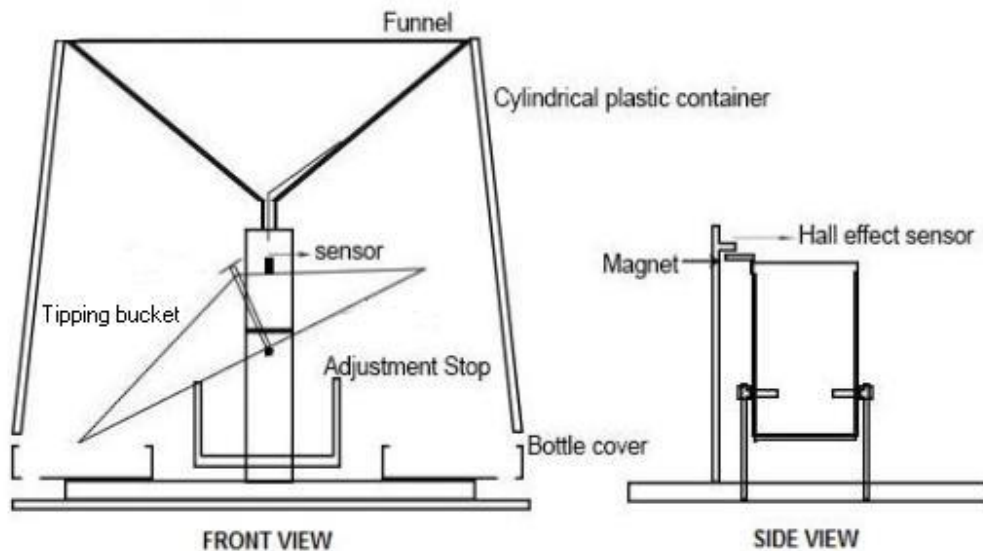


Figure 5: Schematic representation of a tipping bucket type rain gauge (Lopez & Villaruz, 2015, modified).

Other less used rain gauges are capacitance rain gauges and drop-counting gauges. The former is used on buoys in a project in the Pacific and Atlantic oceans, the latter was developed to estimate the instantaneous rainfall rate. Also, non-collecting rain gauges exist such as optical rain gauges that measure precipitation directly as it falls through an infrared beam, precipitation detectors that do not measure the amount of precipitation but only if rain or snow is falling as well as disdrometers that measure individual rain drops (Strangeways, 2006).

2.2.2 Uncertainties and errors in the measurement of precipitation

There are several factors that can influence the correct measurement of precipitation using the above-mentioned precipitation gauges. Initial errors can occur through choosing a wrong sized precipitation gauge, made from material that is not ideal as well as from errors due to incorrect installation. The size of the collector must be small enough to provide accurate readings of small precipitation events and big enough to avoid overflowing during heavier rain. The material of the rain collector should not hold water extensively because all water that holds to surfaces instead of flowing into the collector bottle is lost due to evaporation before being measured (Strangeways, 2006; WMO, 2018a). It should be avoided that any debris enters the funnel as it also holds water. Wire meshes are commonly installed above the funnel to keep debris from entering the rain gauge, but these also hold some water that then will be lost due to evaporation (Strangeways, 2006). Funnels should be shaped in such a way to avoid losing collected rain due to out-splash during heavy rain (Strangeways, 2006; WMO, 2018a). Increasing the steepness and depth of funnels helps prevent out-splash but also leads to an increased surface allowing evaporation losses to occur. Clearly, rain gauges should be installed on levelled ground to give correct measurements (Strangeways, 2006). Nevertheless, rain gauges should not be installed on hard, flat ground such as concrete to avoid in-splashes, but rather on short-cut grass or gravel (WMO, 2018a). Furthermore, choosing the correct site plays an important role in obtaining correct measurements. Ideally, rain gauges are not nearer to an object such as trees, buildings, or other instruments, than four times the height of the object (Strangeways, 2006). If that is not feasible at least twice the height is acceptable (Strangeways, 2006; WMO, 2018a). Regardless, often the recommended distance is not kept. The chosen site must also be representative of the surrounding area to obtain correct areal estimates from single-point measurements. Additionally, wind can have a large influence on

the accuracy of measurements of precipitation (Strangeways, 2006) as it might be the main reason for under-catching precipitation. Wind error can be minimized using natural wind shields like forest clearings (WMO, 2018a) or artificial wind shields on top of rain gauges. Also pit gauges which are buried in the ground or aerodynamical rain gauges can reduce wind effects (Strangeways, 2006). As weighing gauges can also be used in winter to measure solid precipitation, freezing rain or wet snow sticking to the funnel, hence, not reaching the bucket to be measured, adds some uncertainty to the measurement. In addition, timing errors may occur, or the weighing mechanism may be sensitive to temperature or wind. However, human reading errors and evaporation or wetting losses occurring at manual gauges might be reduced (WMO, 2018a). The performance of tipping bucket rain gauges is also affected by bearing friction and in case precipitation remains in a bucket before another precipitation event occurs that collected rain either evaporates or is assigned to the wrong time (Strangeways, 2006) (WMO, 2018a).

2.2.3 Precipitation measurements with radar

Radar was first developed for aviation in the 1940s and was soon used for precipitation measurements. The advantage of radar over rain gauges is that an areal estimate is obtained instead of a single-point measurement. Thus, each radar station can cover several thousand square kilometres. In addition, it is possible to obtain real time precipitation measurements even from remote areas (Strangeways, 2006). The operating principle of radar is as follows: an antenna emits microwaves in different inclined angles into the atmosphere; if the waves hit an object, such as raindrops, snow, or hail, they are reflected and registered by the dish of the antenna (DWD, n.d. a); a schematic representation of the operating principle can be seen in Figure 6. The dish rotates 360 degrees and can therefore detect precipitation in all directions. Due to the rotation, however, it is not a continuous measurement in any one direction. Thus, converting that instantaneous intensity to mean areal values is adding some uncertainty to the data (Strangeways, 2006). Moreover, if trees, buildings, or hills reflect the radar signal it could lead to overestimation of rainfall when raw radar data are not corrected for these so-called ground clutters (Dhiram & Wang, 2016). In order to prevent ground clutters, the antenna is not oriented completely horizontally, but at a slight upward angle. As the distance from the radar site increases, the radar beam is increasingly higher from the ground and consequently precipitation arriving at the ground is not measured (DWD, n.d. b). This also means uncertainty in the measurement of precipitation, as precipitation below the radar beam is not detected (Strangeways, 2006). The distance of precipitation can be determined from the return time of the signal and the strength of the signal provides information about the reflectivity of precipitation (DWD, n.d. a; Strangeways, 2006). The rainfall rate R in millimetre per hour can then be calculated from the radar reflectivity Z with the empirical equation:

$$Z = aR^b \quad (2)$$

The parameters (a) and (b) can have different values; the value of (a) depends on the type of precipitation (e.g., 140 for drizzle or 240 for heavy convective showers), (b) usually takes the value 1.6. Such a wide range of values for (a) poses some uncertainty for the calculation of precipitation intensities from reflectivity (Strangeways, 2006). One assumption for the calculation of the rainfall rate from reflectivity is that the intensity of precipitation increases with increasing reflectivity. However, reflectivity is greater for raindrops than for snowflakes and the biggest for melting snow. This increased reflectivity of melting snow is referred to as *bright band* (DWD, n.d. b). It might lead to an overestimation of the rain intensity while on the other hand drizzle is often underestimated. The bright band can cause differences between radar and rain gauge data of up to 100 % (Strangeways, 2006) and thus should be corrected (Dhiram

& Wang, 2016). Furthermore, it must be taken into account that heavy rain weakens the returned signal through absorption (Strangeways, 2006). While the frequently used Marshall-Palmer relation suggests a parameter (a) of 200 and a parameter (b) of 1.6 (AMS, 2017), some studies, that looked for optimal values in certain regions, determined values for the parameter (a) that were much smaller. For example, one study found that the optimal value for parameter (a) from June to October for the upper Ping River basin in Thailand is 74 (Mapiam & Sriwongsit, 2008), while another study found that rainstorms in Tripoli City, Libya are better described with the parameters $a = 116$ and $b = 1.87$ (Ali & Said, 2009). Hence, for the correct calculation of precipitation amounts, it is necessary to establish the optimal Z-R relationship for a respective region (Ramli & Tahir, 2011). The Z-R relationship also depends on the type of precipitation. The Marshall-Palmer relation is applicable for standard stratiform precipitation while for convective precipitation the standard parameter (a) takes the value 300 and parameter (b) takes the value 1.4 (Dhiram & Wang, 2016). Clearly, Z-R relations are dependent on the type of precipitation and prevailing weather situation, hence, automatic detection of the precipitation type can reduce the uncertainty regarding the correct value for the parameter (a). Another method to determine the correct value of (a) is to measure the variability between a few rain gauges. Hence, a good rain gauge network can enhance the accuracy of radar measurements while radar stations can supply information for a rain gauge network in inaccessible areas but are not precise enough to be used solely (Strangeways, 2006).

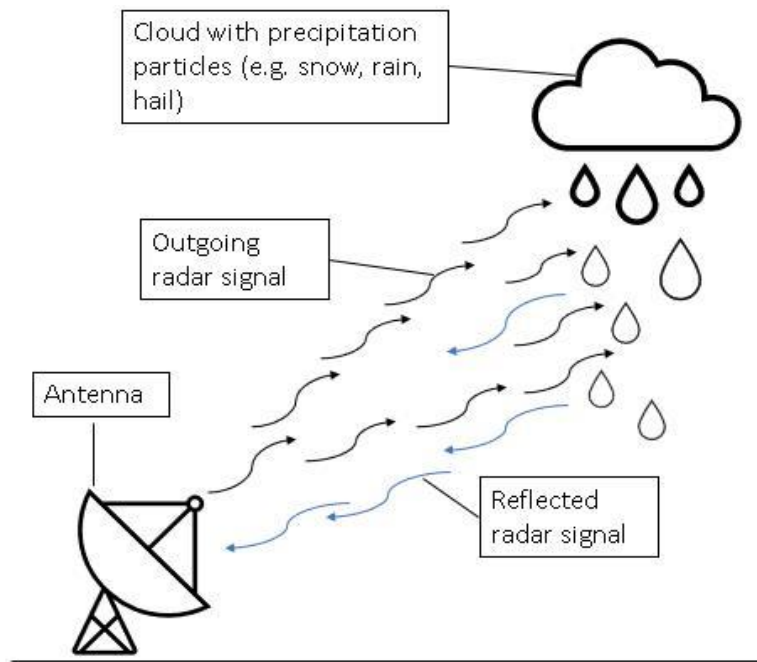


Figure 6: Schematic representation of the operating principle of a weather radar. Outgoing radar signals are reflected by precipitation and returned to the radar dish (own illustration).

2.2.4 Precipitation measurements with satellites

Precipitation was first estimated from satellite images in the 1970s. An advantage of satellites over ground-based measurements is that they can cover large areas although their field of view is dependent on their height in the orbit. But satellites do not measure precipitation directly, only electromagnetic radiation reflected from the atmosphere and the earth's surface (Strangeways, 2006; WMO, 2018b). Different satellites can register radiation of different wavelengths, from which three different principles of radiation measurements are derived. On the one hand, satellites can measure radiation in the visible and infrared range, as well as

passively measure microwaves that are naturally reflected into space from the Earth's surface. But some satellites can also actively emit microwaves and register the reflected signal, just as ground-based radars. Satellite measurements in the visible and infrared can be separated into three techniques: cloud indexing, bispectral method and life-history method (Strangeways, 2006). Cloud indexing looks at clouds from above and derives precipitation amounts from cloud-top temperature determined through infrared measurements. Objects at different temperatures produce different levels of infrared radiation, thus, allowing the satellite to convert the received signal into so-called brightness temperature (Strangeways, 2006; WMO, 2018b). On the other hand, in the visible spectrum, radiation is shown on satellite pictures just as brightness. As bright and cool clouds are associated with higher precipitation probability than cool and dull, or bright and warm clouds, combining information from the visible spectrum with infrared, as done by the bispectral method, can enhance infrared-only methods. Lastly, the life-history method observes the life cycle of clouds to predict precipitation. However, those methods work reliably only for convective precipitation of the tropics, for the mid- and high latitudes microwave measurements are more suitable (Strangeways, 2006). An advantage of microwaves over infrared and visible radiation is that they can travel through clouds until they encounter liquid or frozen particles from which they are reflected (Bührke, 2004; Strangeways, 2006). As with infrared, microwave signals can then be converted into brightness temperature. Algorithms are further needed to estimate precipitation from the observed radiation. To do so, they can either relate brightness temperature to ground-based measurements of rainfall from rain gauges or model physical processes of radiation, absorption and scattering by the ground and hydrometeors. Many different algorithms were developed over time, but there is no single algorithm performing well over all surfaces and in all conditions. Also, their accuracy varies with time and place (Strangeways, 2006). Generally, when satellite data are combined with rain gauge data it produces the best results (Bührke, 2004; Strangeways, 2006). The difficulty in deriving precipitation from passive radiation is because radiation arriving at the satellite is a mixture of ground radiation and radiation from hydrometeors (see Figure 7). Further, absorbed radiation by precipitation particles does not reach the satellite. In addition, the strength of the ground radiation varies depending on nature and condition of the surface, which makes it difficult to assign the different emission sources. At times, the strength of the ground radiation can even mask the radiation from the precipitation. If the algorithm fails to correct for variations in emissions, the received signal could be misinterpreted as rain, even though it has not rained (Strangeways, 2006).

Active microwave measurements with satellites have the same operating principle as ground-based radars. A difference is that satellites have a downward looking perspective resulting in three reflected signals instead of just one. First, the signal is reflected by precipitation particles, followed by an echo from the ground. The last echo comes from microwaves being scattered to the ground through hydrometeors and then returned to the satellite, also called mirror-image echo (see Figure 8). As with ground-based radars, the strength of the echo provides information about the reflectivity, thus, precipitation intensity. A second estimate of intensity is provided by the ground echo as the radar signal is weakened by traveling through precipitation. To estimate the attenuation through precipitation, a rain free echo is needed for comparison. Alternatively, a second frequency that is unaffected by precipitation can be used to measure the ground echo, although another frequency might interact differently with the ground than the frequency used for precipitation measurement. Uncertainties also arise through spatial variability which is bigger for land than for the sea (Strangeways, 2006). An advantage of active over passive sensing is that wavelengths are not determined by the natural object but can be chosen. Also, at least one radar in space is needed to calibrate passive microwave radiometers. In the future, however, the increasing demand for radio frequencies for telecommunications could lead to interference in the passive and active microwave measurement of weather satellites (WMO, 2018b).

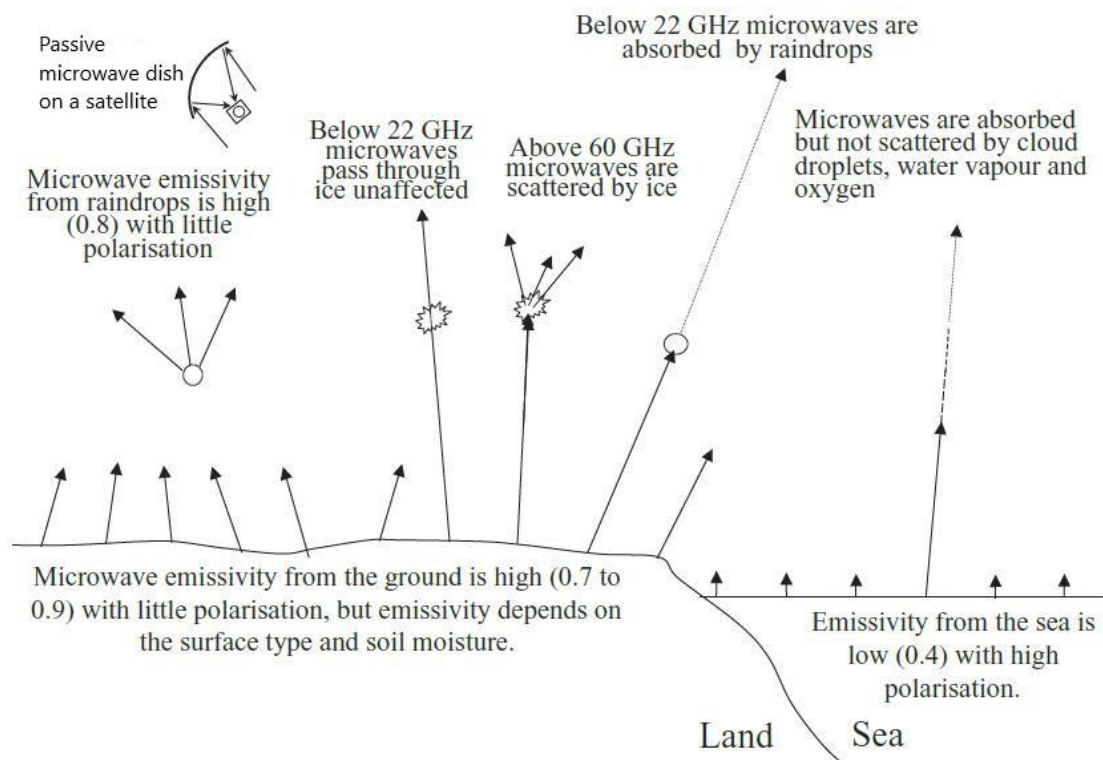


Figure 7: Passive microwave emissions from land, sea and hydrometeors being emitted, scattered or absorbed and eventually received by the satellite. Emissivity describes how effectively a surface can emit radiation (Strangeways, 2006, modified).

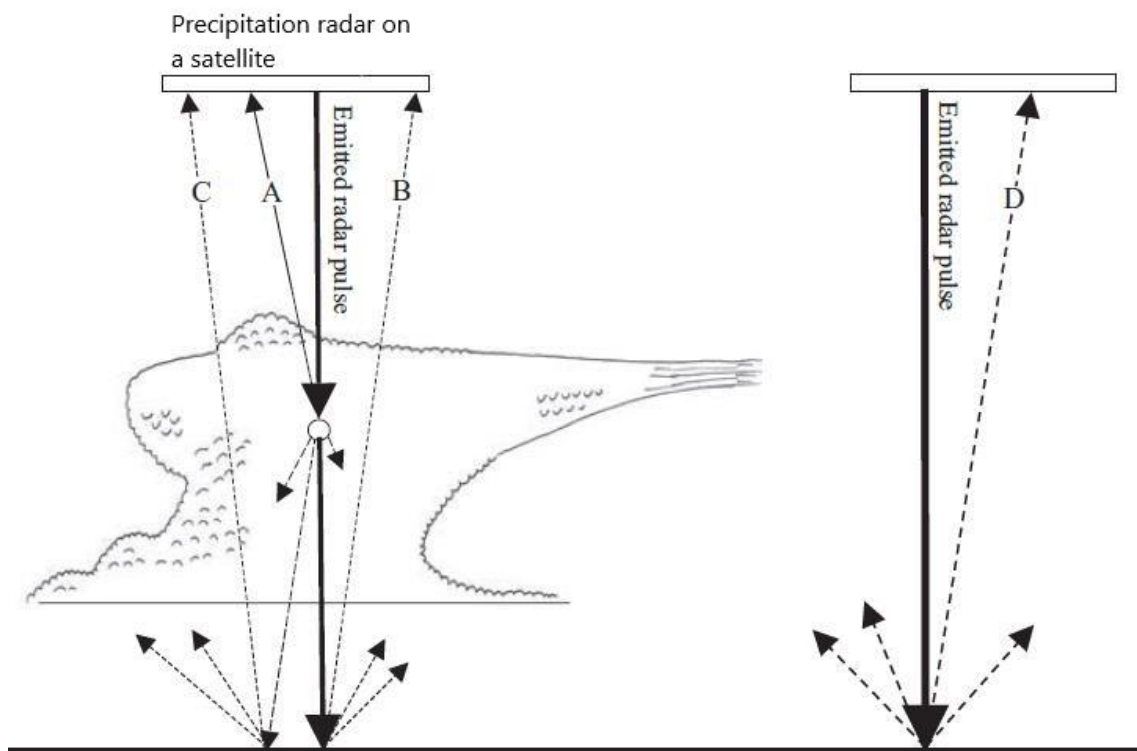


Figure 8: The operating principle of a precipitation satellite radar actively emitting microwaves, which produces three echos: reflected from (A) precipitation, (B) the ground, and (C) scattered by precipitation and reflected from the ground (mirror-image echo). (D) represents the strength of the echo through a precipitation free atmosphere and is for comparison with (B) to estimate how much the signal is attenuated by travelling through precipitation (Strangeways, 2006, modified).

2.2.5 Snow measurement

The uncertainties in snow measurement come from the fact that snow is more susceptible to wind effects and therefore ordinary rain gauges can only be used under certain circumstances or with additional measures such as wind shields. Manual rain gauges can be used at low wind speeds and if gauges are not buried in snow. Further, the snow must have melted to be able to measure the amount. For doing so, the rain gauge is usually heated with electricity or gas. But heating might also lead to evaporation losses. Recording gauges such as weighing, tipping, or syphoning gauges can be used under the same conditions as manual gauges if snow melts naturally and the measuring mechanism does not freeze. To prevent this, internal heaters can be used. Yet, it is important to note that the recorded times will be the times of melting not times of falling. Only weighing gauges without a funnel can directly collect and measure snow as it falls. However, even with those larger snowfall might be difficult to measure due to limited capacity. Many of the above-mentioned problems can be avoided with optical gauges since they do not catch and therefore do not have to melt snow, however, the water content of snowflakes cannot be determined as precisely as for raindrops due to the broad variety of size and density of snowflakes. Thus, estimating snow intensity from light signal is also subject to uncertainties (Strangeways, 2006). According to the WMO (2018c) there are currently no accepted automated methods to measure the depth of snowfall, referring to the amount of snow fallen in a certain period. Manual techniques include using an artificial surface of known size (called snowboard) that is placed on the ground or on previously fallen snow. Snowfall can then accumulate undisturbed and is measured with a ruler after some time, mostly 24h. The procedure is repeated placing the snowboard on the existing snowpack. However, spindrift or melting might interfere with correct measurements.

Probably the best and most accurate method for estimating the amount of snow is to cut sections of fallen snow with an inverted rain gauge funnel by pressing it into the snow until it reaches the ground. The snow in the funnel is then melted and measured. If snow depth is more than the size of the funnel the procedure can be repeated in multiple steps by digging a hole into the snowpack and then using a metal or wooden sheet to cut sections until the ground is reached (Strangeways, 2006; WMO, 2018c). One disadvantage to this method might be the necessity of an observer who takes the samples whenever snow has fallen. Also, the site where the sample is taken should be representative of the area. Otherwise, multiple samples have to be taken (Strangeways, 2006).

Other methods include measuring snow depth with a graduated pole that is fixed to the ground (Strangeways, 2006) or inserted manually before each measurement (WMO, 2018c) and read at intervals, or with an automatic level sensor using ultrasonic echo systems. However, readings can be influenced by spindrift or falling snow as well as air temperature (Strangeways, 2006; WMO, 2018c). Moreover, without the knowledge of the snow's density, water content cannot be deduced from depth. Snow can also be weighed with electronic pressure sensors or float-operated level recorders, so-called "snow pillows" (Strangeways, 2006) which are probably the most frequently used automatic method to measure the water equivalent of snow cover (WMO, 2018c). Over time however, the structure of the snowpack may change, which means that the entire weight may no longer be on the snow pillow and thus be distorting the measurement. Snowmelt lysimeters can measure water that has melted and flows through the snowpack, but timing nor the correct amount of snowfall can be determined with such devices due to evaporation or spindrift. The collected melt water is led to a container and measured manually or automatically by a tipping bucket. As water does not flow fully vertically through the snowpack but chooses the way of least resistance, samples of small lysimeters might not be fully representative (Strangeways, 2006).

Similar to rainfall measurements with radar, the amount of snowfall can also be estimated with the empirical equation mentioned in the radar measurement chapter, but with adjusting

parameter (a) to much larger values (e.g., 540 for dry snow or 2100 for wet snow) (Strangeways, 2006). Yet, looking at three specific events of winter precipitation in the Austrian mountains, Teschl et al. (2005) found that dry snowflakes, ice pellets and rimed graupel are best described by the parameter (a) of 2009, 229 and 1060, respectively. The parameter (a) is in that case part of the equation for the equivalent radar reflectivity factor Z_e , which is to be used when the composition and size of the reflecting particles is not known (AMS, 2012). This illustrates that the uncertainty of measurement is larger for snowfall than for rainfall due to varying water content of differently sized and dense snowflakes. Furthermore, snowfall measurements with radar cannot be calibrated with gauges on the ground in real time due to difficulties of obtaining reliable in-time measurements with conventional gauges as discussed above. The option remaining is to assess the performance of radar measurements in retrospect after the snow has fallen and consequently improve the algorithm applied (Strangeways, 2006).

2.3 Study area

The focus of this thesis is the Greater Vienna region. Vienna is the capital and one of nine states of Austria. It has 1.9 million inhabitants (Statistik Austria, 2021) and extends between 48° 07' 06"N to 48° 19' 23"N and 16° 10' 58"E to 16° 34' 43"E in the northeast of the country, surrounded by the state of Lower Austria. Its altitude ranges from 151 m a.s.l. to 543 m a.s.l. (Stadt Wien, 2019). The climate of Vienna and the surrounding region is sometimes described as Pannonian (Seibert, et al., 2007) and is known to be a particularly dry climate in the Alpine region (Isotta, et al., 2014). Station Hohe Warte is considered as a representative site for East-Austrian climate, receiving on average 620 mm of precipitation annually and maximum 84 mm per day (Formayer & Fritz, 2017). Besides Vienna, the study area also includes stations in Lower Austria, some directly adjacent to Vienna, others located more in the countryside (see Figure 9 and Figure 10). Stations in Lower Austria include the stations Krems, Stockerau, Gross-Enzersdorf and Brunn am Gebirge. Station Krems is located in Krems an der Donau, a town at the Danubian river with 25.000 inhabitants (Statistik Austria, 2020), approximately 60 km westwards of the city of Vienna. The mean annual precipitation sum determined over a period of 30 years (spanning 1981 to 2010) is 551 mm. A similar mean annual precipitation sum over the same period was determined at station Gross-Enzersdorf with 516 mm (ZAMG, s.a. a). The station is located in Gross-Enzersdorf, a municipality with 11.600 inhabitants (Statistik Austria, 2020) 14 km eastwards of the city centre of Vienna, but in fact only 1,5 km from the Viennese state border. The stations Stockerau and Brunn am Gebirge have not been established for a sufficiently long period, thus, to date no long-term precipitation averages exist. Station Stockerau can be found in the city of Stockerau, a small town with around 16.800 inhabitants (Statistik Austria, 2020) about 25 km northwest of the city of Vienna. The station Brunn am Gebirge is located in Brunn am Gebirge, a market township with around 12.000 inhabitants (Statistik Austria, 2020) 14 km southwest of the city centre and about 3 km from the state border of Vienna. Stations were chosen based on their location as well as the time period for which they offer data. In total, data of ten stations are analysed for this thesis which are marked in Figure 10 and found in Table 1.

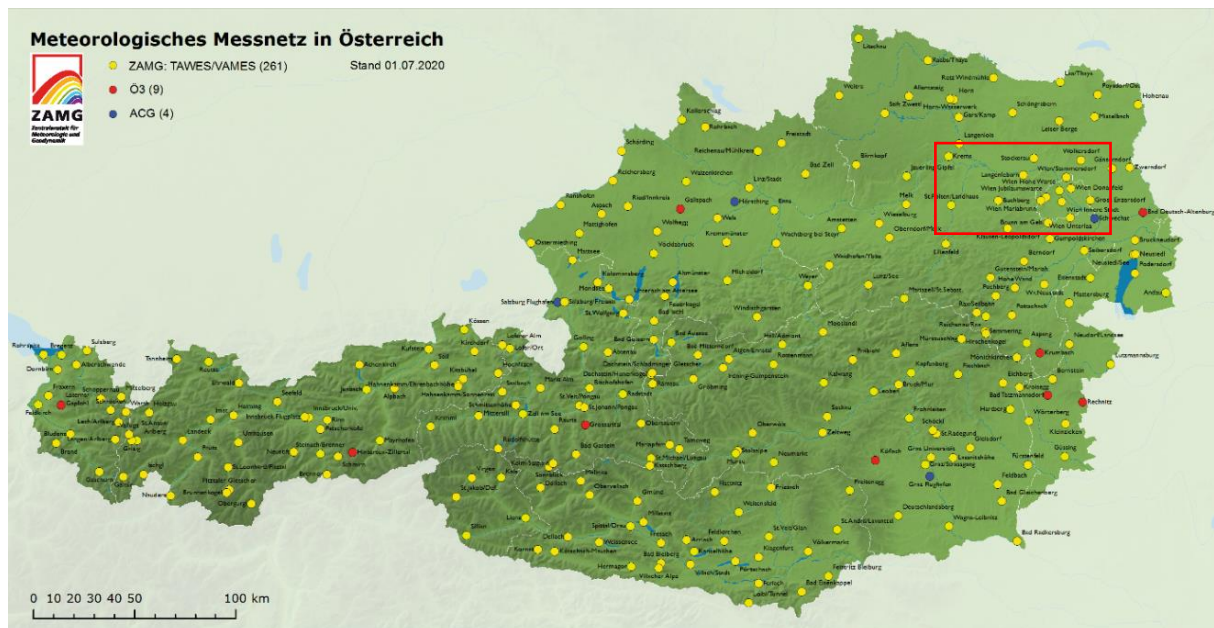


Figure 9: Meteorological measurement network of the ZAMG in Austria, red rectangle representing the study area (ZAMG s.a. b, modified).



Figure 10: Stations used in thesis marked with red crosses (ZAMG s.a. b, modified).

Table 1: Stations in the study area and their geographical characteristics.

Station	Metres a.s.l.	Latitude	Longitude
Wien-Innere Stadt	177	48.19833333°	16.36694444°
Wien-Hohe Warte	198	48.24861111°	16.35638889°
Gross-Enzersdorf	154	48.19972222°	16.55916667°
Krenns	202	48.41861111°	15.62222222°
Wien-Donauefeld	160	48.25722222°	16.43138889°
Wien-Mariabrunn	225	48.20694444°	16.22944444°
Stockerau	203	48.39694444°	16.1925°
Wien-Unterlaa	200	48.125°	16.41944444°
Brunn am Gebirge	291	48.10694444°	16.27°
Wien-Stammersdorf	191	48.30583333°	16.40555556°

3 Methods

The following section describes which sensors are used by ZAMG to collect precipitation data used in this thesis. Further, how data are processed before being made public and how data are stored and delivered to the end-user.

3.1 Data collection

The ZAMG station network covers the whole of Austria across all altitudes and climate zones (see Figure 9). It comprises over 260 measurement stations, most of which are partially automated TAWES stations where data are recorded every 10 minutes. At about 65 stations, in addition to the automatic measurements, additional observations are recorded daily by supervisors according to the SYNOP key at 6 a.m. and 6 p.m. UTC (ZAMG, s.a. b). The SYNOP key is a globally applicable key proposed by the World Meteorological Organization to report surface observations (WMO, 2011). At about three quarters of these stations, additional observations are recorded by staff on climate sheets and transmitted to ZAMG monthly. Observations include type of cloud cover, lower limit of cloud cover, visibility, and type of precipitation, in other words data that cannot be (optimally) recorded by the available instrumentation (ZAMG, s.a. b). Regarding the stations used in this thesis, automated precipitation sensors have been used starting in 1995. Before that, measurements were taken by hand for stations that existed before 1995 (see Table 2 and Table 3). Also, different types and models of precipitation gauges are used depending on the station, but the two main types are the tipping bucket rain gauge and the weight-operated rain gauge. Except at stations Brunn am Gebirge and Gross-Enzersdorf, weighing gauges are the type of sensor used today. The model of the weighing rain gauge used at most stations is the MPS TRWS 503.

3.2 Data processing

ZAMG checks its data in multiple steps to ensure high quality. First, directly after the precipitation is measured, data are subjected to an automated check to ensure that no large errors are passed on to the system or that no implausible values are published. The main check is then carried out using the software application Austria Quality Service (AQUAS). AQUAS is suitable for fully or partially automated weather stations and implausible values are either deleted or flagged in real time. The final check is carried out by an examiner. After data have undergone quality control, data sets are imported into the climate database and are available for research purposes. Since 1984 ZAMG started to examine historical data. Historical climate sheets are digitized and checked for completeness as well as internal, climatological, temporal, spatial and statistical consistency (ZAMG, s.a. c). Data that were provided for this thesis are checked for the years 2006-2020. For earlier years unchecked measurement data are available from the respective stations.

3.3 Data management

Precipitation measurements are saved as CSV files. Precipitation is measured in millimetre [mm]. For daily data, if there is no precipitation it is indicated with negative values (-1) whereas the value zero (0) indicates that precipitation was smaller than 0.1 (<0.1) and thus could not be measured. As this thesis focusses on extreme precipitation, negative values are set to 0 to avoid statistical impairments. Furthermore, 10-minute data are supplemented with a 'RRM'-

value, which is the sum of the rain detector showing how many minutes of the 10-minute measurement interval rain could be detected. Therefore, the RRM value lies between zero and ten. Quality flags are indicated with large negative values e.g., -99 or -999. Missing data are indicated with three minuses (“---”) in the CSV-files.

4 Empirical analysis

For the empirical analysis ten stations were chosen in the study area described under section 2.3. The subchapters below provide an overview of the data used, the implementation in R, as well as calculations and definitions used in this analysis.

4.1 Data

For the empirical analysis 10-minute precipitation data were requested from ZAMG. The received data files contained the station ID, time stamp, rain rate “RR” in mm of a 10-minute interval and the sum of the precipitation indicator “RRM”. However, 10-minute data were not available for each station for the same period, as can be seen in Table 2. Due to different availability of 10-minute precipitation data, the main study period was limited to 01.01.2006 - 31.12.2020. This is also the period where ZAMG provides internally checked data as described in Chapter 3.2. The reference period should, as far as possible, cover a 15-year period to ensure comparability with the main study period. At the same time, the largest possible number of measurements at each station should be used. Therefore, the years 1991-2005 were chosen as the reference period for sub-daily analyses, as both conditions are fulfilled best. Since, on the one hand, stations started recording 10-minute precipitation data at different times, but also due to missing values after the start of recording, there are different recording periods for individual stations in the respective periods. However, as missing values are considered in the calculation of hourly sums, calculated values are averaged for comparison over the time since establishment of the respective station. For most stations missing values comprise less than a month and only stations Innere Stadt and Gross-Enzersdorf have missing data in the reference period adding up to 1.5 years and 1.2 years, respectively. Because missing data of those stations amount to years they are subtracted from the number of years with available data when calculating averages. For the main study period, values are missing in total for less than one month for all stations, except for those stations that were only established after 2006.

Daily data were requested from ZAMG for analyses. As can be seen in Table 3 daily data are available for a longer time period for certain stations. Daily measurements represent 24-h sums which refer to a time frame from 7am to 7am (CET) of the following day. Regarding missing values of daily data, station Donauefeld has one missing value on 03.12.2020 for the main study period; however, the days before and after this missing value had little to no precipitation, thus, that missing value in particular is regarded less relevant for this thesis. The other stations have a complete set of daily measurements available from 2006 onward. Based on previous studies, a reference period from 1979-1993 is used to be able to compare the presented analysis for the study area to those findings. For that period, station Mariabrunn has multiple months with missing values, in total Mariabrunn is lacking precipitation measurements for 826 days. Station Innere Stadt has missing values in this period because it was only established in 1985, other stations have data available consistently. Naturally, those that were established after 1993 have no data available for the reference period (see Table 3).

Table 2: Availability of 10-minute rainfall data for the different stations in the study area. Stations are listed in time chronological order of the start of their records.

Station	Data available from
Innere Stadt	01.01.1985
Hohe Warte	05.11.1992
Gross-Enzersdorf	15.06.1993
Krems	07.05.1996
Donaufeld	01.07.1996
Mariabrunn	17.02.1997
Stockerau	04.06.1997
Unterlaa	09.09.1997
Brunn am Gebirge	25.09.2008
Stammersdorf	02.01.2009

Table 3: Availability of daily rainfall data for the different stations in the study area. Stations are listed in time chronological order of the start of their records.

Station	Data available from
Hohe Warte	01.09.1852
Gross-Enzersdorf	01.01.1936
Krems	01.01.1943
Mariabrunn	01.01.1951
Unterlaa	01.01.1966
Innere Stadt	01.01.1985
Donaufeld	01.07.1996
Stockerau	01.06.1997
Brunn am Gebirge	25.09.2008
Stammersdorf	10.12.2008

4.2 Implementation in R

For each station, 10- minute data came stored in multiple CSV files in two to three different formats. The formats differed in the way that some files had the timestamp separated in two columns for date and time, others had a single date and time column but had the date formatted in different ways. The CSV files were imported in R and brought to a uniform format. For a certain period, data were stored in a format without a decimal point and therefore records data ten times greater than actually measured. Thus, to bring these data to the same order of magnitude as the remaining files, these measurements were divided by ten. Some files contained overlapping dates, the duplicates were thus removed and finally all files were merged in one data frame by date and time. Moreover, because the 10-minute data came in UTC format, but daily data was measured in Central European wintertime throughout the year, the time zone of 10-minute data was converted to UTC+1. The final data frame contains a date and time column as well as the RR value and RRM value of each station. Data are quality controlled by ZAMG only from 2006 onwards. Therefore, before that year, there are sometimes precipitation measurements even if the rain detector has not registered any precipitation. Hence, by including these measurements, there is more precipitation obtained than listed in the daily data of ZAMG. Thus, if the sum of the 10-minute values is larger than the total daily rain depth provided by ZAMG for that day, that RR value is assumed to be a measurement error and set as NA.

4.3 Data analysis

The following paragraphs describe how thresholds for heavy and hourly precipitation as well as heavy precipitation events were determined. Further, a short introduction into extreme value statistics is provided.

4.3.1 Determining daily, hourly and event heavy precipitation

To determine a threshold for heavy precipitation days (HPDs) the 98th percentile of precipitation in the reference period, including wet and dry days, is calculated, analogously to Seibert et al. (2007). All days with precipitation above the calculated threshold are then classified as heavy precipitation days in the reference as well as the main study period. Other than daily data, which were provided by ZAMG, sub-daily values are calculated from available 10-minute precipitation data. Hourly precipitation can be calculated either using full hours on the clock or as rolling totals. Clock-based hourly precipitation is calculated by grouping precipitation by date and hour and then summing up 10-minute values (further called clock-time hour sum, or short CTHS). In contrast, hourly rolling totals are summed over six consecutive 10-minute values also going beyond clock hours with the function "rollapplyr". For initial comparative analyses and threshold calculations, only the maximum 1h value per day of rolling sums (further called maximum rolling sum per day, short MRSD) is extracted to avoid double-counting of values. For that same reason, the calculated rolling sums from 0:00-0:40 o'clock are excluded from the selection of MRSD. This is because the "rollapplyr" function sums up six values into the past e.g., the rolling hour sum of 0:30 a.m. is a sum of the values from 11:40 p.m. to 0:30 a.m., thus rolling sums between midnight and 00:40 a.m. contain values from the previous day and hence could be counted twice. The CTHS is used to analyse mean precipitation change, but to examine heavy precipitation, rolling totals are used as they can potentially represent larger hourly precipitation values. To determine heavy hourly precipitation, the 98th percentile of dry and wet hours of MRSD in the reference period is used to find a threshold to classify heavy hourly precipitation. The calculated threshold is then used to find multiple heavy precipitation hours per day, which might have been excluded when only choosing the maximum rolling sum per day. An additional minimum period of one hour between heavy precipitation sums ensures that no 10-min value is counted twice. In order to have a clear distinction from MRSD, those sums are referred to as total heavy hour sums (THS).

For the classification of rain events, a MIT of 20 minutes is used in this thesis whereby all events are counted as precipitation events that have no more than 10 consecutive minutes without rain within them. If there are more than 10 minutes without rain, events will be treated as two separate events. This approach is considered most suitable for heavy precipitation analyses because convective precipitation is known to be short-lived, often lasting less than two hours. Thus, a short MIT of 20 minutes is chosen to account for that kind of precipitation. Further, to classify heavy precipitation events, the 98th percentile of the mean event rain rate of all events – including dry periods - is calculated to be used as a threshold. It is important to make a distinction between event rain depth and event rain rate to make events of different durations comparable with each other.

4.3.2 Theory of extreme value statistics

"Extreme-value statistics, or statistics of extremes, is concerned with the occurrence and sizes of rare events, be they larger or smaller than usual" (Davison, 2005, p. 1877). Initially being developed to study flood levels (Charras-Garrido & Lezaud, 2013), it has since been used in many different areas, from finance to environmental sciences (Davison, 2005; Gilli & K llezi, 2006; Charras-Garrido & Lezaud, 2013; Gomes & Guillou, 2015). The aim is to predict statistical probabilities of events that have not or hardly occurred before (Gilli & K llezi, 2006; Charras-Garrido & Lezaud, 2013), so-called extreme values, hence extreme value theory, to avoid negative impacts of such events (Gomes & Guillou, 2015). Extreme values can be identified using one of two approaches. The traditional and most common way is the so-called Block-Maxima-Approach where the maximum value within a continuous time interval, e.g., days, months, or years, is chosen (Davison, 2005; Gilli & K llezi, 2006; Gomes & Guillou,

2015). Those block maxima (M_n) are selected from a sample of independent and identically distributed random variables (X_1, \dots, X_n) with a common cumulative distribution function (cdf) (Davison, 2005; Gilli & K llezi, 2006; Charras-Garrido & Lezaud, 2013; Gomes & Guillou, 2015). The issue that the cdf is unknown and hard to estimate (Charras-Garrido & Lezaud, 2013) is solved by the Fisher-Tippett-Gnedenko Theorem which says that if a limit exists for maxima, the cdf of M_n approximates to one of the following three distributions (Davison, 2005):

$$\text{Gumbel: } F(x) = \exp[-e^{-x}], \quad -\infty < x < \infty,$$

$$\text{Fr chet: } F(x) = \begin{cases} 0, & x \leq 0, \\ \exp(-x^{-\alpha}), & x > 0, \alpha > 0, \end{cases} \quad (3)$$

$$\text{Weibull: } F(x) = \begin{cases} \exp[-(-x)^\alpha], & x < 0, \alpha > 0, \\ 1, & x \geq 0. \end{cases}$$

Nowadays the three distributions are combined into the generalized extreme-value (GEV) distribution

$$H_\xi(x) = \begin{cases} \exp^{-(1+\xi x)^{-1/\xi}} & \text{if } \xi \neq 0 \\ \exp^{-\exp^{-x}} & \text{if } \xi = 0 \end{cases} \quad (4)$$

with values of x for which $1 + \xi x > 0$ (Gilli & K llezi, 2006). The parameter ξ is called the extreme value index (Charras-Garrido & Lezaud, 2013; Gomes & Guillou, 2015) or shape parameter (Davison, 2005) and characterizes the GEV. The GEV can be obtained when the distribution is known by setting $\xi = \alpha^{-1}$ (Fr chet), $\xi = -\alpha^{-1}$ (Weibull) or $\xi = 0$ (Gumbel) as the limiting case. As in practice the distribution is not known the following parameter specifications of the GEV are used:

$$H_{\xi,\sigma,\mu}(x) = H_\xi\left(\frac{x-\mu}{\sigma}\right) \quad x \in \mathcal{D}, \mathcal{D} = \begin{cases}]-\infty, \mu - \frac{\sigma}{\xi}[& \xi < 0 \\]-\infty, \infty[& \xi = 0 \\]\mu - \frac{\sigma}{\xi}, \infty[& \xi > 0 \end{cases} \quad (5)$$

Equation (5) represents the GEV of unnormalized maxima, with μ and σ as the location and scale parameter while equation (4) represents the GEV of normalized extrema. We recall that the aim of extreme value analysis is to predict the probabilities of extreme values, so the so-called $1/p$ -year return level is of interest. $1/p$ is the return period while the return level corresponds to the quantiles of the estimated GEV and is obtained using estimates of the shape, location, and scale parameters (Gilli & K llezi, 2006):

$$\hat{R}^k = \begin{cases} \hat{\mu} - \frac{\hat{\sigma}}{\hat{\xi}} \left(1 - \left(-\log \left(1 - \frac{1}{k} \right) \right)^{-\hat{\xi}} \right) & \hat{\xi} \neq 0 \\ \hat{\mu} - \hat{\sigma} \log \left(-\log \left(1 - \frac{1}{k} \right) \right) & \hat{\xi} = 0 \end{cases} \quad (6)$$

Instead of using only maxima within a certain period to identify extreme values, the so-called peak-over-threshold (POT) method considers all values above a certain high threshold. The

advantage over the block-maximum approach is that data are used more efficiently and all values exceeding a certain threshold are considered in the analysis, i.e., no extreme values are dropped from the analysis just because a higher value is already present in a period/block (Davison, 2005; Gilli & K llezi, 2006; Charras-Garrido & Lezaud, 2013). The excess cdf F_u is defined as

$$F_u(y) = P(X - u \leq y \mid X > u), \quad 0 \leq y \leq x_F - u \quad (7)$$

where X is a random variable and u a sufficiently high threshold (Gomes & Guillou, 2015). Extreme value theory also provides a generalized distribution function for the POT method which is referred to as the generalized Pareto distribution (GP):

$$G_{\xi,\sigma}(y) = \begin{cases} 1 - \left(1 + \frac{\xi}{\sigma}y\right)^{-1/\xi} & \text{if } \xi \neq 0 \\ 1 - \exp^{-y/\sigma} & \text{if } \xi = 0 \end{cases} \quad (8)$$

.

for $y \in [0, (x_F - u)]$ if $\xi \geq 0$ and $y \in \left[0, -\frac{\sigma}{\xi}\right]$ if $\xi < 0$.

$y = x - u$ is referred to as exceedances or excess over the threshold and corresponds to the differences of the values x and the threshold u . σ represents the scaling parameter while ξ is the shape parameter or tail index (Gilli & K llezi, 2006; Gomes & Guillou, 2015).

In this thesis, the POT method is used to determine the 2- to 200-year return levels of daily heavy precipitation at each station. This way all heavy precipitation days are considered opposed to the Block-Maxima method which might consider days that are not classified as heavy if a year had particularly moderate precipitation rates. As a threshold for the POT analysis the determined value for heavy precipitation days in the study area, namely 15.0 mm, is used. This corresponds to the averaged value of the 98th percentile of precipitation of all dry and wet days in the reference period at all stations. This is compared to an extreme value analysis where the threshold corresponds to the 98th percentile for each individual station over the entire period in which records exist.

5 Results and discussion

The following chapter presents the results of the analysis regarding change in frequency, mean rain rates as well as seasonality of heavy precipitation. First, existing studies are reproduced for the study area, then analyses are presented for daily, hourly, and event-based precipitation. Before starting the analyses, the consistency of data was checked for the main study period by calculating daily sums with 10-minute data and comparing them with daily measurements provided by ZAMG. The assumption is that calculated sums should match daily totals provided by ZAMG. Daily sums are calculated from 7:10 am to 7:00 am CET of the following day. Most of the time the calculated sum matches the daily sum, but some discrepancies are identified. Inconsistencies can be partly attributed to missing 10-minute data, which also leads to 35 heavy precipitation days not occurring in the calculated sums. Further, there are differences of 0.1 mm on days with complete data, which emerge probably due to rounding errors. And finally, there are few days where the calculated total is exceeding the daily precipitation sum provided by ZAMG. This might be because of measurement/recording/reporting errors; however, the reason for that could not be certainly determined.

5.1 Reproduction of previous studies

In order to verify if results of previous studies generally still apply for the study, those studies were reproduced using the ten chosen stations in the study area. The studies reproduced were a study by Seibert et al. (2007) providing thresholds to identify heavy precipitation days in different regions in Austria, as well as a study by Blöschl et al. (2017) analysing changes in seasonal precipitation.

5.1.1 Thresholds to identify heavy precipitation days

As described in Chapter 2.1.1, the use of percentiles is common to identify heavy precipitation and previous studies used the 98th percentile to identify heavy precipitation days in Austria. For instance, Seibert et al. (2007) found that for the Eastern Region of Austria the 98th percentile of precipitation exceeded 13 mm/d for the period of 1979-1993, thus, days exceeding this threshold can be considered heavy precipitation days. When recalculating the 98th percentile for the period Seibert et al. (2007) used in their study, with station data used in this thesis, it results in about 15 mm/d, 2 mm/d more than the authors of the study found for the same period for the Eastern Region of Austria. Differences in the 98th percentile most likely can be attributed to different sizes of the studied regions (and thus stations included in the analysis). While this thesis focusses on the Greater Vienna region and the study area extends only a little beyond the borders of Vienna, the region defined as Eastern Austria in the study by Seibert et al. (2007) comprises a substantially larger area also including, for instance, the northern part of Burgenland. Moreover, when calculating the 98th percentile for the main study period from 2006-2020, even larger differences emerge. The 98th percentile across all stations for the main study period is about 18 mm/d indicating that there might have been a change either in frequency or mean rain rate of precipitation which led to an increase of precipitation in the upper percentiles. The 98th percentile for each station for both time periods is reported in Table 4. NA values represent stations which were not yet established until 1993, thus not having any precipitation data available (see also Table 3 in Chapter 4.1 about availability of data).

Table 4: 98th percentile values in [mm/d] of daily precipitation at each of the 10 stations for the main study period (2006-2020) as well as for the reference period used by Seibert et al. (2007). Note that (*) indicates stations where data are not available throughout the period. Value for the study area in parentheses shows the mean calculated with all stations including those that were not established in the reference period.

Station	1979-1993	2006-2020	Change in %
Innere Stadt	13.7*	19.7	44
Hohe Warte	15.6	18.5	19
Gross-Enzersdorf	14.2	16.5	16
Krems	14.6	16.6	13
Donaufeld	NA	(16.8)	NA
Mariabrunn	17.7*	20.9	18
Stockerau	NA	(18.2)	NA
Unterlaa	14.3	16.5	15
Brunn am Gebirge	NA	(18.8*)	NA
Stammersdorf	NA	(17.4*)	NA
Mean value of all stations	15.0	18.1 (18)	21

5.1.2 Seasonality of precipitation in study area

Blöschl et al. (2017) analyse hydrological baseline data and other research results to draw conclusions on climate change in Austria with regard to the impacts on water management as briefly described in Chapter 2.1.2. They compare changes in the period from 1996-2014 to a reference period from 1976-1995. Regarding changes of precipitation in different seasons, they report an increase of summer precipitation by 14 % in Austria, while the North-East of the country showed the most profound increase of up to over 40 %. Regional differences in the North-East are apparent and focussing on the study area, the increase of summer precipitation ranges between 20-40 %. A comparable increase to summer precipitation was observed in autumn (13 % for all of Austria); however, the most profound increase was found in the West in that season. Regarding winter precipitation, most of the country does not show a clear signal, but due to a significant decrease in the south, the overall trend for Austria is -7 %. Spring precipitation shows only a slight increase of 6 % for the whole country.

To reproduce seasonal precipitation changes in the study area, mean values of precipitation were calculated for different seasons and compared to the mean values calculated for the reference period. Only stations that existed and provided data in the reference period were used. Further, it should be noted that seasons were defined as standard meteorological seasons (DJF, MAM, JJA, SON). As can be seen in Table 5, calculations show that mean spring precipitation increased in the study area more than twice as much as observed for all of Austria. Mean summer precipitation increased only by about 24 %, while mean autumn precipitation shows only an increase of 10 % among the selected stations. It is noted that the statistical robustness of these changes is hard to assess given the averaging of the data over the study area and small number of stations considered as well as large interannual variability within the data sets. Similar to the analysis for all of Austria, mean winter precipitation decreased in the Greater Vienna region, but only by about 3 %. Additionally, calculations were performed for the main study period comparing seasonal means to the reference period from 1979-1993

which is used for the frequency analysis. Results show a similar seasonal change as the calculations using the reference period from Blöschl et al. (2017) (see Table 6).

Table 5: Seasonal mean precipitation (RR in [mm/d]) in the study area for the time periods used in Blöschl et al. (2018). Note that the mean value was calculated only with stations in the study area that existed in the reference period.

Season	Mean precipitation in [mm/d]		Change in %
	1974-1995	1996-2014	
Spring	1.5	1.7	16
Summer	2.1	2.6	24
Autumn	1.4	1.6	10
Winter	1.1	1.1	-3

Table 6: Seasonal mean precipitation (RR in [mm/d]) in the study area for the study period and reference period used in the frequency analysis. Note that the mean value in column three was calculated only with stations that existed in reference period.

Season	Mean precipitation in [mm/d]		Change in %	Mean precipitation in [mm/d] 2006-2020, all stations
	1979-1993	2006-2020		
Spring	1.5	1.8	17	1.7
Summer	2.1	2.5	21	2.6
Autumn	1.5	1.7	14	1.7
Winter	1.2	1.1	-3	1.1

5.2 Daily precipitation analysis

Mean daily precipitation, calculated including dry and wet days, increased across the study area by around 14 % compared to the reference period. For individual stations the increase varied between 3 – 35 % (see Table 7). Such an increase could result either from an increase in mean rainfall rate or from an increase in the number of precipitation days. However, the number of precipitation days increased only marginally from 137.5 wet days per year in 1979-1993 to 139.5 wet days in 2006-2020. Thus, the increase of overall daily mean precipitation must result from increased daily precipitation on wet days, which indeed increased by 13 % across the study area. For individual stations, changes are found with different robustness given that increases are ranging between 2 and 31 % (see Table 8).

Table 7: Mean daily precipitation [mm], calculated including wet and dry days, for the reference (1979-1993) and main study period (2006-2020). Note that (*) indicates stations where data are not available throughout the entire period. Value for the study area in parentheses shows the mean calculated with all stations including those that were not established in the reference period.

Station	1979-1993	2006-2020	Change in %
Innere Stadt	1.4*	1.9	35
Hohe Warte	1.7	1.9	15
Gross-Enzersdorf	1.4	1.6	14
Krems	1.4	1.5	3
Donaufeld	NA	(1.7)	NA
Mariabrunn	2.0*	2.2	10
Stockerau	NA	(1.7)	NA
Unterlaa	1.4	1.5	11
Brunn am Gebirge	NA	(2.0*)	NA
Stammersdorf	NA	(1.7*)	NA
Study area	1.6	1.8 (1.9)	14

Table 8: Mean precipitation of rainy days [mm] for the reference and main period at each station. Note that (*) indicates stations where data are not available throughout the entire period. Value for the study area in parentheses shows the mean calculated with all stations including those that were not established in the reference period.

Station	1979-1993	2006-2020	Change in %
Innere Stadt	3.9*	5.1	31
Hohe Warte	4.0	4.7	17
Gross-Enzersdorf	3.9	4.3	11
Krems	4.0	4.1	2
Donaufeld	NA	(4.4)	NA
Mariabrunn	4.8*	5.3	12
Stockerau	NA	(4.5)	NA
Unterlaa	4.2	4.3	3
Brunn am Gebirge	NA	(4.9*)	NA
Stammersdorf	NA	(4.5*)	NA
Study area	4.1	4.6 (5.1)	13

As described in Chapter 5.1.1, the calculated threshold for heavy precipitation days (HPDs) in Eastern Austria by Seibert et al. (2007) is not fully representative for the study area, so the value of 15.0 mm/d is used instead to identify HPDs in the further analysis. This value represents the 98th percentile of the chosen stations in the study area for the reference period and appears as most suitable to analyse changes in heavy precipitation days over time. The following paragraphs include analyses regarding daily heavy precipitation and describe changes in frequency, mean rain rate, seasonality as well as correlations of annual precipitation and daily heavy precipitation.

5.2.1 Frequency of daily heavy precipitation

As discussed earlier, the increase of daily rain depth for the 98th percentile could either be attributed to an increase in the frequency of heavy precipitation days or a rise in the mean daily rain rate. Indeed, calculations show that the number of days per year exceeding 15 mm of precipitation increased at every station in the study area for the main study period compared to the reference period. The annual average per station was calculated with the time frame of available data in each period. For instance, station Innere Stadt has only nine years of data for the reference period because it was only established in 1985, thus the identified days having more than 15 mm precipitation were averaged over nine years to make it comparable to the 15 year long main study period. Similarly, station Mariabrunn was averaged over 12.74 years due to missing values in the reference period. Stations Brunn am Gebirge and Stammersdorf were established after 2006, thus not having 15 years of data available. Those stations were averaged over 12.25 and 12 years, respectively. The increase among stations varies between 20-100 %, with an average for the study area of 43 % more HPDs than in the reference period. On average, there are now three HPDs per year more than in 1979-1993 (see Table 9). The biggest increase can be observed for station Innere Stadt, where the number of HPDs doubled in 2006-2020 compared to the two previous decades. This increase might be distorted to some degree because of lack of data for the whole reference period, nevertheless, also in absolute numbers station Innere Stadt is among the stations showing the most heavy precipitation days per year in recent years. It should be noted that the numbers reported are averages and the number of heavy precipitation days on a year-to-year basis can vary substantially. Generally, most stations experienced between 3-17 HPDs (3-13 days in the reference period) except station Mariabrunn, which had at least 9 days and a maximum of 23 HPDs in the main study period (8-17 in the reference period). Interested readers can find the plots regarding the distribution of heavy precipitation days over both periods in the supplements (see Appendix A, Figure A1 and Figure A2).

Table 9: Average number of days per year with precipitation >15mm for the reference period and main study period, as well as the increase expressed as a percentage. Note that () indicates stations where data are not available throughout the entire period. Value for the study area in parentheses shows the mean calculated with all stations including those that were not established in the reference period.*

Station	1979-1993	2006-2020	Change in %
Innere Stadt	6.1*	12.3	101
Hohe Warte	8.0	11.7	47
Gross-Enzersdorf	5.8	9.0	55
Krems	6.8	8.5	25
Donaufeld	NA	(9.4)	NA
Mariabrunn	11.1*	14.1	27
Stockerau	NA	(10.9)	NA
Unterlaa	7.1	8.5	20
Brunn am Gebirge	NA	(11.0*)	NA
Stammersdorf	NA	(9.6*)	NA
Study area	7.5	10.7 (10.5)	43

These findings also suggest that there must have been a decrease in the number of days with weak or moderate precipitation as the frequency of heavy precipitation days increased more

than the total number of precipitation days reported in Chapter 5.2. This would also explain the increase in rain depth of precipitation days as heavy precipitation as per its definition has a higher mean rain rate, thus increasing the overall rain depth.

5.2.2 Mean rain rate of daily heavy precipitation

Aside from increased frequency of heavy precipitation days, an increase in mean daily rain rate might also have contributed to a change in the 98th percentile of precipitation in the main study period. Indeed, the daily mean of heavy precipitation in the study area increased by 7 % from 22.9 mm/d in the reference period to 24.7 mm/d. However, the mean rain rate of the strongest precipitation days in both periods remained approximately the same. Daily mean rain rate in the main study period ranges from 15.0 mm/d as the chosen threshold for HPDs up to 116 mm/d due to an exceptionally heavy precipitation day at station Mariabrunn. However, for most stations the maximum daily mean rain rate does not exceed 75 mm/d, except station Mariabrunn which experienced three days with precipitation above 75 mm/d and station Innere Stadt which had one. Several stations have a maximum daily mean rain rate below 65 mm/d as can be seen in Figure 11. Figure 11 also shows a grouping among heavy precipitation days. Many HPDs seem to be grouped below 35 mm/d and only a few above. When extracting the heaviest 20 precipitation days, this grouping is confirmed. The mean daily rain rate of the 20 heaviest days is above 33 mm/d (see Figure 12) grouping all other heavy precipitation days below this threshold.

In the reference period, daily mean rain rate reaches 120 mm/d, which is higher than the maximum daily mean rain rate in the main study period (see Figure 13). This is due to one exceptionally heavy day at station Mariabrunn. Although, contrary to the main study period that station had no other day with a rain depth above 75 mm (see Figure 13 and Figure 11). Similar to the main study period, there were only four days with a rain depth bigger than 75 mm, found at three stations. Other than that, the mean rain rate seems to stay below 50 mm/d, except for a few outliers, and HPDs seem to be grouping below and above 25 mm/d, which is generally lower than in the main study period. This grouping is confirmed when plotting the strongest 20 heavy precipitation days (see Figure 14). For all stations but Innere Stadt those days have 25 mm or more of precipitation. This might be due to the limited amount of data for station Innere Stadt and thus fewer heavy precipitation days in general. Overall, the plot of the main study period seems to be denser than the plot of the reference period which displays the increased frequency of heavy precipitation days in recent years.

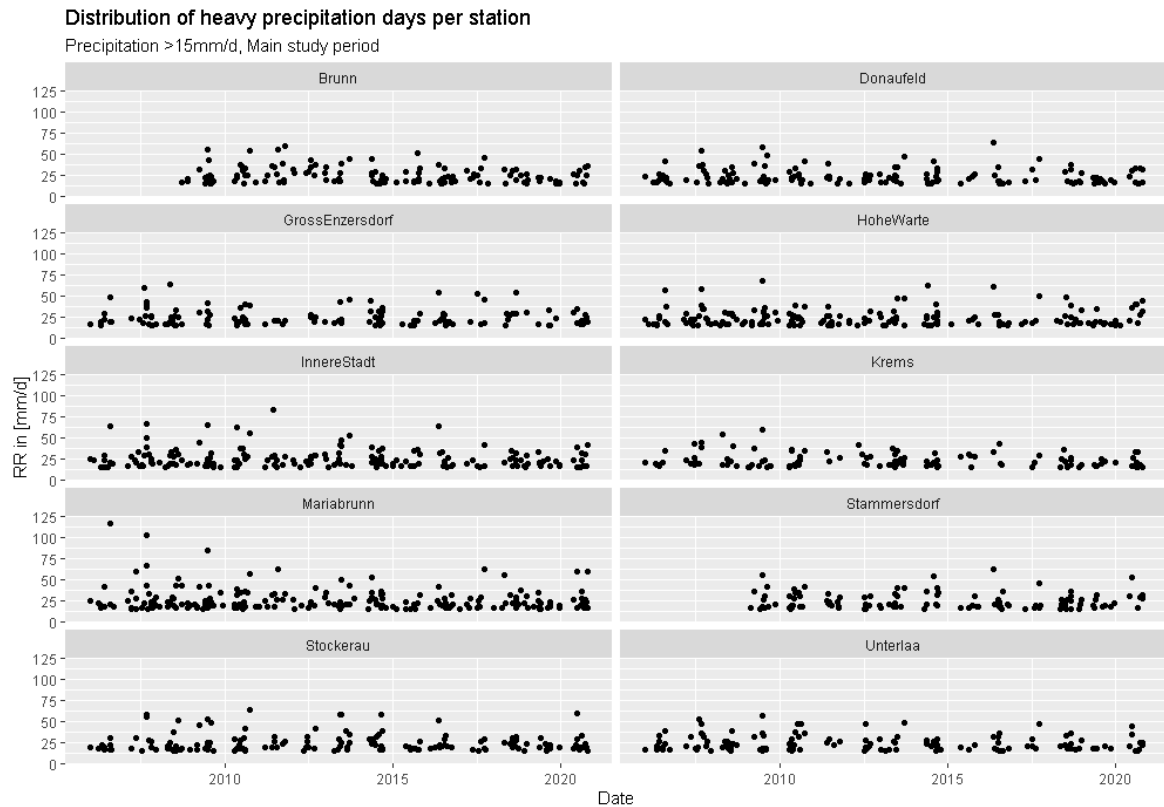


Figure 11: Occurrence of heavy precipitation days (>15mm/d) across all stations for 2006-2020.

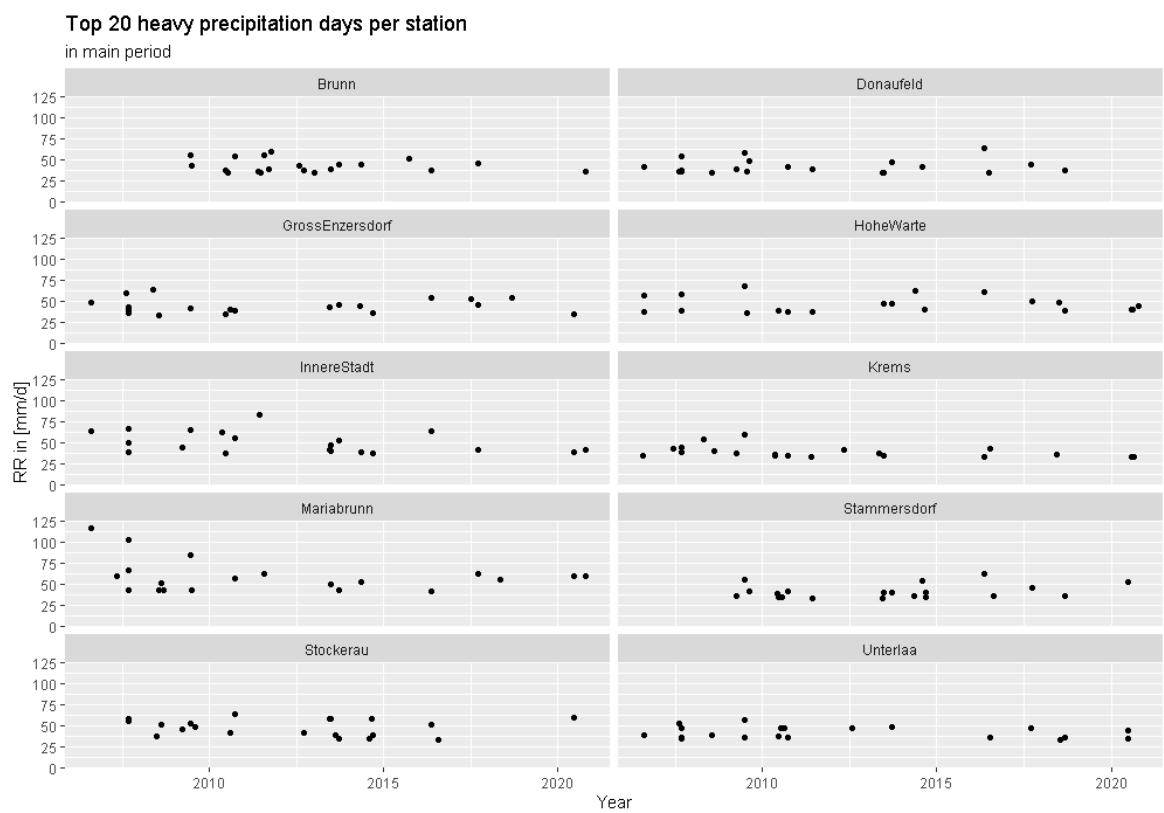


Figure 12: Strongest twenty heavy precipitation days at each station from 2006 - 2020, Brunn am Gebirge and Stammersdorf from 2008-2020.

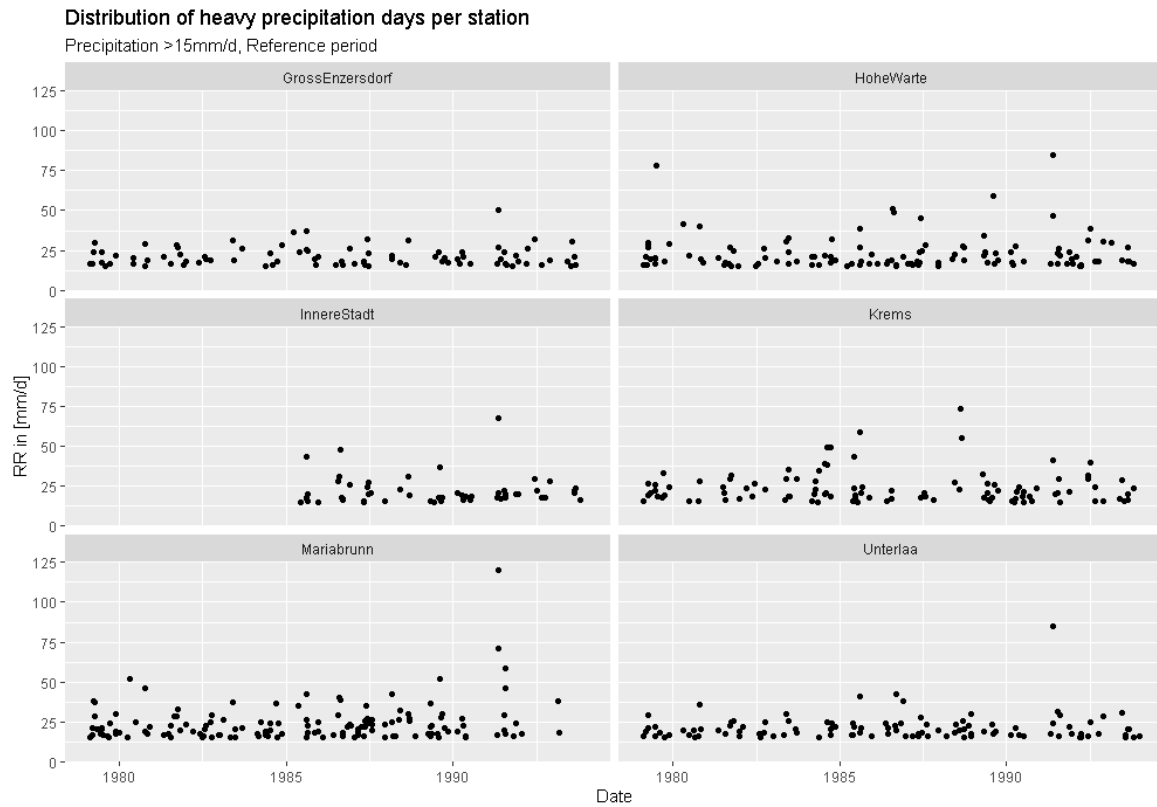


Figure 13: Occurrence of heavy precipitation days (>15mm/d) across all stations for 1979-1993.

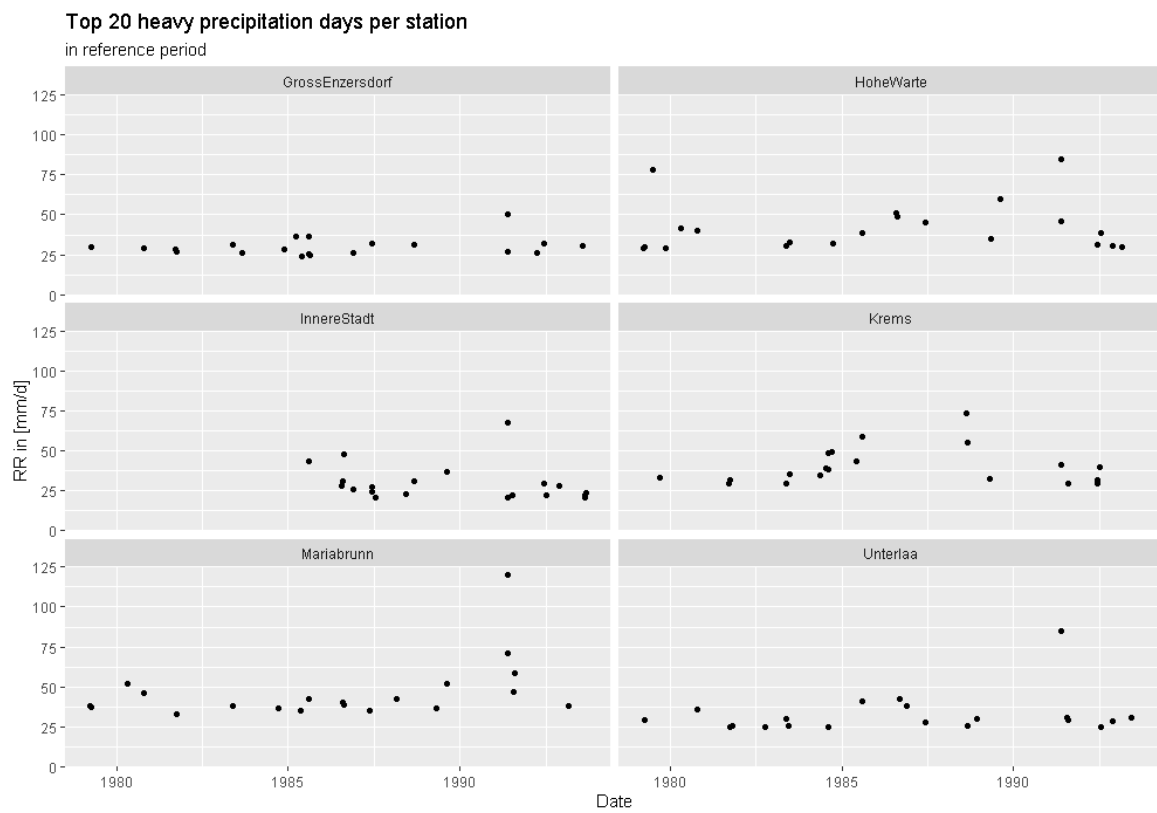


Figure 14: Strongest twenty heavy precipitation days at each station in the reference period from 1979-1993, Innere Stadt from 1985-1993.

Percentiles offer a good opportunity to look at values within a distribution. So instead of looking at the general distribution of heavy precipitation days in terms of mean rain rate or at the rain depth of the strongest 20 precipitation days, which are in the highest percentiles, we can look at how daily rain depth varies across days for both periods. Therefore, we look at the 25th, 50th and 75th percentile indicating the maximum daily rain depth of a quarter, half and three quarters of all HPDs. The observation that most days have less than 35 mm/d and only few have more is confirmed by the calculation of the 75th percentile, showing that 75 % of all HPDs have less than 31 mm of precipitation. Generally, comparing the percentiles of daily rain depth of both periods they did not change profoundly, but did increase for most stations in all percentiles. Only for station Krems the daily rain depth decreased for the 50th and 75th percentile (see Table 10).

Table 10: 25th, 50th and 75th percentile of precipitation (RR) in [mm/d] of heavy precipitation days (RR > 15mm/d) for the reference and main period of analysis. Note that () indicates stations where complete data are not available throughout the period.*

Station	1979-1993			2006-2020		
	0.25	0.5	0.75	0.25	0.5	0.75
Innere Stadt	16.8*	19.4*	22.8*	17.6	22.2	28.9
Hohe Warte	16.8	19.5	26.4	17.1	20.7	26.9
Gross-Enzersdorf	16.8	19.3	24.2	17.8	21.2	28.6
Krems	17.4	21	26.9	17.8	20.7	26.7
Donaufeld	NA	NA	NA	17.1	20.7	27.2
Mariabrunn	17.1*	20.6*	26.2*	17.8	21.2	28.3
Stockerau	NA	NA	NA	17.6	20.1	26.6
Unterlaa	16.5	19.3	23.3	17.8	21.5	29.2
Brunn am Gebirge	NA	NA	NA	17.7*	22.4*	30.6*
Stammersdorf	NA	NA	NA	17.8*	20.7*	29.9*

A profound increase can be observed at station Innere Stadt. While only 25 % of all HPDs in the reference period had precipitation over 22 mm/d, in 2006-2020 this is true for over 50 % of all heavy precipitation days. Although, the value for the reference period might be distorted to some extent due to missing data before 1985. However, a similar increase in the 75th percentile can also be observed at station Unterlaa and Gross-Enzersdorf, which have complete data coverage. According to findings of Ban et al. (2015) the magnitude of daily and sub-daily heavy precipitation is constrained by the availability of moisture, which might explain the small

changes in mean rain rate. However, if the Greater Vienna region continues to become wetter, the magnitude of heavy precipitation might change as well. Furthermore, increases could be observed despite both periods being within phases of high convective activity identified by Blöschl et al. (2017). Hence, the increase is not merely based on comparing periods with increased and decreased convective activity. Furthermore, daily heavy precipitation accumulates over 24 hours and thus is not so dependent on short-term convective activity. Further, an increase in all percentiles with similar convective activity in both periods could indicate that advective precipitation or the occurrence of frontal depressions has increased as well. Although there is low confidence that the occurrence of extratropical cyclones has changed recently (IPCC, 2021).

5.2.3 Seasonality of daily heavy precipitation

As expected, most HPDs in the study area occurred in summer whereas the winter season shows the smallest number of HPDs (see Appendix A, Figure A3 and Figure A4). These results are consistent with those of Villarini et al. (2011). This is physically most likely related to warmer temperatures and thus higher convective activity in the summer season. Interestingly, in the reference period the differences in the number of HPDs between summer and the other seasons were less pronounced while in the main study period the summer season clearly stands out. Moreover, an increase in the number of HPDs can be observed. While there were at most 3.5 HPDs on average in summer in the reference period, in the main study period some stations experienced up to 5.5 HPDs in summer. As discussed in section 5.1.2, seasonal precipitation changes for the study area differed slightly from the results obtained by Blöschl et al. (2017) for the whole eastern region of Austria. As results were similar for both reference periods, for consistency the reference period from 1979-1993 is further used to calculate seasonal differences in heavy precipitation.

While winters generally got drier (3 % decrease in mean winter precipitation), heavy winter precipitation increased by almost 9 % (see Table 6 for mean precipitation and Table 11 for mean heavy precipitation). Summers got wetter by 21 % whereas mean heavy summer precipitation increased by only 8 %. Contrary to mean precipitation, which had the largest increase in summer and spring, mean daily heavy precipitation increased the most in autumn and even slightly decreased in spring in the study area. If this larger amount of heavy precipitation in autumn happened mostly in September it could be associated with late summer precipitation as warm temperatures in September might favour convective precipitation. Indeed, most of the HPDs in Autumn occurred in September ($n = 209$) while October and November had only about half ($n = 97$) and one fifth ($n = 42$) the amount of HPDs as September in the main study period. Analysing the distribution of heavy precipitation days over the month of September, however, it is evenly distributed without any tendency to be concentrated early in the month (see Appendix A, Figure A5). Depending on the year, heavy precipitation days can even occur more often in autumn than in summer. For instance, in 2007, most stations experienced more heavy precipitation days in autumn than in summer (see Figure 15). 2007 was also a year with many heavy precipitation days at most stations (refer to Appendix A, Figure A1). However, 2009 for example, also a year with many heavy precipitation days, had few to no HPDs in autumn and most events occurred in summer. In fact, many stations such as Gross-Enzersdorf, Stockerau and Unterlaa had HPDs only in spring and summer and none in autumn and winter in 2009. It should be noted that the only heavy precipitation in autumn 2008 at station Brunn am Gebirge came from an incomplete yearly record; the station was established at the end of 2008, thus only recorded rain data for 3 months.

Table 11: Seasonal mean heavy precipitation ($RR > 15\text{mm/d}$) in $[\text{mm/d}]$ in the study area. Note that the mean value in column three was calculated only with stations that existed in reference period.

Season	Mean heavy precipitation		Change in %	Mean heavy precipitation 2006-2020, all stations
	1979-1993	2006-2020		
Spring	23.6	23.5	-0.2	23.4
Summer	23.4	25.2	8	25.0
Autumn	22.0	26.7	21	23.5
Winter	18.6	20.2	9	25.2

Seasonal percentage of heavy precipitation days per year

Precipitation $> 15\text{mm/d}$, Main study period

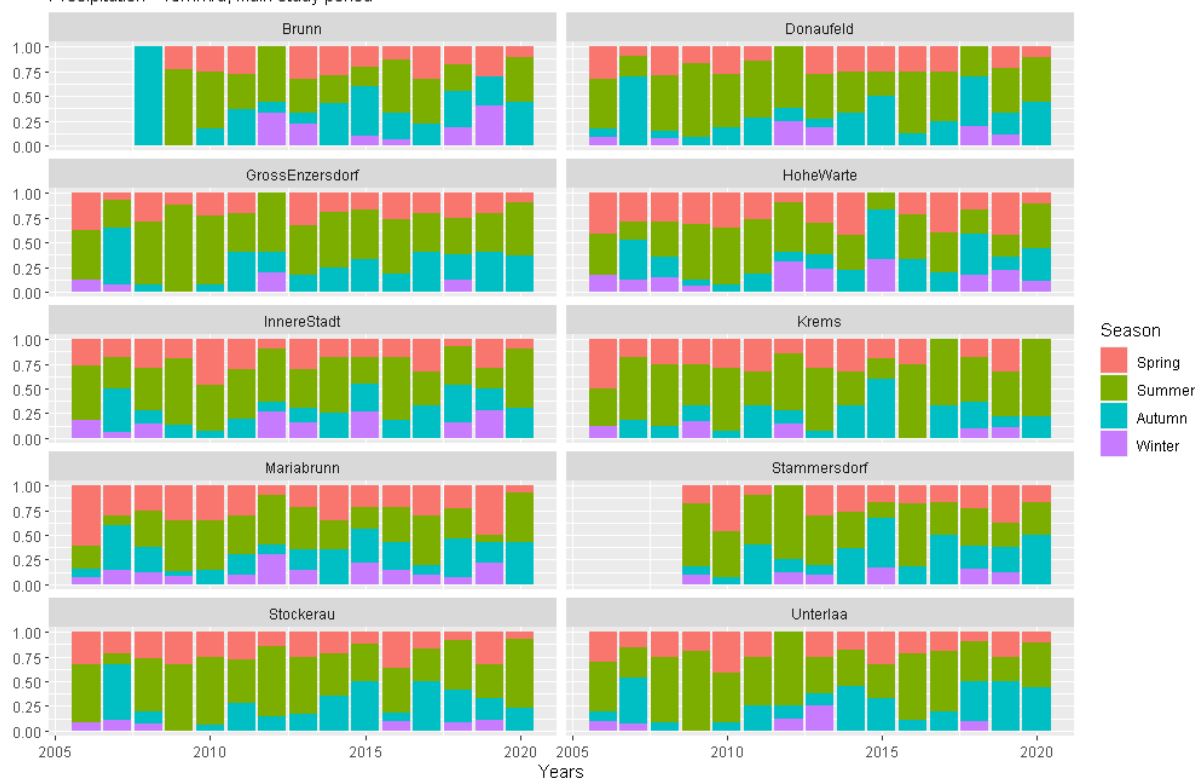


Figure 15: Seasonal fraction of heavy precipitation days per year in 2006-2020. Note, that station Brunn was only established at the end of 2008.

5.2.4 Correlation analysis of seasonal and annual heavy precipitation

The Pearson correlation method was carried out for the main study period from 2006-2020 to investigate how annual, spring and summer precipitation correlate with annual heavy precipitation. Spring and summer season were defined more generously with spring including the months January to April and summer including the months May to August. The sum of

annual as well as spring precipitation in mm was plotted against the sum of annual heavy precipitation in mm and the number of heavy precipitation days for the main study period. Only years with complete data were considered to calculate annual precipitation sums. Thus, the year 2008 was not considered for stations Brunn am Gebirge and Stammersdorf as those stations had less than 3 months of data in that year. The same was done with calculations for annual heavy precipitation and number of heavy precipitation days per year. Correlation is calculated for the study area; plots of each individual station can be found in Appendix A.3. Significance is tested at $\alpha = 0.05$.

Depths of annual precipitation and annual heavy precipitation were found to be strongly positively correlated, $R = 0.9$, $p < 0.001$ (see Figure 16). This result was expected as heavy precipitation as per its definition has high precipitation amounts, thus, years with a lot of heavy precipitation are naturally years with high annual precipitation sums. 81 % of the variability in annual precipitation sums can be explained by heavy precipitation ($R^2 = 0.81$). For the individual stations there is also significant and strong correlation of annual precipitation and annual heavy precipitation (see Appendix A, Figure A6). A similarly strong correlation was found for annual precipitation amounts and number of heavy precipitation days, $R = 0.84$, $p < 0.001$ (see Figure 17), which also might result from the definition of heavy precipitation days, since heavy precipitation days bring a higher amount of rain and, thus, the total annual precipitation increases with a higher number of such days. The number of heavy precipitation days explains about 70 % of the variability in annual precipitation ($R^2 = 0.71$). For the individual stations the correlation is similar, except for station Brunn am Gebirge, where it was non-significant, and station Donaufeld where the two variables were moderately correlated, $R = 0.67$, $p = 0.007$ (see Appendix A, Figure A7).

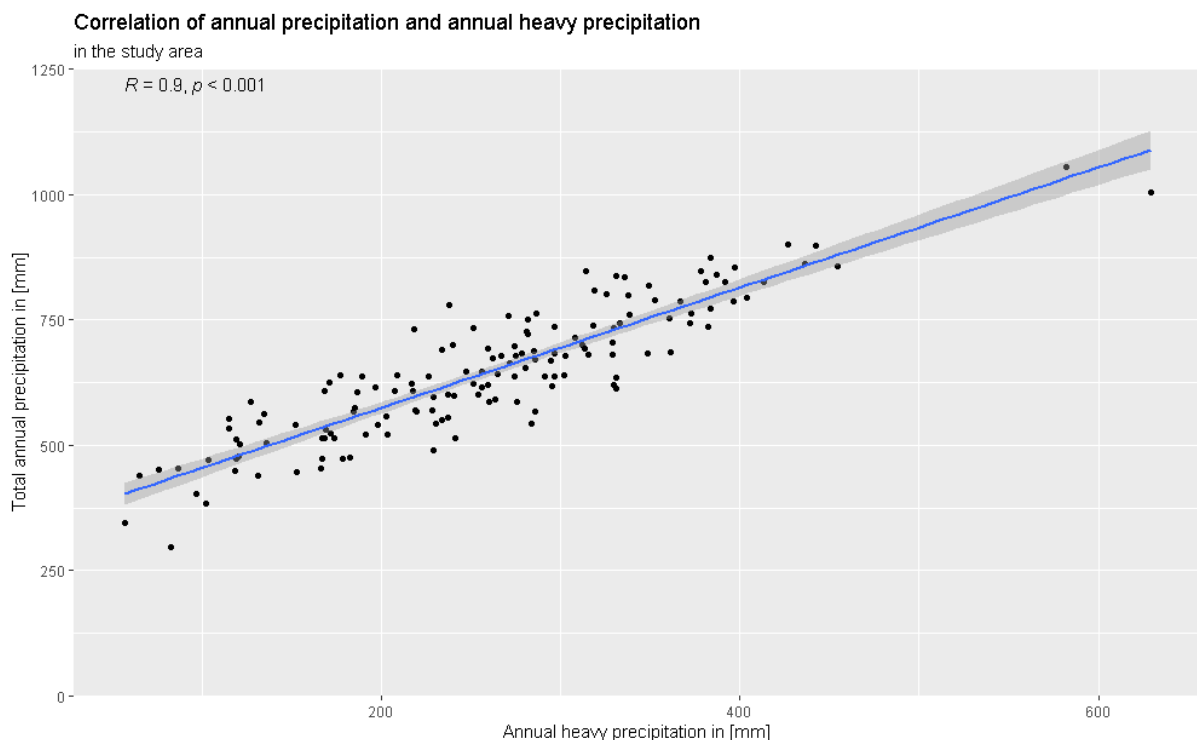


Figure 16: Correlation of total annual precipitation and annual heavy precipitation in mm in the study area. Significance accepted at $\alpha = 0.05$.

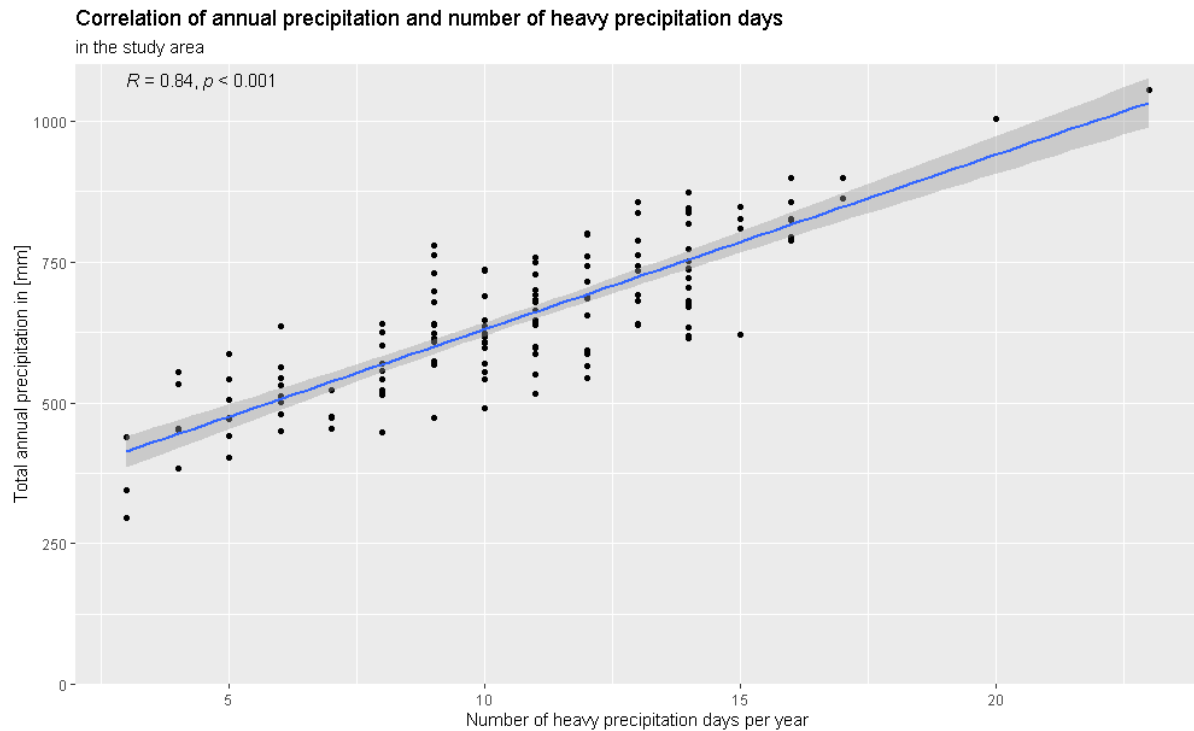


Figure 17: Correlation of total annual precipitation [mm] and annual number of heavy precipitation days in the study area. Significance accepted at $\alpha = 0.05$.

Further, it was investigated if wet springs correlate with heavy precipitation throughout the year. Interestingly, annual heavy precipitation and spring precipitation were found to be moderately correlated, $R = 0.52, p < 0.001$ (see Figure 18). 27 % of variability in annual heavy precipitation can be explained by spring precipitation ($R^2 = 0.27$). Looking at the individual stations, correlation was non-significant for all stations but Gross-Enzersdorf, $R = 0.54, p = 0.038$ (see Appendix A, Figure A8). As expected, spring precipitation and the number of heavy precipitation days also were found to be moderately correlated, $R = 0.51, p < 0.001$ (see Figure 19). For the individual stations, however, correlation was not significant (see Appendix A, Figure A9).

In addition, it was investigated how spring precipitation and summer precipitation correlate with heavy precipitation in summer. Spring precipitation and heavy summer precipitation were found to correlate weakly, $R = 0.36, p < 0.001$ (see Figure 20), for each individual station correlation was non-significant (see Appendix A, Figure A10). Thus, only 13 % of the variability in heavy summer precipitation can be explained as preconditioned by spring precipitation ($R^2 = 0.13$). Correlation of spring precipitation and the number of heavy precipitation days in summer was also found to be weak, $R = 0.32, p < 0.001$ (see Figure 21), and non-significant for individual stations (see Appendix A, Figure A11). There is a strong correlation between summer precipitation and heavy summer precipitation, $R = 0.93, p < 0.001$ (see Figure 22). Over 86 % of the variability in summer precipitation can be explained by heavy precipitation in summer ($R^2 = 0.865$), as more heavy precipitation in summer increases total summer precipitation. Although only 13 % of all precipitation days in summer were heavy precipitation days, the effect on total summer precipitation is significant as heavy precipitation days contribute 51 % of precipitation in terms of rain depth (see Table A1 in Appendix A). All stations show similarly strong correlation of those two variables (see Appendix A, Figure A12). Likewise, there is a strong correlation between annual summer precipitation and the number of days with heavy precipitation in summer, $R = 0.86, p < 0.001$ (see Figure 23). When analysed at the

individual station level, correlation is similarly strong or even stronger, such as, e.g., for station Gross-Enzersdorf, $R = 0.95$, $p < 0.001$ (see Appendix A, Figure A13).

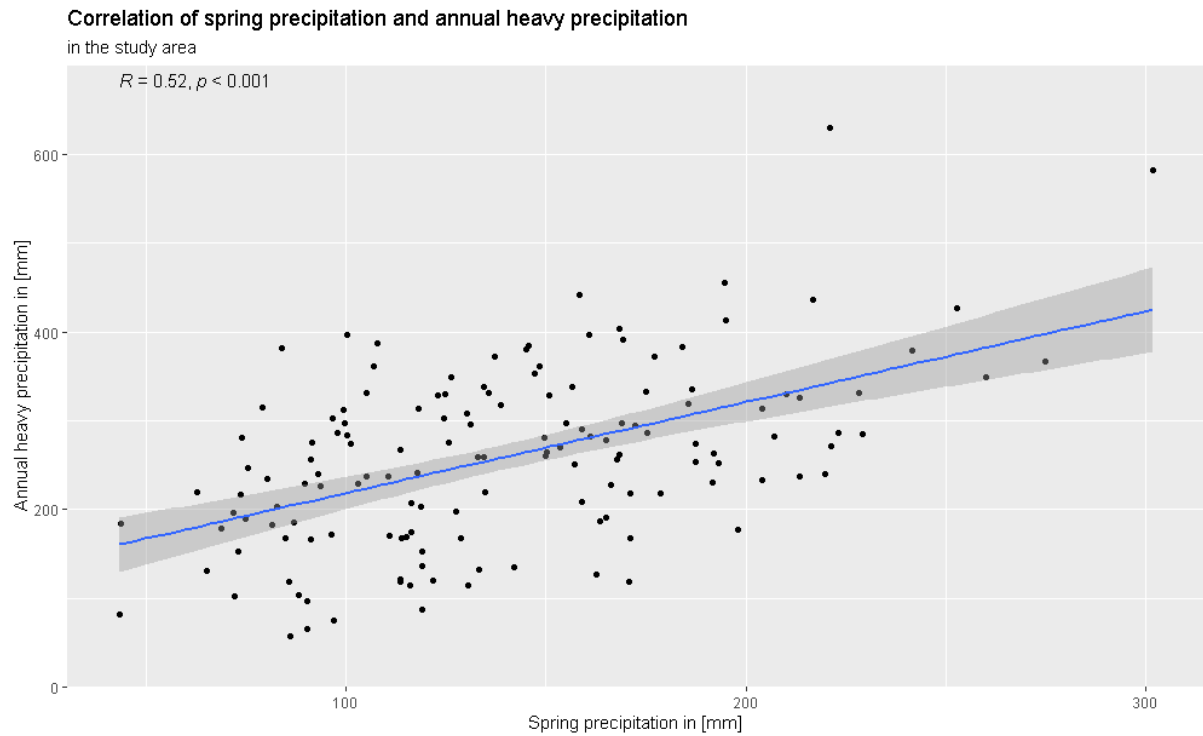


Figure 18: Correlation of spring precipitation and annual heavy precipitation in mm in the study area. Significance accepted at $\alpha = 0.05$.

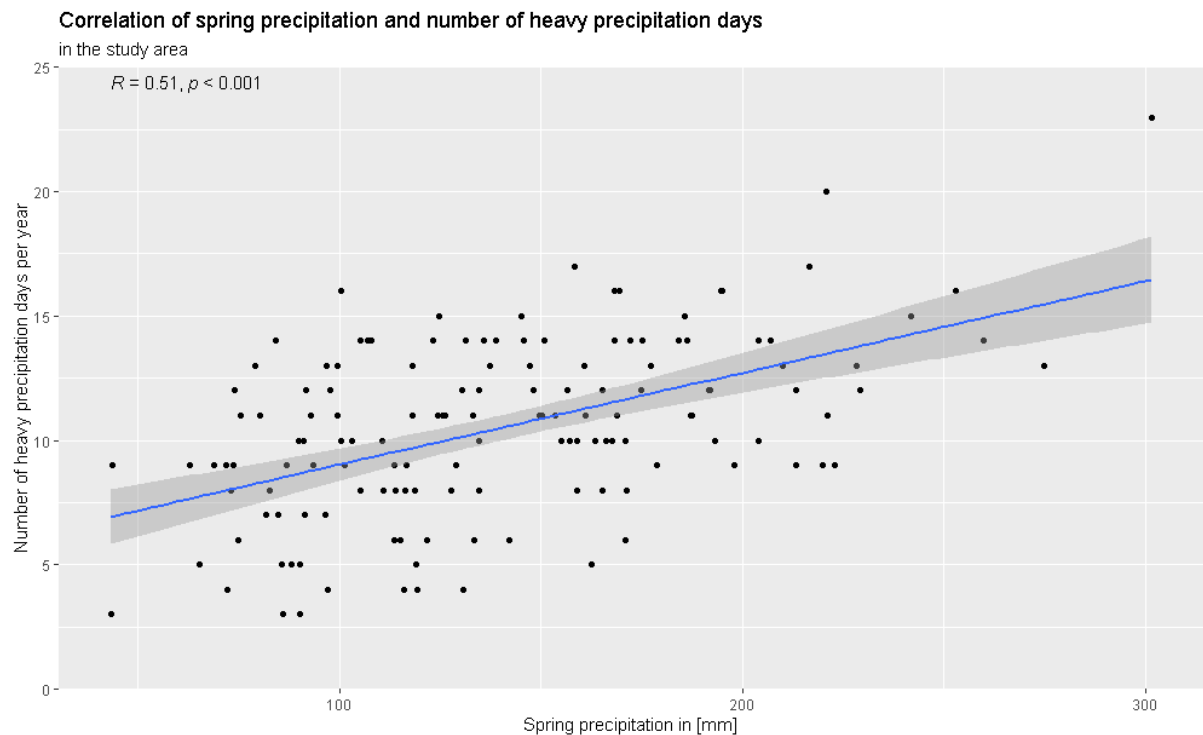


Figure 19: Correlation of spring precipitation [mm] and annual number of heavy precipitation days in the study area. Significance accepted at $\alpha = 0.05$.

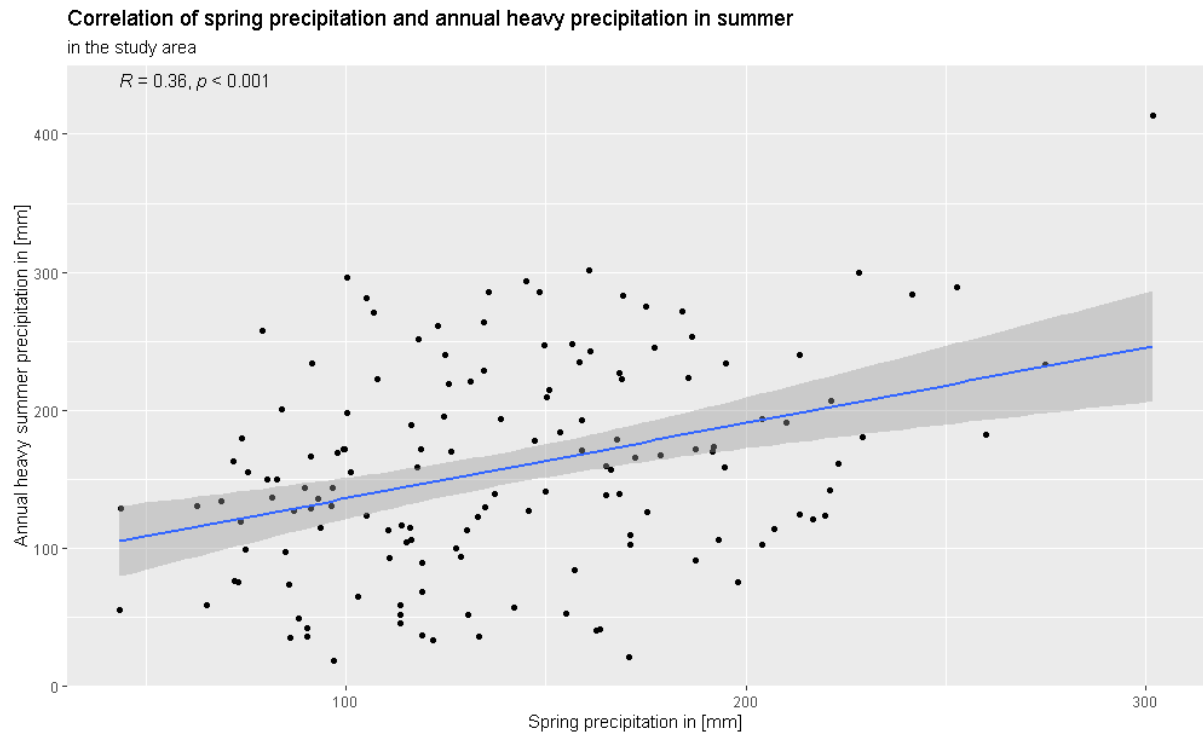


Figure 20: Correlation of spring precipitation and annual heavy summer precipitation in mm in the study area. Significance accepted at $\alpha = 0.05$.

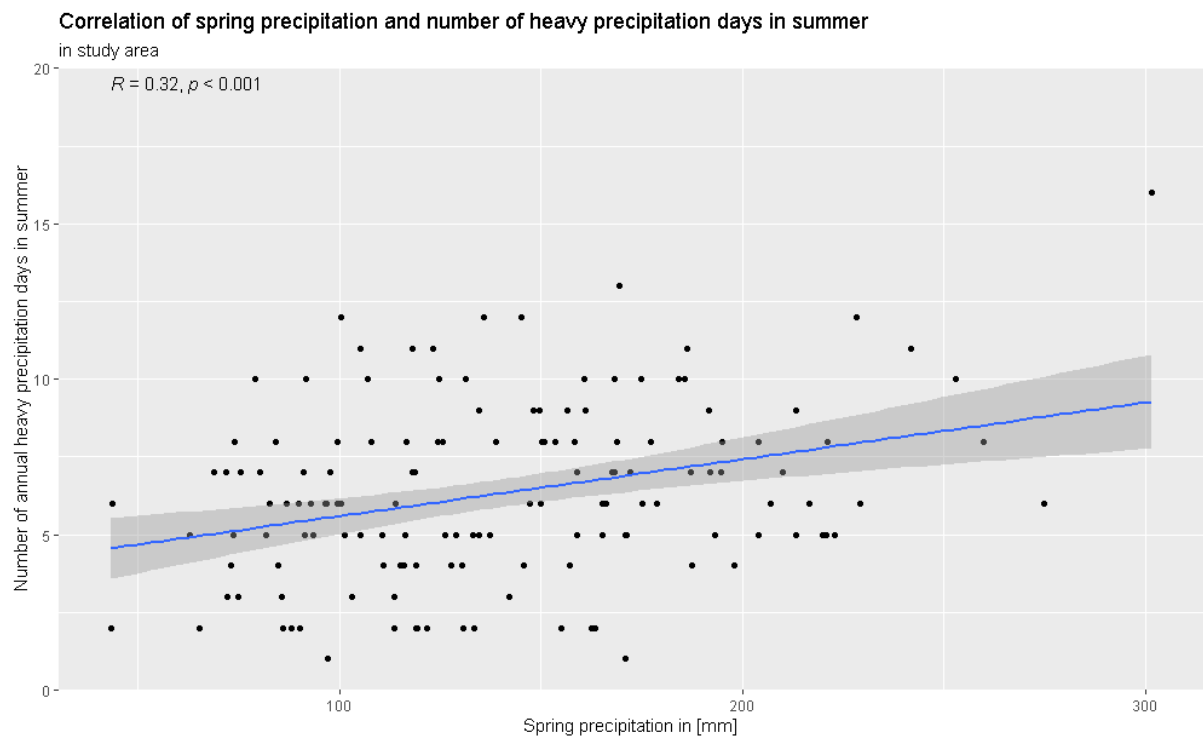


Figure 21: Correlation of spring precipitation [mm] and annual number of heavy precipitation days in summer in the study area. Significance accepted at $\alpha = 0.05$.

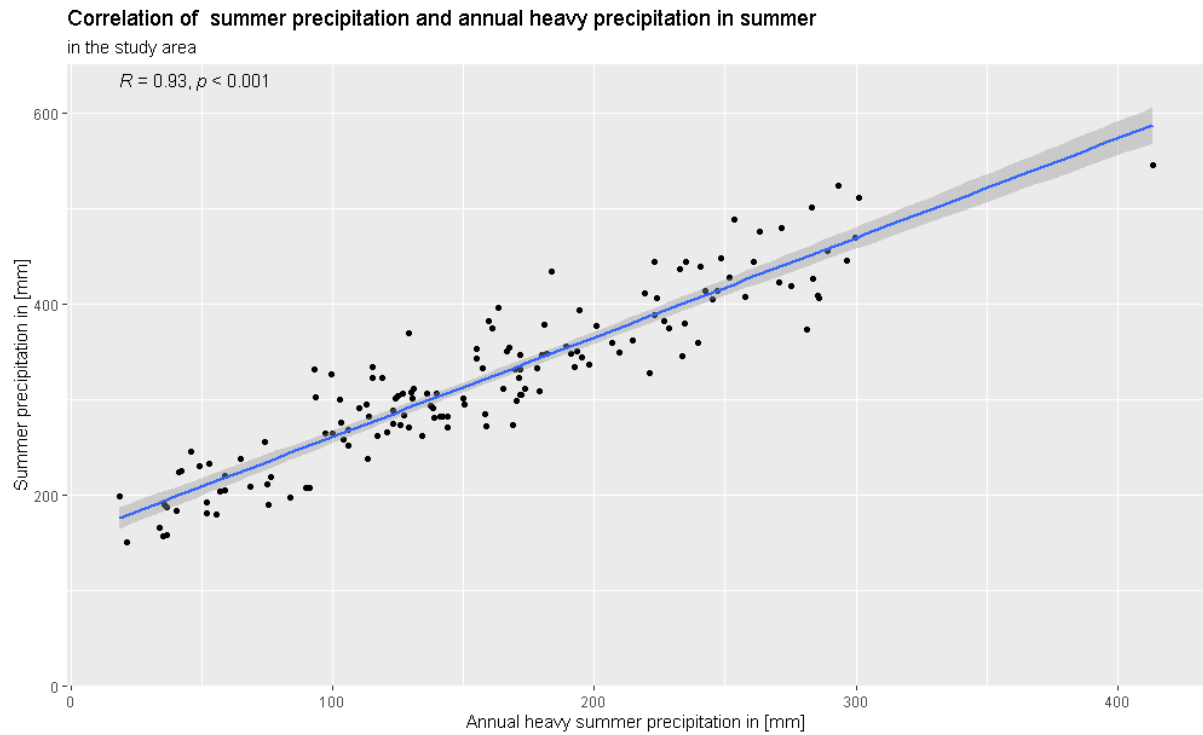


Figure 22: Correlation of summer precipitation and annual heavy precipitation in summer in mm in the study area. Significance accepted at $\alpha = 0.05$.

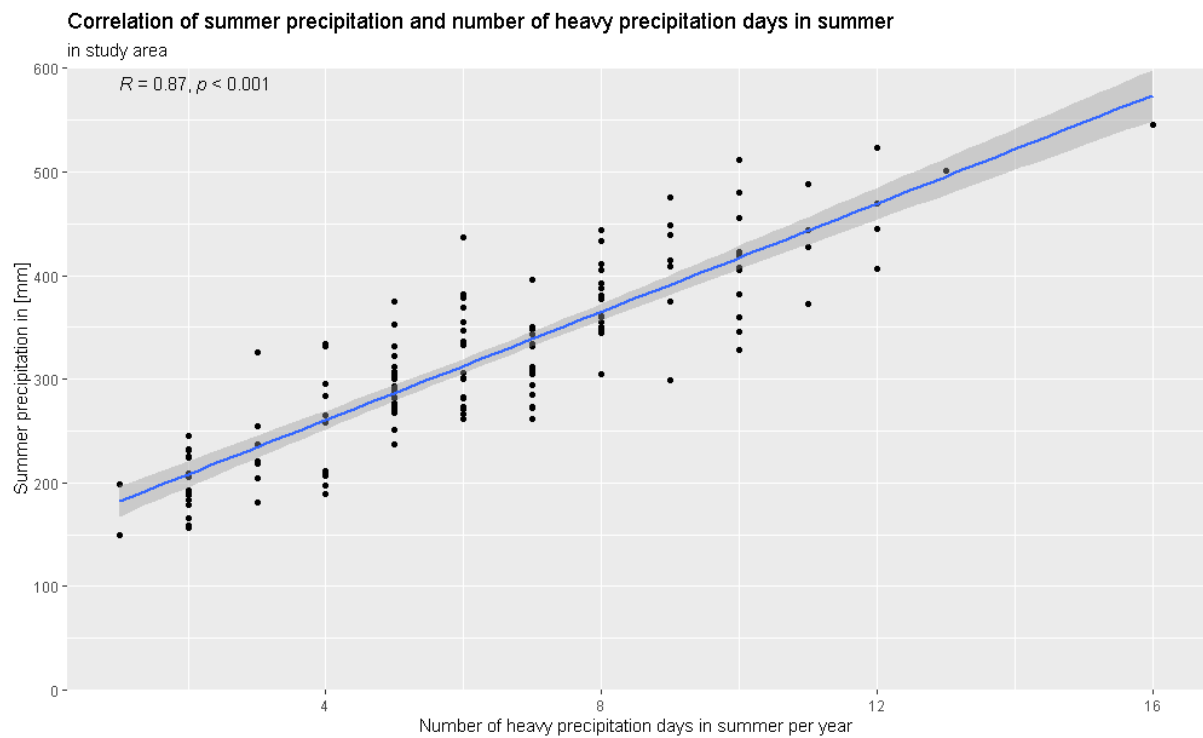


Figure 23: Correlation of summer precipitation [mm] and annual number of heavy precipitation days in summer in in the study area. Significance accepted at $\alpha = 0.05$.

5.3 Hourly precipitation analysis

Hourly precipitation is calculated based on time of day and as a rolling total. Clock-time based 1h sums are used to calculate mean hourly precipitation as they illustrate hourly precipitation throughout the day, whereas rolling sums are used for heavy precipitation analyses, as explained in Chapter 4.3. Mean hourly precipitation, including dry and wet hours, increased across the study area by about 10 % compared to the reference period. For individual stations it increased up to 20 %, and generally precipitation increased at all stations except station Krems, where mean hourly precipitation decreased by 4 % (see Table 12). Such an increase at most stations could result either from an increase in mean rainfall rate or from an increase in the number of precipitation hours. However, the number of precipitation hours decreased by 4 % from 1.95 wet hours per day in 1991-2005 to 1.86 wet hours per day in 2006-2020. Thus, the increase of overall mean hourly precipitation must result from increased hourly precipitation of wet hours, which indeed increased by 15 % across the study area, for individual stations, the increase ranges between 3-25 % (see Table 13), meaning more rain fell in a shorter period.

Table 12: Mean precipitation of CTHS (dry and wet hours) [mm/h] for the reference period (1991-2005) and main study period (2006-2020) at each station in the study area. Note that () indicates stations where data are not available throughout the entire period. Value for the study area in parentheses shows the mean calculated with all stations including those that were not established in the reference period.*

Station	1991-2005	2006-2020	Change in %
Innere Stadt	0.066*	0.079	20
Hohe Warte	0.075*	0.079	6
Gross-Enzersdorf	0.056*	0.064	14
Krems	0.064*	0.061	-4
Donaufeld	0.062*	0.068	9
Mariabrunn	0.087*	0.091	5
Stockerau	0.059*	0.068	15
Unterlaa	0.053*	0.063	18
Brunn am Gebirge	NA	(0.079*)	NA
Stammersdorf	NA	(0.071*)	NA
Study area	0.065	0.071 (0.072)	10

While CTHS portray precipitation throughout the day well, rolling totals are used for heavy precipitation analyses as they best represent maximum possible hourly precipitation and thus portray the heaviness of precipitation more realistically. However, since only one maximum value per day (further referred to as MRSD) is selected, precipitation is not realistically represented throughout the day. This can be seen when calculating the mean precipitation of MRSD. Thereby an increase of 17 % is shown, almost twice as much compared to calculations with CTHS, while mean precipitation of wet hours even increased by 21 %. For the same reason, mean precipitation in absolute numbers is larger by a factor of ten for rolling sums (see Appendix B, Table B1 and Table B2). Nevertheless, the importance of rolling totals for heavy precipitation analyses becomes evident when comparing maximum CTHS with maximum MRSD in both periods. Only in five cases the maximum possible 1h-precipitation also falls within a clock-based hour, in all other cases the maximum 1h-precipitation is higher for rolling sums (see Table 14). Tendencies (decreasing/increasing) are the same for both sum calculation

methods, except for the station Krems. There, compared to the reference period, a decrease of maximum 1h sum is recorded for CTHS and an increase for MRSD.

Table 13: Mean hourly precipitation of CTHS >0mm/h (wet hours only) for the reference period (1991-2005) and main study period (2006-2020) at each station in the study area. Note that (*) indicates stations where data are not available throughout the entire period. Value for the study area in parentheses shows the mean calculated with all stations including those that were not established in the reference period.

Station	1991-2005	2006-2020	Change in %
Innere Stadt	0.80*	1.00	25
Hohe Warte	0.76*	0.91	20
Gross-Enzersdorf	0.82*	0.90	10
Krems	0.84*	0.87	3
Donaufeld	0.78*	0.88	14
Mariabrunn	0.85*	0.97	14
Stockerau	0.77*	0.90	17
Unterlaa	0.77*	0.89	16
Brunn am Gebirge	NA	(0.90*)	NA
Stammersdorf	NA	(0.90*)	NA
Study area	0.80	0.92 (0.91)	15

Table 14: Maximum recorded hourly precipitation [mm/h] for the CTHS and MRSD calculation method for the reference and main study period. The numbers in bold show an increase in the maximum recorded rainfall total for each respective period. The trend column is showing the change of maximum hourly sums between periods for both calculation methods. Note that (*) indicates stations where data are not available throughout the entire period. Value for the study area in parentheses shows the mean calculated with all stations including those which were not established in the reference period.

Station	CTHS		MRSD		Trend	
	1991-2005	2006-2020	1991-2005	2006-2020	CTHS	MRSD
Innere Stadt	31.5*	35.4	34.1*	47.0	↑	↑
Hohe Warte	39.3*	33.9	42.6*	39.1	↓	↓
Gross-Enzersdorf	38.3*	50.9	38.3*	50.9	↑	↑
Krems	34.9*	32.8	39.0*	40.7	↓	↑
Donaufeld	19.7*	33.3	24.4*	39.7	↑	↑
Mariabrunn	46.1*	43.7	46.1*	43.7	↓	↓
Stockerau	22.9*	28.9	23.9*	33.5	↑	↑
Unterlaa	28.2*	44.5	30.9*	44.5	↑	↑
Brunn am Gebirge	NA	(39.4*)	NA	(40.6*)	NA	NA
Stammersdorf	NA	(35.0*)	NA	(36.7*)	NA	NA
Study area	32.6	37.9 (37.8)	34.9	42.4 (41.6)	↑	↑

To classify heavy precipitation, a threshold is calculated from hourly precipitation in the reference period. Like for daily analyses, the 98th percentile of dry and wet hours is used to determine heavy precipitation. As further analyses are based on rolling totals, the threshold is calculated with MRSD. The 98th percentile in the study area for the reference period corresponds to 5.9 mm/h, over 1 mm/h less than in recent years (see Table 15). The threshold of 5.9 mm/h (> 5.9) is used to select all heavy precipitation hours calculated as rolling totals, which are at least one hour apart to avoid double-counting of 10-minute values. Those hours are further referred to as total heavy hour sums (THS). As with daily precipitation, the increase in the 98th percentile may be due to more hours that can be classified as heavy precipitation or to a stronger mean rain rate. The following subsections present the results in this regard using THS.

Table 15: 98th percentile of hourly precipitation [mm/h] calculated with MRSD for the reference period (1991-2005) and main study period (2006-2020) at each station in the study area. Note that () indicates stations where data are not available throughout the entire period. Value for the study area in parentheses shows the mean calculated with all stations including those that were not established in the reference period.*

Station	1991-2005	2006-2020	Change in %
Innere Stadt	5.7*	7.7	36
Hohe Warte	5.9*	7.3	24
Gross-Enzersdorf	5.8*	6.6	14
Krems	6.8*	6.9	3
Donaufeld	5.4*	6.9	29
Mariabrunn	6.3*	7.5	20
Stockerau	5.6*	6.8	21
Unterlaa	5.6*	6.0	7
Brunn am Gebirge	NA	(6.8*)	NA
Stammersdorf	NA	(7.0*)	NA
Study area	5.9	7.0 (7.0)	19

5.3.1 Frequency of hourly heavy precipitation

As discussed earlier, the increase of the mean hourly rain rate in the 98th percentile either could be attributed to an increase in frequency of heavy precipitation hours (HPH) or a rise in the mean hourly rain rate itself. Indeed, calculations show that the number of hours per year, having more than 5.9 mm of precipitation, increased at every station between 12 % and 57 % compared to the reference period. An exception is station Krems, where HPHs per year have decreased by 11 % in recent years. Overall, the increase across the whole study area amounts to 25 % (see Table 16). The annual average of each station was calculated using the number of years of available data per station in each period, as discussed in Chapter 4.1. On average there are about two hours more of heavy precipitation per year in the main study period. The smallest increase could be observed at station Mariabrunn with 12 % and station Gross-Enzersdorf with 20 %; at all other stations, the number of heavy precipitation hours has increased by 25 % or more. Interestingly, station Krems was the station with most HPHs in the reference period aside from station Mariabrunn and is now among the stations with the fewest heavy precipitation hours on an annual average.

As with the daily analyses, these are average values, and the number of heavy precipitation hours varies considerably per year. Most stations had at least three to five HPHs per year in the main study period, only station Unterlaa had less, namely one, and station Innere Stadt had at least eight (see Table 17). In contrast, in the reference period most stations had three to four HPHs as a minimum, only stations Donaufeld and Innere Stadt had less, namely two, and station Krems had at least six. Regarding the maximum number of HPHs in a year, most stations had not more than 18 in the main period, except stations Innere Stadt, Mariabrunn and Stockerau, which had 23, 22 and 21, respectively. In the reference period, the maximum number of HPHs shows more variation. While some stations had only around 11 or 12 HPHs in a year, others such as station Krems even had 27. Although this is due to an exceptional year (2002); in other years of the reference period station Krems had no more than 13 hours of heavy precipitation. Beyond that, such a high number of heavy precipitation hours was not reached again by any station in the main study period. On the contrary, there was a decrease in the maximum number of HPHs in a year at the stations Krems and Mariabrunn in recent years. It should be noted that - depending on when the stations were established - not all stations recorded precipitation data for a whole year. That is the case for stations Brunn am Gebirge in 2008, Hohe Warte in 1992 and Unterlaa in 1997. This must be considered when analysing the amount of heavy precipitation hours. Interested readers will find the plots regarding the distribution of heavy precipitation hours over both periods in the supplement (see Appendix B, Figure B1 and Figure B2).

Table 16: Average number of heavy precipitation hours per year in each respective period at each station in the study area using THS. Numbers are averaged over years in each period and at each station. Note that () indicates stations where data are not available throughout the entire period. Value for the study area in parentheses shows the mean calculated with all stations including those that were not established in the reference period.*

Station	1991-2005	2006-2020	Change in %
Innere Stadt	8.8*	13.7	57
Hohe Warte	8.5*	11.5	36
Gross-Enzersdorf	9.0*	10.8	20
Krems	11.9*	10.6	-11
Donaufeld	7.3*	9.9	37
Mariabrunn	12.3*	13.8	12
Stockerau	8.4*	12.2	45
Unterlaa	6.9*	8.9	29
Brunn am Gebirge	NA	(11.3*)	NA
Stammersdorf	NA	(12.2*)	NA
Study area	9.1	11.4 (11.5)	25

Table 17: Minimum and maximum number of heavy precipitation hours in a year in each respective period for each station in the study area. Note that (*) indicates stations where data are not available throughout the entire period. Value for the study area in parentheses shows the mean calculated with all stations including those that were not established in the reference period.

Station	1991-2005		2006-2020		Change	
	Min	Max	Min	Max	Min	Max
Innere Stadt	2*	16*	8	23	↑	↑
Hohe Warte	3*	16*	3	17	→	↑
Gross-Enzersdorf	3*	15*	5	17	↑	↑
Krems	6*	27*	4	18	↓	↓
Donaufeld	2*	12*	5	16	↑	↑
Mariabrunn	4*	23*	5	22	↑	↓
Stockerau	4*	20*	4	21	→	↑
Unterlaa	3*	11*	1	15	↓	↑
Brunn am Gebirge	NA	NA	(5*)	(17*)	NA	NA
Stammersdorf	NA	NA	(4*)	(20*)	NA	NA
Study area	3	18	4 (4)	19 (19)	↑	↑

5.3.2 Mean rain rate of hourly heavy precipitation

As in the case of daily precipitation, an increase in mean hourly rain rate may also have contributed to a change in the 98th percentile of hourly precipitation in the main study period. The mean rain rate of heavy hours increased from 10.0 mm/h on average in the reference period to 10.6 mm/h in the main study period. The mean rainfall rate of heavy precipitation hours has thus increased by 6 % in the study area. This is less than Formayer & Fritz (2017) calculated for a station in Vienna. According to their results, an increase in the hourly rain rate of heavy precipitation of 8.5 % per degree of warming can be expected. This difference may be due to the fact that the authors calculated percentiles only with wet events that had more than 1mm/h of precipitation, whereas in this study dry hours were also included for the calculation of thresholds of heavy precipitation hours. Aside from global warming, the increase could be related to the fact that the main study period partly falls within the phase of high convective activity identified by Blöschl et al. (2017) while the reference period is mostly within the phase of lower convective activity. However, the increase in mean rain rate and also frequency of hourly heavy precipitation is smaller than for daily heavy precipitation. Although the mean increased the mean rain rate of the strongest hours remained approximately the same. The hourly mean rain rate in the main study period ranges from 5.9 mm/h as the chosen threshold to identify heavy hourly precipitation, up to 50.9 mm/h at station Gross-Enzersdorf. However, for most stations the maximum mean rain rate does not exceed 45 mm/h, except station Innere Stadt, which had two hours in the main study period with rain depths of 46.1 mm and 47 mm (see Figure 24). Figure 24 also shows a grouping of heavy hourly precipitation below and above 15mm/h. When extracting the heaviest 20 precipitation hours, this grouping is confirmed (see Figure 25). For every station, except station Brunn, the mean rain rate of the twenty heaviest precipitation hours is above 15 mm/h, grouping all other heavy precipitation hours below this threshold. For station Brunn that threshold is around 10 mm/h.

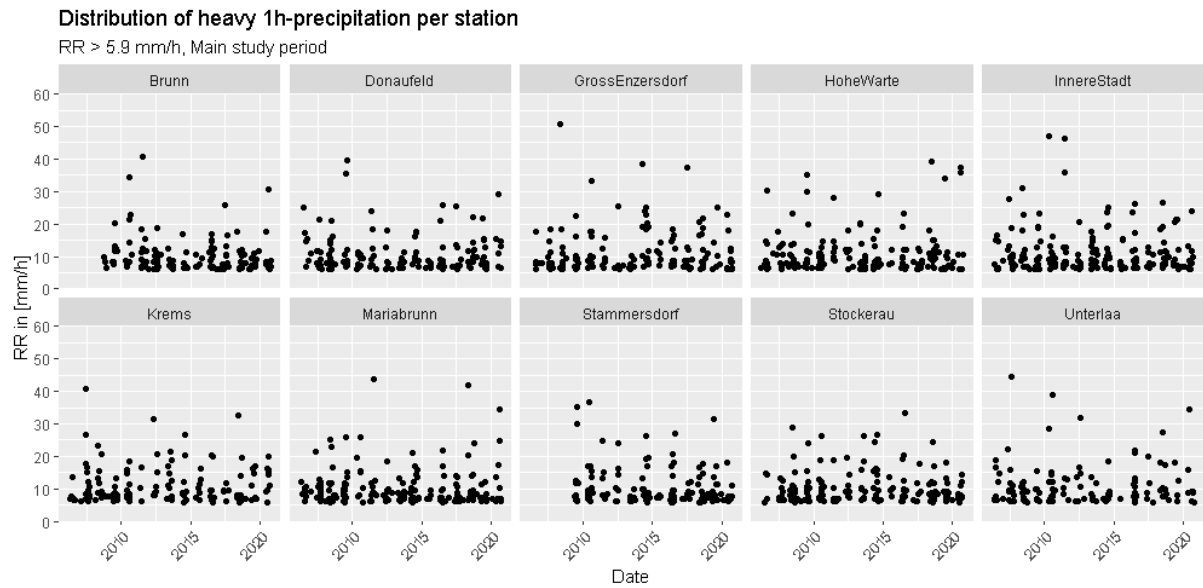


Figure 24: Occurrence of heavy precipitation hours, 2006-2020. Note, stations Brunn am Gebirge and Stammersdorf recorded data only since late 2008.

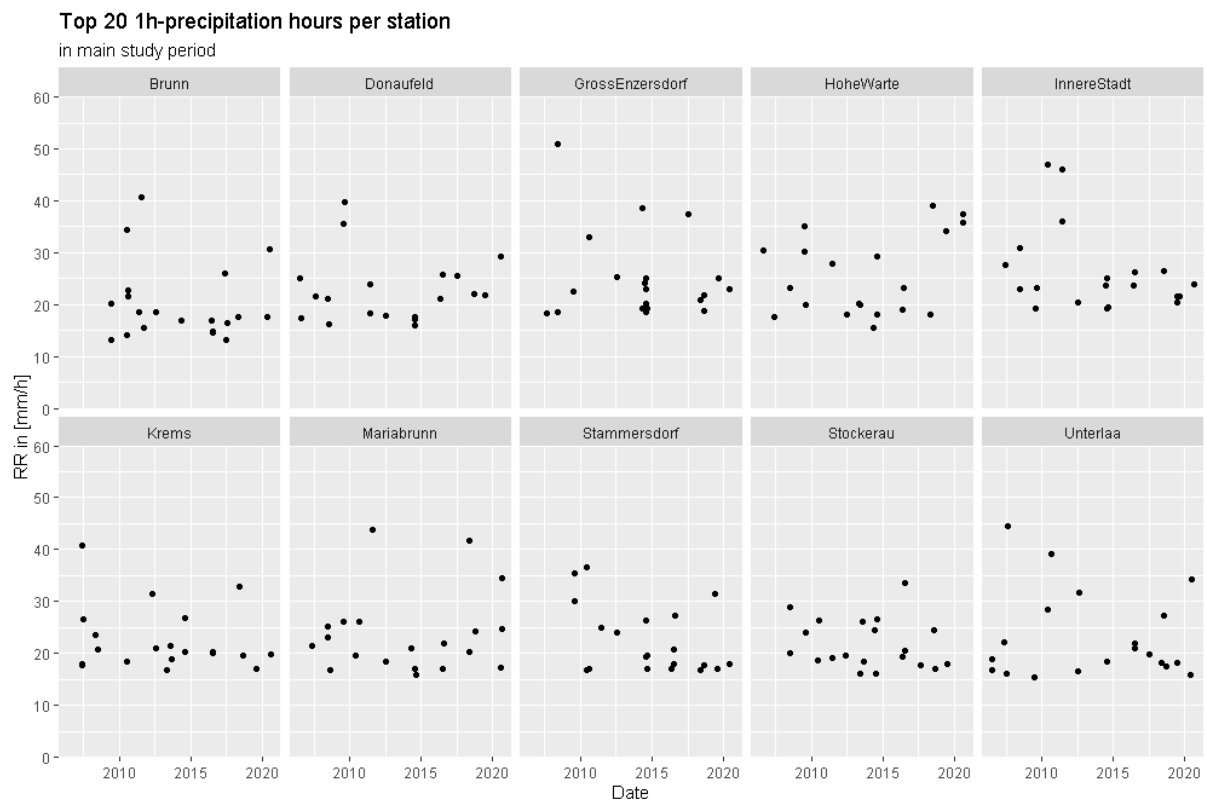


Figure 25: Strongest twenty heavy precipitation hours at each station 2006-2020. Note, stations Brunn am Gebirge and Stammersdorf recorded data only since late 2008.

In the reference period, the hourly mean rain rate reaches up to 46 mm/h, which is lower than the maximum mean rain rate in the main study period (see Figure 26). Contrary to the main study period, where all stations but Hohe Warte, Stockerau and Stammersdorf exceeded 40 mm/h of precipitation at least once, heavy precipitation hours at most stations in the reference period stay below 40 mm/h. In addition, at station Unterlaa hourly precipitation does

not exceed 35 mm/h in the reference period, which is also the case at station Innere Stadt. Likewise, heavy precipitation at the stations Donaufeld and Stockerau remains below 25 mm/h. The stations exceeding 40 mm/h are Hohe Warte with two hours above this value and station Mariabrunn with one hour. In contrast, there were eight hours in the main study period with mean rain rate greater than 40 mm/h. At stations Mariabrunn and Innere Stadt, except for three hours, mean rain rate even remained below 25 mm/h. Comparing Figure 24 and Figure 26, the increase not only of mean rain rate of heavy hourly precipitation but also the increase in frequency of heavy precipitation hours becomes obvious. Further, heavy precipitation hours seem to group below, and above 10 mm/h opposed to 15 mm/h in recent years. Extracting the twenty heaviest hours at each station, it appears for the reference period that this grouping only applies to some stations (see Figure 27), however, still lying below 15 mm/h. The minimum rain rate of the twenty heaviest hours at station Unterlaa is below 10 mm/h, showing that there is a clear increase in the main study period.

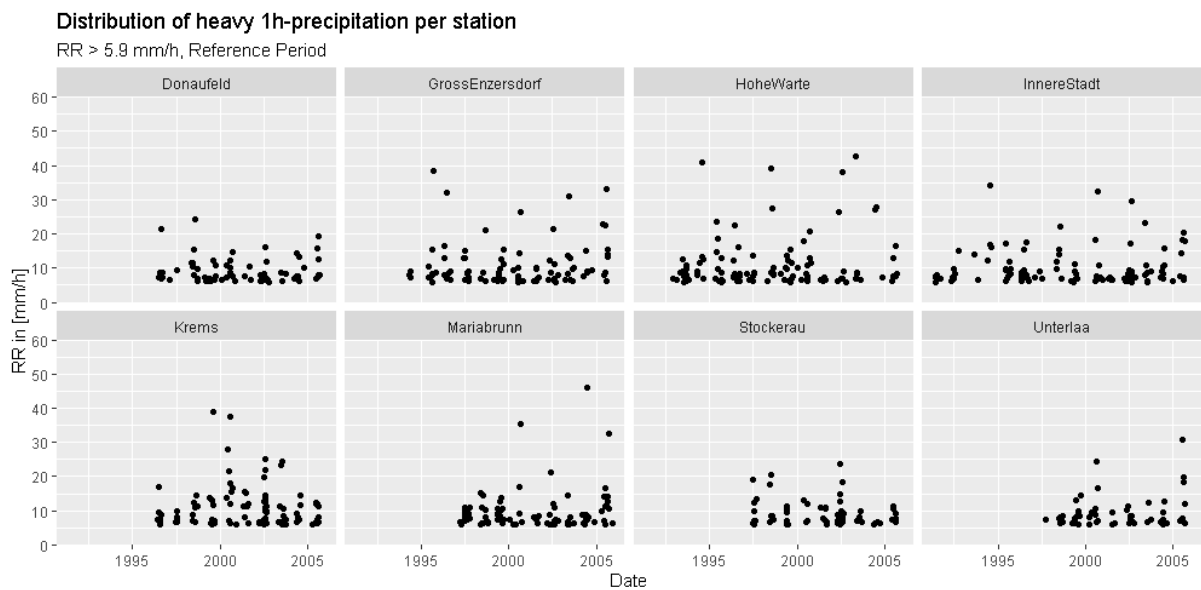


Figure 26: Occurrence of heavy precipitation hours 1991-2005. Note, not all stations recorded data since 1991 (refer to Chapter 4.1 for more details).

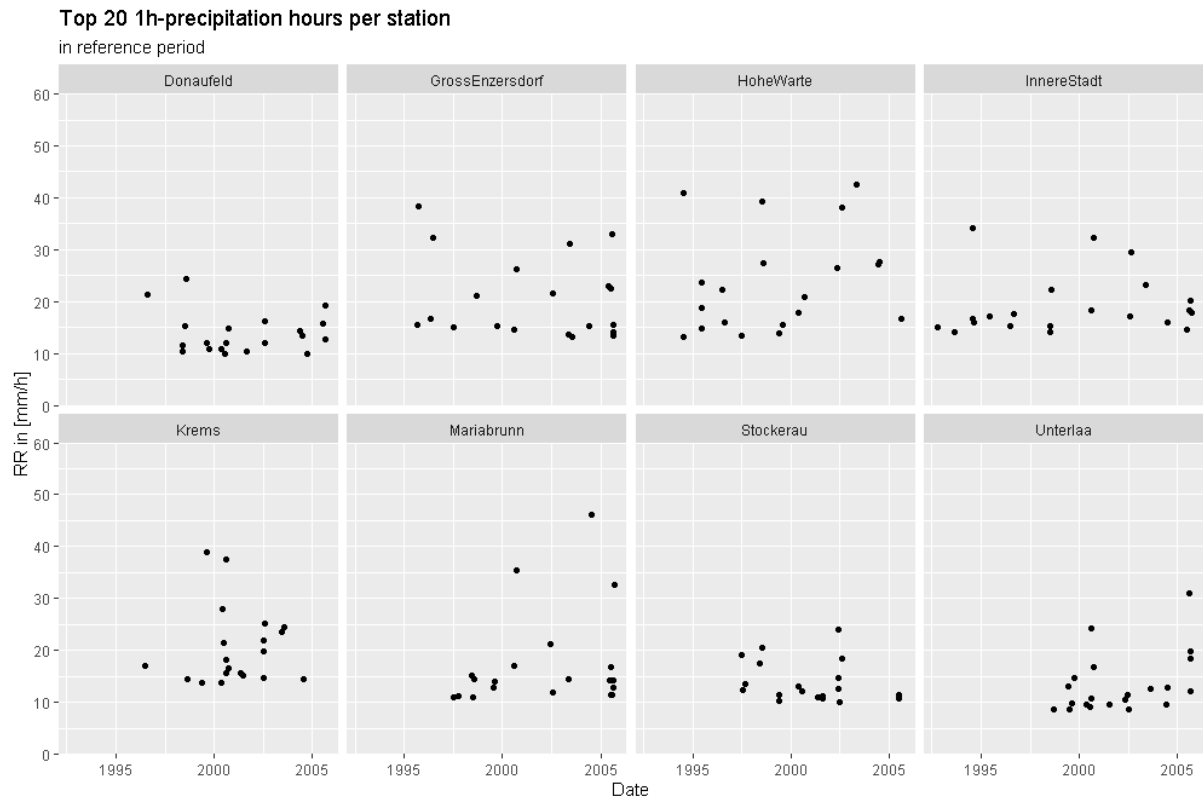


Figure 27: Strongest twenty heavy precipitation hours at each station 1991-2005. Note, not all stations recorded data since 1991 (refer to Chapter 4.1 for more details).

Although the minimum rain rate of the strongest events increased at station Gross-Enzersdorf, the calculation of percentiles shows that the mean rain rate decreased or remained the same in the 25th and 50th percentiles. Further, the 75th percentile confirms the observation that most hourly totals have less than 15 mm/h, which shows that less than 25 % of all hourly sums have more than that amount of precipitation recorded (see Table 18). In fact, for most stations 75 % of all hours have even less than 12 mm of precipitation recorded in the main study period and are generally lower in the reference period, not exceeding 14 mm/h at any station. Compared to the reference period, there was an increase in hourly precipitation in all percentiles except for the stations Gross-Enzersdorf as mentioned above, as well as stations Innere Stadt and Hohe Warte, where the mean rain rate decreased in the 25th and 75th percentile, respectively. For station Gross-Enzersdorf this change is substantially smaller compared to the change in daily precipitation where the station was among those with the largest increase in the 75th percentile. The most pronounced increase was noticeable at station Unterlaa where mean hourly mean rain rate of the 75th percentile increased by 27 %, which is about the same increase as for daily precipitation at that station. This increase is not unexpected, as the comparison of Figure 24 and Figure 27 has already shown an increase of the mean rain rate of hours with heavier precipitation. Moreover, at the 50th percentile the increase for mean hourly rain rate is even greater than for mean daily rain rate at station Unterlaa. While there was a decrease of the daily mean rain rate at station Krems, the mean rain rate of hourly heavy precipitation recorded an increase in all percentiles. Other than that, the hourly mean rain rate of heavy precipitation increased less than the daily mean rain rate.

Table 18: 25th, 50th and 75th percentile of precipitation (RR) in [mm/h] of heavy precipitation hours (RR > 6mm/h) for the reference and main study period. Note that (*) indicates stations where complete data are not available throughout the entire period.

Station	1991-2005			2006-2020		
	0.25	0.5	0.75	0.25	0.5	0.75
Innere Stadt	7.0*	7.7*	10.2*	6.8	8.4	12.0
Hohe Warte	6.8*	8.2*	12.1*	6.9	8.6	11.7
Gross-Enzersdorf	6.8*	8.2*	12.0*	6.8	8.4	12.4
Krems	6.7*	8.1*	12.1*	7.0	8.6	13.5
Donaufeld	6.7*	7.6*	10.4*	7.2	8.5	12.0
Mariabrunn	6.4*	7.8*	10.1*	6.9	8.2	10.6
Stockerau	6.7*	7.6*	10.3*	6.8	8.6	11.0
Unterlaa	6.7*	7.6*	9.6*	6.8	8.9	12.2
Brunn am Gebirge	NA	NA	NA	6.8*	8.7*	11.4*
Stammersdorf	NA	NA	NA	6.9*	8.1*	11.6*

5.3.3 Seasonality of hourly heavy precipitation

Like heavy precipitation days, most of the heavy precipitation hours occurred in summer. However, the differences among seasons were much more pronounced for hourly heavy precipitation than for daily heavy precipitation with distinctly more heavy precipitation in summer than in any other season. This could be related to the fact that short-lived, convective precipitation occurs mainly at warm temperatures (Lenderink & van Meijgaard, 2010) and thus one-hour convective heavy precipitation is less likely to occur in winter. In the case of heavy precipitation on a daily basis, on the other hand, several precipitation hours/events can accumulate over the course of the day and will be classified as a heavy precipitation day when a certain threshold is reached. Overall, the amount of heavy precipitation hours increased in every season compared to the reference period. At station Krems, the number of heavy precipitation hours decreased in summer, although there were increases in other seasons (see Appendix B, Figure B3 and Figure B4). Interestingly some years show hourly heavy precipitation occurring only during the summer season (see Figure 28), although on a daily basis in those years there were heavy precipitation days in other seasons identified as well. This suggests that daily heavy precipitation accumulates from precipitation that is not classified as heavy precipitation on smaller time resolutions. It should be noted that the sole heavy precipitation in autumn in 2008 at station Brunn am Gebirge is not representing a full year as the station was established at the end of 2008, thus recorded only rain data for three months. This is also the case for the year 1992 at station Hohe Warte and 1997 at station Unterlaa.

While mean daily heavy precipitation has increased the most in autumn, this is not the case when the data are analysed on an hourly basis (see Table 19). However, due to different reference periods for daily and hourly analyses, the results are not directly comparable. For this reason, mean hourly precipitation was determined for the reference period 1991-2005, as well as for the main study period, using CTHS. The calculations show that mean precipitation increased most in spring and autumn and only half as much in summer and winter. In each case, there was an increase in mean precipitation in every season (see Table 20). Since there was a decrease in mean hourly heavy precipitation in autumn, the increase in mean hourly precipitation in this season must be due to an increase in weak or moderate precipitation below the threshold of 5.9 mm/h. Regarding other seasons, mean heavy precipitation has increased to the same extent as mean precipitation. Although the increase of mean heavy precipitation

is similar for summer and winter, the number of hours with heavy precipitation in winter almost doubled while in summer the amount increased only by 44 %, marking the smallest increase among all seasons (see Table 21). This suggests that the increased amount of heavy precipitation hours in winter brought less heavy precipitation than half the amount of heavy precipitation hours in summer. This is expected as summer temperatures offer better conditions for strong convective precipitation with higher mean rain rates. The strongest increase could be observed in autumn where the amount of heavy precipitation hours doubled in recent years. Since less heavy precipitation fell over more hours, it can be assumed that hourly heavy precipitation decreased in severity in autumn. In summer, the number of heavy precipitation hours increased stronger than the mean of hourly heavy precipitation, also indicating that the severity of hourly precipitation decreased in that season. A similar observation can also be made for spring.

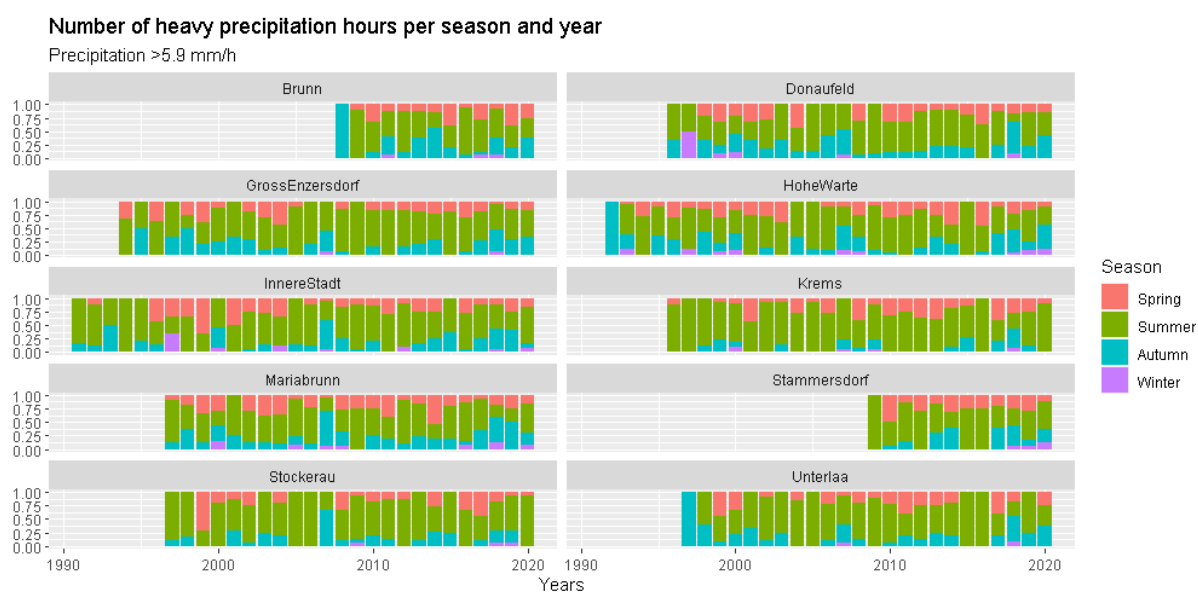


Figure 28: Seasonal fraction of heavy precipitation hours per year for the reference (1991-2005) and main study period (2006-2020). Note, stations Brunn am Gebirge, Hohe Warte and Unterlaa have not data for every season in their first year of establishment.

Table 19: Mean hourly heavy precipitation [mm/h] per season for the reference and the main study period.

Season	1991-2005	2006-2020	Change in %
Spring	8.9	10.2	15
Summer	10.4	11.4	10
Autumn	9.8	8.8	-10
Winter	7.1	7.9	11

Table 20: Mean hourly precipitation [mm/h] per season in the study area for reference and the main study period, using CTHS.

Season	1991-2005	2006-2020	Change in %
Spring	0.06	0.07	12
Summer	0.09	0.10	8
Autumn	0.06	0.07	12
Winter	0.04	0.05	9

Table 21: Number of heavy precipitation hours per year and season for the study area; calculated with averages per station.

Season	1991-2005	2006-2020	Change in %
Spring	13.7	22.2	62
Summer	46.7	67.4	44
Autumn	11.1	23.1	108
Winter	1.3	2.3	83

5.4 Event analysis

While studies often focus on daily and hourly resolutions of heavy precipitation and the definite time frame offers a good opportunity to compare results across studies and time periods, daily and hourly resolutions do not illustrate real rain conditions very well. Precipitation can last a few minutes to over 24 hours. Thus, dividing rainy periods into events is the best way to represent different time lengths of precipitation according to real conditions. As discussed earlier, the number and characteristics of events depends highly on the conditions that are used to define events. How events are defined in this thesis is described in detail in Chapter 4.3.1. Since events are calculated from 10-minute data, the reference period is the same as for hourly analyses. With the chosen definitions, over 400 rain events per year are identified in the study area for both periods, on average that is more than one precipitation event per day. This is due to the fact, that periods are counted as an event even if gauges registered precipitation only for a few minutes as long as dry periods did not exceed 10 minutes within the event. The number of rain events decreased by 11 % in the study area while mean event rain rate increased by 11 % (see Appendix C, Table C1 and Table C2). Hence, event precipitation got stronger in recent years. Mean event rain depth (excluding dry events) increased by 23 % from 1.23 mm to 1.51 mm while mean rain event duration increased only moderately, namely 12 % from 0.86 h to 0.96 h, further confirming the assumption that the magnitude of rain events has increased. Like for daily and hourly analyses, the 98th percentile is used to find a threshold for heavy precipitation events. For this purpose, the event rain rate is calculated dividing the event rain depth by the event duration to make events of different lengths and with various rain depths comparable with each other. Calculations show that there was an increase of mean event rain rate in the 98th percentile by 28 %, from 3.1 mm/h to 4.0 mm/h (see Table 22). Station Gross-Enzersdorf stands out with a substantially smaller event rain rate in the 98th percentile

compared to other stations in the reference period. A detailed analysis of this station record shows that there were many long-lasting dry periods, especially in 2004 and 2005 and many dry periods lasted several days. Since this is unverified data, it could be a measurement error, but a comparison with the daily data shows correspondences of dry periods with dry days. It is therefore assumed that this finding is not due to a data error. The following subchapters will analyse to what extent the increase in the 98th percentile is due to a change in the frequency of heavy rain events or a change in the magnitude of the mean event rain rate. Lastly, seasonal changes of heavy precipitation events are presented.

Table 22: 98th percentile of mean event rain rate [mm/h] calculated with dry and wet events for the reference period (1991-2005) and main study period (2006-2020) at each station in the study area. Note that () indicates stations where data are not available throughout the entire period. Value for the study area in parentheses shows the mean calculated with all stations including those that were not established in the reference period.*

Station	1991-2005	2006-2020	Change in %
Innere Stadt	3.4*	4.2	24
Hohe Warte	3.0*	3.9	31
Gross-Enzersdorf	1.9*	4.2	115
Krems	3.6*	4.0	12
Donaufeld	3.4*	3.9	13
Mariabrunn	3.2*	3.9	20
Stockerau	3.2*	4.2	30
Unterlaa	3.3*	3.8	15
Brunn	NA	(3.6*)	NA
Stammersdorf	NA	(4.0*)	NA
Across study area	3.1	4.0 (4.0)	28

The 98th percentile of mean event rain rate in the reference period is used as a threshold to identify heavy precipitation events. The following examples illustrate the importance of using the mean rain rate instead of the total event rain depth to identify heavy precipitation events. The longest precipitation event was recorded at station Hohe Warte beginning on the 23rd of February 1993 which lasted 37 hours with a rain depth of 48.5 mm. This event would most likely be classified, at least in part, as a heavy precipitation day because of the amount of rain that fell over the course of 24 hours. And indeed, the 24th of February 1993 was classified as a heavy precipitation day according to the definitions used in this thesis. For this event, however, the mean event rain rate is not sufficiently high to be classified as a heavy precipitation event, as it is only 1.3 mm/h due to the length of the event. The event with the greatest amount of rain was measured at station Mariabrunn. It began on the 7th of August 2006, lasted 25.5 hours and brought 119.9 mm of precipitation. This precipitation event was also partly classified as a heavy precipitation day and with a mean event rain rate of 4.7 mm/h it is also classified as a heavy precipitation event according to the definitions used in this study. However, if the 98th percentile was calculated only with rain events excluding dry periods, this event would have fallen out of the definition of heavy precipitation events. These two examples show how dependent the classification of heavy precipitation is on the employed definitions and the importance of including dry periods in the calculation of thresholds to identify heavy precipitation like Ban et al. (2015) recommend. After having heavy precipitation events identified as any event with a mean rain rate exceeding 3.1 mm/h (>3.1) some descriptive statistics were performed. The findings are that mean rain depth of heavy precipitation events increased less than the mean of all precipitation events, namely by 13 % from 7.6 mm to 8.6 mm, while the mean rain depth of all precipitation events (excluding dry events) increased by 23 % from 1.23 mm to 1.51 mm. Mean event duration of heavy precipitation events increased

to the same extent as mean event duration of all precipitation events (excluding dry events), namely by 12 % from 1.39 h to 1.55 h compared to 0.86 h to 0.96 h.

5.4.1 Frequency of heavy precipitation events

For the frequency analysis it is necessary to average the count of heavy precipitation events per station over the years of available data for every station in each period to account for different time frames of data collection at each station. The calculations show that the frequency of heavy precipitation events per year has increased by 10 % in the study area, from around 22 to 24.5. For individual stations, the increase ranges between 4-36 % (see Table 23). Between 2006-2020, the largest number of heavy precipitation events per year was found at station Hohe Warte. Nevertheless, the strongest increase in the frequency of events could be observed at station Stockerau. On the other hand, a decrease in frequency of events could be observed at station Krems. However, these numbers present only averages, and the number of events can vary considerably. Most stations had not more than 25 heavy precipitation events in most years in the reference period. In the main study period, it could be observed that substantially more years had at least 25 heavy precipitation events. Interested readers can find the plots showing the number of events per year for each station in both periods in the supplements (see Appendix C, Figure C1 and Figure C2). The maximum recorded number of events in a year increased at all stations in recent years except at stations Innere Stadt and Gross-Enzersdorf. While the minimum recorded number of heavy events per year has increased considerably at some stations, it remained unchanged at station Unterlaa, and decreased slightly at stations Hohe Warte, Krems and Donauefeld (see Table 24). Hence, not only the average number of events per year increased, but at most stations there was also an increase of minima and maxima of recorded events in single years. It should be noted that the event analysis is based on 10-minute data, and not all stations recorded precipitation for a whole year in the year of their establishment, for example stations Brunn am Gebirge in 2008 and Unterlaa in 1997. This should be considered when analysing the frequency of heavy precipitation in those years.

Table 23: Average number of heavy precipitation events ($RR > 3.1$ mm/h) per year in each respective period at each station in the study area. Numbers are averaged over available years in the respective period. Note that () indicates stations where data are not available throughout the entire period. Value for the study area in parentheses shows the mean calculated with all stations including those that were not established in the reference period.*

Station	1991-2005	2006-2020	Change in %
Innere Stadt	23.7*	26.4	11
Hohe Warte	23.5*	27.1	15
Gross-Enzersdorf	22.0*	23.6	7
Krems	23.9*	23.6	-1
Donauefeld	20.8*	22.0	6
Mariabrunn	25.5*	26.5	4
Stockerau	18.8*	25.5	36
Unterlaa	19.6*	21.1	8
Brunn	NA	(24.7*)	NA
Stammersdorf	NA	(24.5*)	NA
Across study area	22.2	24.5 (24.5)	10

Table 24: Minimum and maximum number of heavy precipitation hours in a year in each respective period for each station in the study area. Note that (*) indicates stations where data are not available throughout the entire period. Value for the study area in parentheses shows the mean calculated with all stations including those that were not established in the reference period.

Station	1991-2005		2006-2020		Change	
	Min	Max	Min	Max	Min	Max
Innere Stadt	8*	36*	19	34	↑	↓
Hohe Warte	14*	33*	13	37	↓	↑
Gross-Enzersdorf	9*	33*	15	31	↑	↓
Krems	18*	30*	11	33	↓	↑
Donaufeld	14*	29*	13	30	↓	↑
Mariabrunn	14*	37*	20	39	↑	↑
Stockerau	9*	25*	12	35	↑	↑
Unterlaa	13*	32*	13	32	→	→
Brunn	NA	NA	(11*)	(32*)	NA	NA
Stammersdorf	NA	NA	(16*)	(35*)	NA	NA
Across study area	12.4	31.9	14.5 (14.3)	33.9 (33.8)	↑	↑

5.4.2 Mean rain rate of heavy precipitation events

As it was the case in the daily and hourly analyses, not only an increase in frequency of heavy precipitation events, but also an increase in the magnitude of events, thus the mean event rain rate itself, could also have led to an increase of the mean event rain rate in the 98th percentile in recent years. Indeed, the mean of heavy precipitation events saw the largest increase compared to the means of daily and hourly precipitation, namely 12 % from 7.6 mm in the reference period to 8.6 mm in the main study period. Similarly to hourly heavy precipitation, this might be related to different phases of convective activity. The increase can be seen when looking at the distribution of mean rain rates of both periods. For the period from 2006-2020, the mean rain rate of heavy precipitation events ranges between 3.1 mm/h as the chosen threshold for heavy precipitation up to 91.8 mm/h. This is due to an exceptionally heavy event at station Brunn am Gebirge on the 26th of July 2020, where it rained 30.6 mm in less than 20 minutes. Other than that, the mean event rain rate does not exceed 54 mm/h and usually stays below 43 mm/h. An exception to this is station Hohe Warte which had one event with mean rain rate of 54 mm/h, as well as station Stammersdorf, which had four events with mean event rain rate in between this range (see Figure 29). Those individual events lasted between 20 and 50 minutes and had rain depths of 14.5 mm to 36.7mm. Figure 29 also shows a grouping of events below and above 10 mm/h, which is confirmed by plotting the strongest twenty events at each station (see Figure 30). The strongest events have a minimum mean event rain rate of 10 mm/h (at many stations even 15 mm/h) grouping all other events below this threshold.

In the reference period, the strongest mean event rain rate was recorded at station Gross-Enzersdorf on the 25th of July 2005, where it rained 19.4 mm in 20 minutes resulting in a mean event rain rate of 58.2 mm/h (see Figure 31). Other than that, the mean event rain rate does not exceed 40 mm/h except during three precipitation events which were recorded at stations Innere Stadt, Gross-Enzersdorf and Krems with precipitation of 15.3 mm, 7.5 mm and 28 mm and event durations of 20, 10 and 40 minutes, respectively. The mean event rain rate of most

events is well below 10 mm/h and events seem to group above and below that threshold. This is confirmed when extracting the heaviest 20 events (see Figure 32). The strongest events have precipitation of at least 10 mm/h, only station Donaufeld seems to have a slightly lower minimum mean event rain rate. Comparing Figure 30 and Figure 32, a clear increase in the mean event rain rate of the strongest heavy precipitation events is evident for most stations except for stations Krems and Stockerau where the increase compared to the reference period was of minor extent.

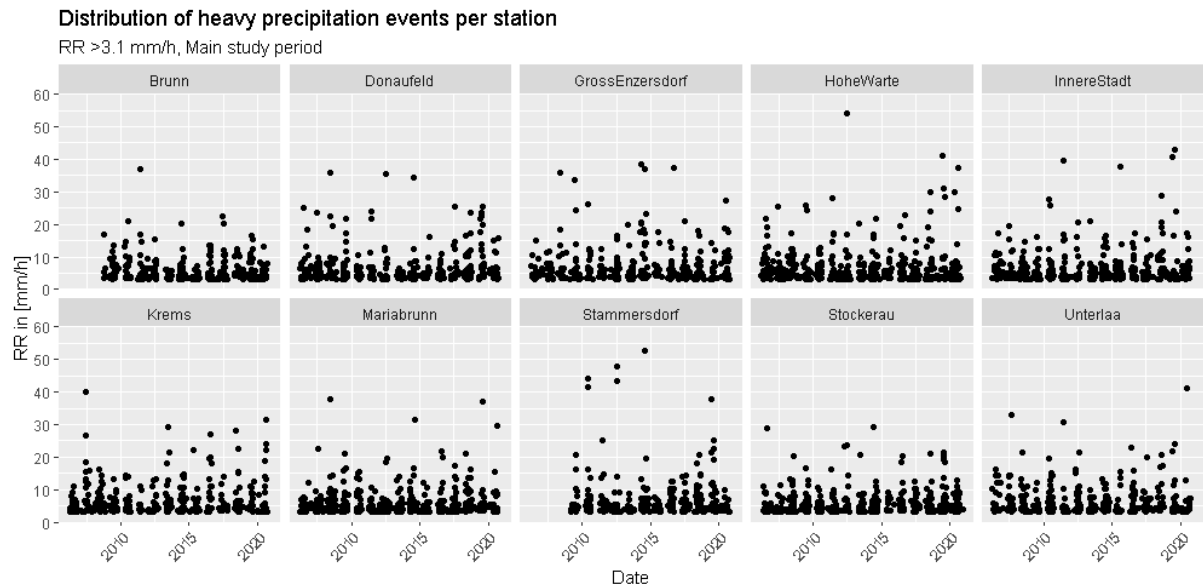


Figure 29: Occurrence of heavy precipitation events, 2006-2020. Note, stations Brunn am Gebirge and Stammersdorf recorded data only since late 2008. Also, the heaviest event with 91.8mm/h at station Brunn am Gebirge is excluded in this illustration to allow for a better analysis and comparison of the remaining heavy precipitation events.

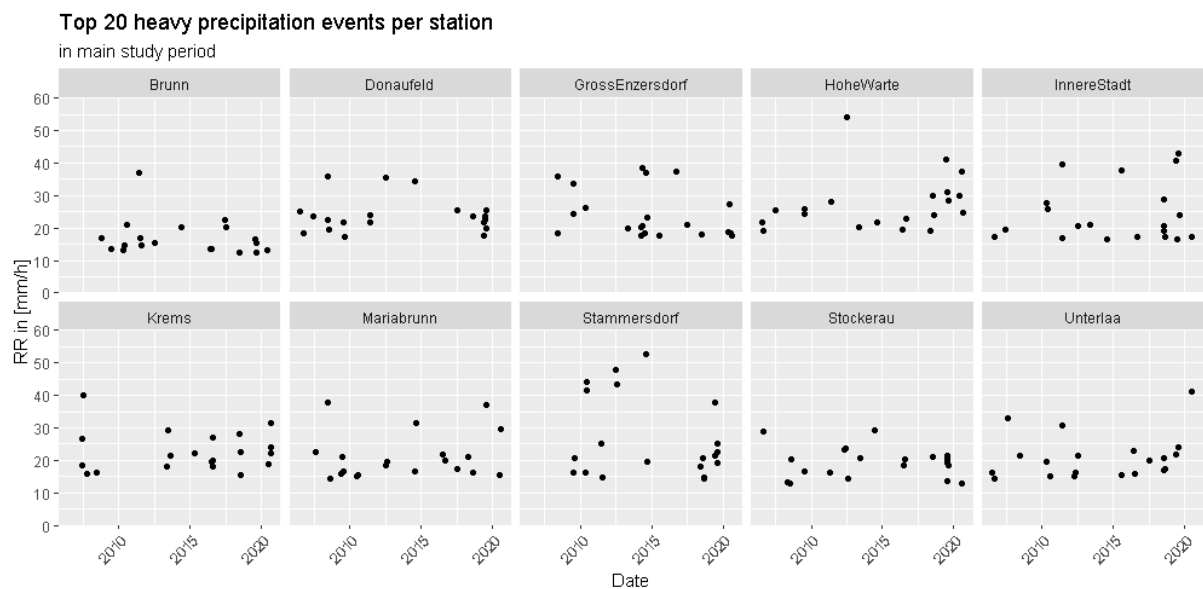


Figure 30: Strongest twenty events for each station, 2006-2020. Note, the heaviest event with 91.8mm/h at station Brunn am Gebirge is excluded in this illustration to allow for a better analysis and comparison of the remaining heavy precipitation events.

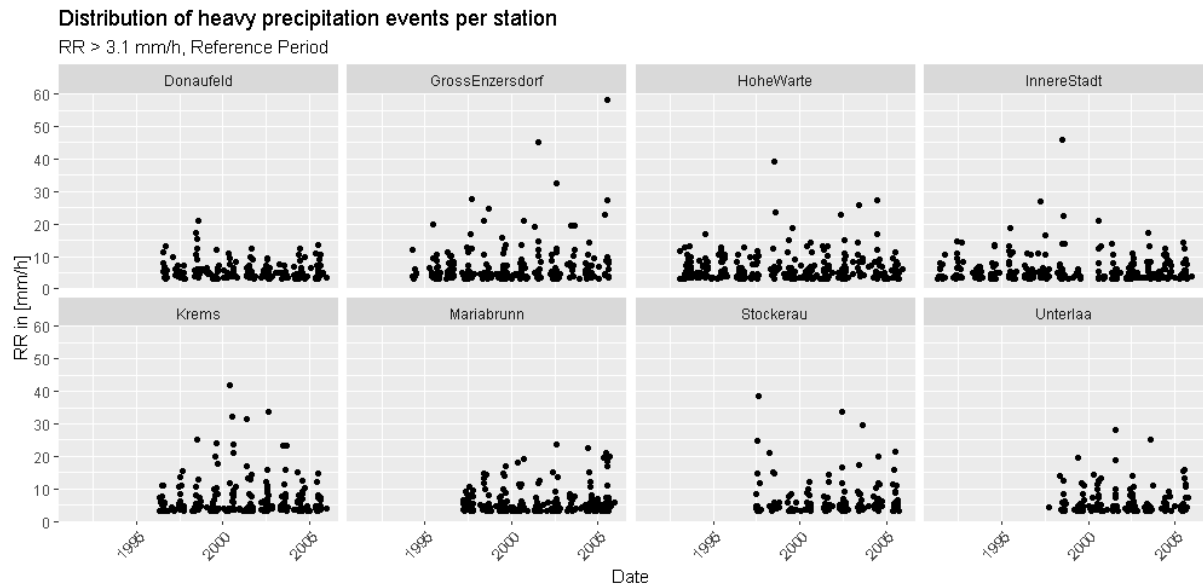


Figure 31: Occurrence of heavy precipitation events, 1991-2005. Note, not all stations recorded data since 1991 (refer to Chapter 4.1 for more details).

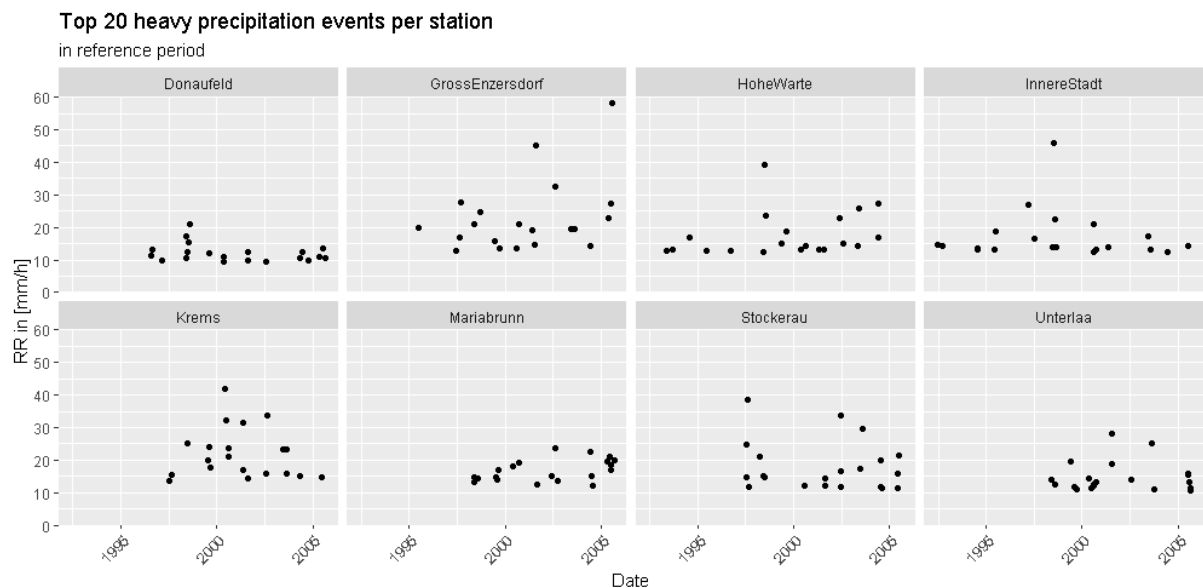


Figure 32: Strongest twenty heavy precipitation hours at each station 1991-2005. Note, not all station recorded data since 1991 (refer to Chapter 4.1 for more details).

Those observations are confirmed by calculating the mean event rain rate of heavy precipitation for different percentiles. The mean event rain rate in the 75th percentile does not exceed 8.0 mm/h at any station in both periods, meaning less than 25 % of all heavy precipitation events had precipitation stronger than 8.0 mm/h (see Table 25). In fact, for most stations 75 % of all heavy precipitation events had precipitation even less than 7.2 mm/h recorded. At almost all stations the mean event rain rate increased in nearly all percentiles, except at stations Hohe Warte and Stockerau where the mean event rain rate decreased slightly for the weakest quarter of heavy precipitation events and at station Krems where mean event rain rate decreased for the strongest 25 %. However, station Krems had the biggest mean rain rate in the 75th percentile in the reference period, hence even the decreased mean rain rate in the main period is among the highest of all stations. The strongest increase can be

observed at stations Unterlaa and Donaufeld in the 50th and 75th percentile, respectively. For most stations, the 25th percentile changed the least while the biggest increases could be seen in higher percentiles.

Overall, there is no clear correspondence between the changes for different percentiles and stations of the event analyses with hourly and daily analyses. Depending on the station and percentile, the results are either similar for all three temporal resolutions or differ (incoherently). For some stations, hourly and event analyses correspond and in other percentiles and stations, event and daily analyses correspond. As explained in the beginning of this chapter, this might be since some events are classified as heavy precipitation days based on rain depth fallen in 24 hours while those same days would not be classified as heavy when considering mean event rain rate. Likewise, the threshold to be classified as a heavy precipitation hour is higher than the threshold for heavy precipitation events, thus considering different magnitudes of precipitation. This might indicate that a threshold based on the maximum rolling sum per day for heavy precipitation hours yields a too high value in terms of mean rain rate.

Table 25: 25th, 50th and 75th percentile of mean rain rate [mm/h] of heavy precipitation events (RR > 3.1 mm/h) for the reference and main study period. Note that () indicates stations where complete data are not available throughout the entire period.*

Station	1991-2005			2006-2020		
	0.25	0.5	0.75	0.25	0.5	0.75
Innere Stadt	3.6*	4.3*	6.3*	3.8	4.8	7.2
Hohe Warte	3.7*	4.9*	7.2*	3.6	5.0	7.6
Gross-Enzersdorf	3.7*	4.7*	7.2*	3.9	5.1	7.4
Krems	3.6*	4.6*	7.9*	3.7	4.8	7.6
Donaufeld	3.7*	4.6*	6.0*	3.8	4.8	7.0
Mariabrunn	3.6*	4.3*	6.5*	3.8	4.8	6.8
Stockerau	3.9*	4.7*	6.9*	3.6	4.8	7.2
Unterlaa	3.6*	4.2*	7.1*	3.8	4.9	8.0
Brunn am Gebirge	NA	NA	NA	3.7*	4.8*	7.2*
Stammersdorf	NA	NA	NA	3.9*	4.9*	7.3*

5.4.3 Seasonality of heavy precipitation events

Naturally, most heavy precipitation events occurred during the summer season and other seasons had distinctly fewer heavy precipitation events. The differences between periods are more pronounced than in daily analyses, but weaker than in hourly analyses. The results of the event analyses seem to lie in between the other two. This is understandable, as most events categorised as heavy did not last considerably longer than one hour, but there were also events that lasted over 24 hours, so both time units are partially represented (see Appendix C, Figure C3 and Figure C4). Compared to the reference period, the change in frequency of events per season is mixed among seasons and stations (see Appendix C, Figure C5 and Figure C6). In most seasons, the number of events either remained unchanged or increased. Only at the Krems station was a decrease in events recorded in summer. Stockerau station is the only

station where an increase could be observed in all seasons. On an event basis, there are no years in which heavy precipitation only occurred in one season as it happened for hourly precipitation (see Figure 33). On the one hand, this might be because the 98th percentile of events equalled 3.1 mm/h while hourly precipitation was classified as heavy with a mean rain rate of 5.9 mm/h. At the same time, heavy precipitation events have mostly lasted less than two hours. Hence, event precipitation should be representing hourly precipitation to a certain degree. However, due to the smaller threshold, weaker events are also included than was previously the case with hourly analyses. On the other hand, some events lasted over 25 hours, hence, allowing to include precipitation that accumulated over a longer period of time. If one were to look at individual hours on those days, such precipitation probably does not reach the necessary mean rain rate to be called heavy on an hourly basis and would thus, depending on the amount of precipitation, only be found in daily heavy precipitation analyses. This again shows how dependent heavy precipitation analyses are on the definitions and time resolutions chosen. However, it also becomes clear that the approach of dividing precipitation into events instead of arbitrary time intervals captures heavy precipitation most comprehensively.

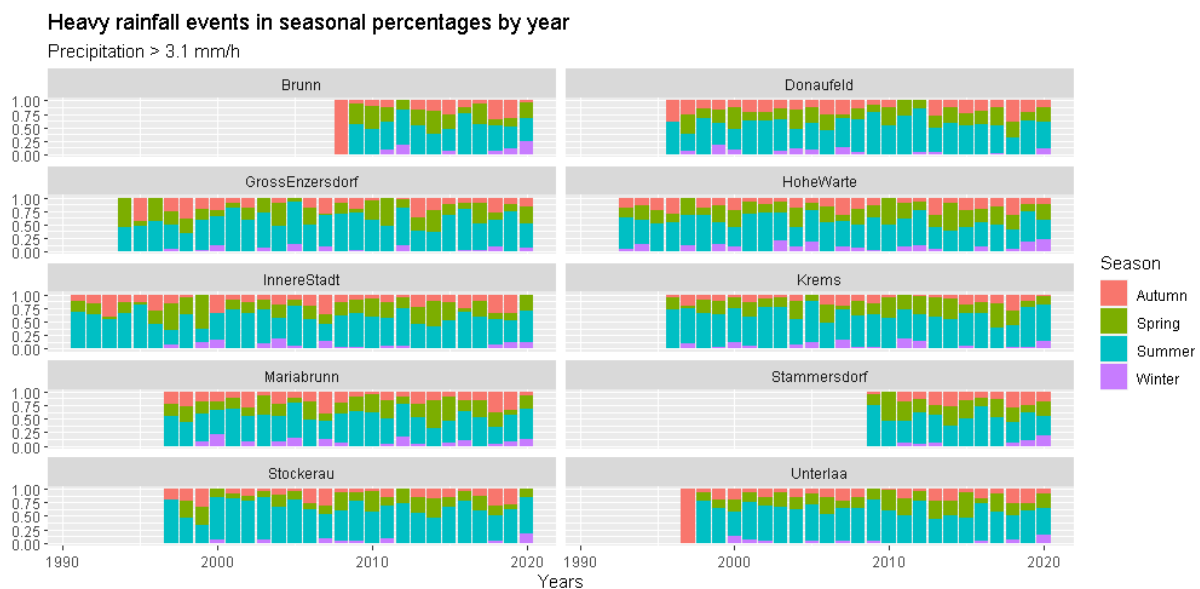


Figure 33: Seasonal fraction of heavy precipitation hours per year for the reference (1991-2005) and main study period (2006-2020). Note, stations Brunn am Gebirge, Hohe Warte and Unterlaa have not data for every season in their first year of establishment.

The change of mean rain rate across seasons for heavy precipitation events differs from the results of daily and hourly heavy precipitation. While the mean rain rate of daily heavy precipitation has increased the most in autumn and the mean rain rate of hourly heavy precipitation increased in all seasons but autumn, the mean rain rate of heavy precipitation on an event basis increased in all seasons but in winter (see Table 26). Event precipitation change is not directly comparable to the results of daily precipitation because different reference periods are used; however, it is interesting that results differ that much between hourly and event analyses as mean event duration is close to one hour, thus, should be representing heavy precipitation similarly as hourly analyses. If one looks at the duration of heavy events per season, events that last 10-25 hours are mainly found in summer and autumn (see Appendix C, Figure C7 and Figure C8). This could be one explanation why the change in seasonal precipitation corresponds more to the change in daily heavy precipitation than to the change in hourly heavy precipitation. Although mean event rain rate of heavy precipitation decreased by 5 % in winter, mean rain depth of heavy precipitation increased in winter by 22 % along with

mean event duration of heavy events, which increased by 28 % (see Appendix C, Table C3 and Table C4). However, this is easily explained as mean duration of heavy precipitation events has increased stronger than mean precipitation, meaning less rain fell over a longer period of time, which leads to a decrease in the mean rainfall rate, although the total amount of rainfall has also increased in winter.

Table 26: Mean rain rate in [mm/h] of heavy precipitation events ($RR > 3.1$ mm/h) per season in the study area for the reference and main study period.

Season	1991-2005	2006-2020	Change in %
Spring	5.7	6.0	6
Summer	6.8	7.5	10
Autumn	5.4	5.7	6
Winter	4.6	4.4	-5

Overall, mean rain rate of dry and wet events increased in all seasons considerably (see Table 27). This is because the mean rain depth of rain events has increased in all seasons (see Table 28). The increase also occurred in events with precipitation of less than 3.1 mm/h (see Table 29), so the increase in mean event rain rate is not only due to an increased rain depth of heavy precipitation events, but also due to increased precipitation among moderate or weak events. Although mean event rain rate increased for moderate and weak events and decreased for winter heavy precipitation, it should not be mistakenly assumed that rainfall events in winter must have weakened into moderate events. On the contrary, since the mean rainfall depth has increased in all seasons, no direct derivation can be made from the changes of mean rain rates of different intensity categories to changes in their frequency. As mean rain depth has increased for weak, moderate, and heavy events in winter it can be concluded that winters became wetter in the main study period. At the same time heavy precipitation in winter decreased in heaviness, but without falling below the threshold for heavy precipitation. Furthermore, the number of rain events has also increased in all seasons except summer. In summer there was a slight decrease in precipitation events (see Table 30). Overall, there has been a decrease in summer precipitation events in recent years with a simultaneous increase in heavy precipitation events in summer (see Table 31). This suggests that some events in the upper tail of the distribution have now reached the threshold to be classified as heavy. The strongest increase could be observed in spring where the number of heavy events increased by 33 %.

Table 27: Mean rain rate [mm/h] of events (including dry and wet events) for the reference and main study period.

Season	1991-2005	2006-2020	Change in %
Spring	0.4	0.6	56
Summer	0.6	1.0	51
Autumn	0.4	0.5	30
Winter	0.3	0.4	29

Table 28: Mean rain depth [mm] of events (including dry and wet events) for the reference and main study period.

Season	1991-2005	2006-2020	Change in %
Spring	1.2	1.5	24
Summer	1.8	2.4	34
Autumn	1.2	1.5	23
Winter	0.8	0.9	17

Table 29: Mean rain depth [mm] of weak and moderate events ($0 \text{ mm/h} < \text{RR} < 3.1 \text{ mm/h}$) for both periods.

Season	1991-2005	2006-2020	Change in %
Spring	0.9	1.1	12
Summer	1.0	1.3	27
Autumn	1.0	1.1	13
Winter	0.7	0.9	17

Table 30: Number of all precipitation events ($\text{RR} > 0 \text{ mm/h}$) in the study area for the reference and main study period.

Season	1991-2005	2006-2020	Change in %
Spring	849	1052	12
Summer	958	948	-1
Autumn	942	1048	11
Winter	936	1138	22

Table 31: Average annual number of heavy precipitation events ($\text{RR} > 3.1 \text{ mm/h}$) per season in the study area.

Season	1991-2005	2006-2020	Change in %
Spring	36.8	48.9	33
Summer	103.0	107.0	4
Autumn	27.4	31.7	16
Winter	8.4	8.6	3

5.5 Return periods of daily heavy precipitation maxima

As a final step in the analysis of extreme precipitation in the Greater Vienna region an extreme value analysis was carried out using the peak-over-threshold approach to determine 2- to 200-year return levels of daily heavy precipitation. As already described in Chapter 4.3.2, the calculated threshold value for heavy precipitation days, namely the averaged 98th percentile of

all days in the reference period in the entire study area, is used as the threshold value for the POT analysis. Calculations in Chapter 5.1.1 show that this threshold is 15.0 mm. The generalized pareto distribution (GP) was used to describe the distribution of daily heavy precipitation at each station. The parameters of the GP distribution were estimated using the maximum likelihood method. Before analysing the return periods, the goodness-of-fit of the GP distribution was examined by comparing the modelled and empirical probability density functions (PDF). A selection of plots can be found below. Figure 34 shows the probability density distribution of heavy precipitation days for station Hohe Warte, which has been established the longest and thus has most observations ($n = 1596$). Figure 35 in contrast shows the probability density distribution of HPDs at station Stammersdorf with the least observations ($n = 115$). Naturally, the more observations are available the better the model fits the real distribution, but also for station Stammersdorf the modelled fit seems acceptable. However, estimated return periods should be viewed with caution since the station only has data for the last 12 years. This is also the case for station Brunn am Gebirge. Table 3 in Chapter 4.1 shows how long data are available for each station. The above-mentioned issue of having only limited data for certain stations becomes also evident in Figure 36 and in Figure 37, the modelled fits predict extreme values well except for those most extreme. This makes sense as low- and mid-level extremes are represented more often in the data. This is however only the case if sufficient data are available. For stations like Stammersdorf that have been established only recently and hence only little data are available the model fit is not very strong. Confidence bounds show here a wide range even for short return periods (see Table 32).

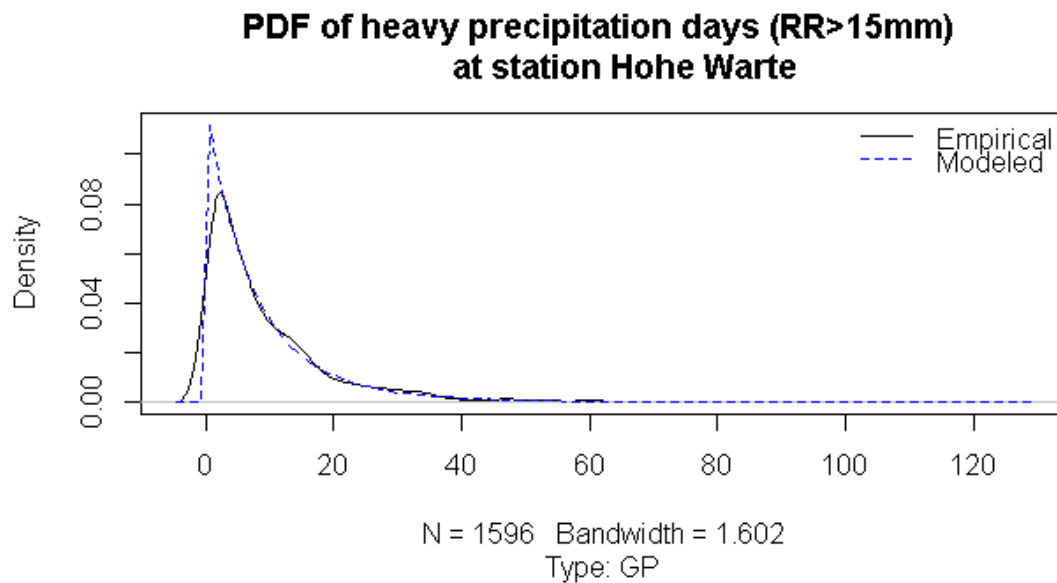


Figure 34: Probability density function (PDF) of the generalized pareto distribution of daily heavy precipitation at station Hohe Warte. Black solid line represents the probabilities of excesses related to the threshold $u = 15\text{mm}$, blue dashed line represents the model distribution that was calculated based on those excesses.

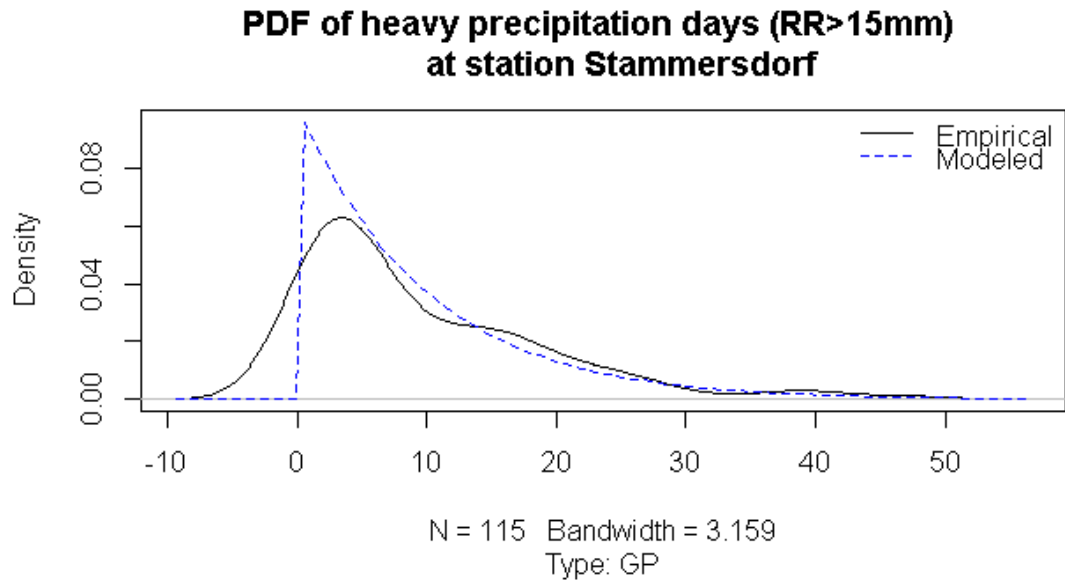


Figure 35: Probability density function (pdf) of the generalized pareto distribution of daily heavy precipitation at station Stammersdorf. Black solid line represents the probabilities of excesses related to the threshold $u = 15\text{mm}$, blue dashed line represents the pdf that was calculated based on those excesses.

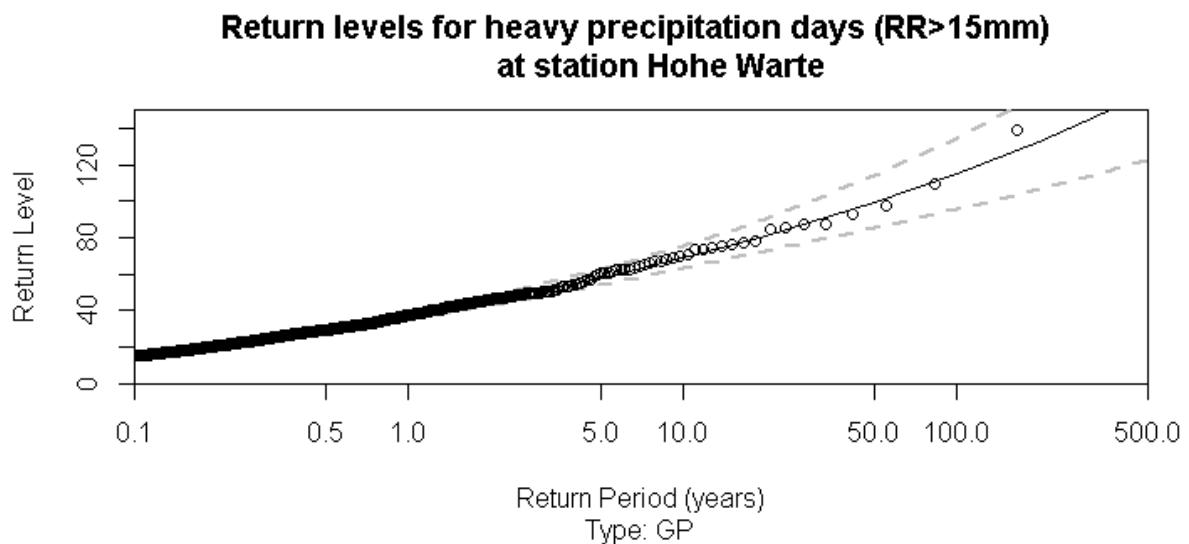


Figure 36: Calculated return levels for different return periods at station Hohe Warte. Confidence bounds are calculated for return periods > 1 year.

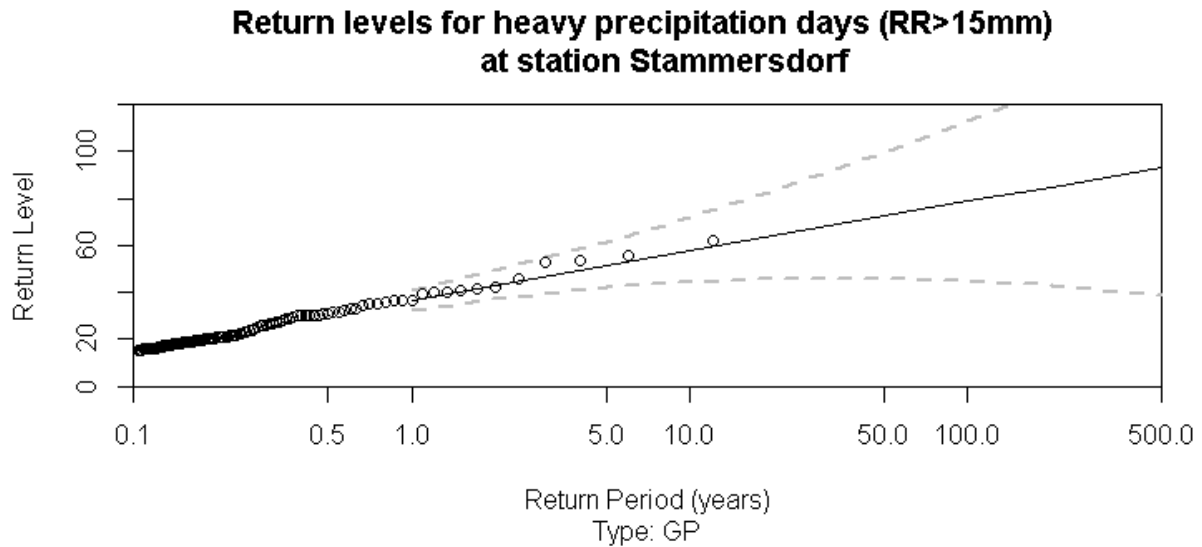


Figure 37: Calculated return levels for different return periods at station Stammersdorf. Confidence bounds are calculated for return periods > 1 year.

After analysing the mean rain rates in the main study period as well as the reference period, it is interesting to see in the next step with which probabilities maxima occur. For this purpose, the return periods of these maxima are determined, and the corresponding probabilities are calculated. The maximum found for station Hohe Warte during the analysis of daily mean rain rates in the main study period equalled to 67.5 mm, this represents a return level that can be found between a 5-to-10-year return period; hence the probability that in any one year this rate is exceeded lies at 10 to 20 %. The same return period is found for the daily maximum at station Stockerau. For most stations, however, the maximum daily precipitation value found in the main study period corresponds to a return level with a return period of 10-to-20 years, hence the chance that this rate is exceeded lies at 5 to 10 %. Station Mariabrunn and station Innere Stadt had the highest maximum values found in the main study period, namely 116 mm and 83.9 mm, respectively. Those values were calculated to have a return period of 20-to-50 years, which means the likelihood that such a rate is exceeded in any one year lies at 2 - 5 %. Interestingly, the maximum mean rain rate at station Unterlaa found in the reference period, namely 84.7 mm, corresponds to a return level with a return period of 100-to-200 years. At the other stations the maxima in the reference period exceeded the maxima of the main study period, and values correspond to a return level with return periods of 20-to-50 years, except at stations Gross-Enzersdorf and Innere Stadt, where maxima in the reference period were smaller than in the main study period and thus correspond to return levels with return periods of 2-to-5 years and 5-to-10 years, respectively. Table 32 shows return levels and return periods for each station.

Table 32: GP ($u_1 = 15\text{mm}$) return levels and return periods for the stations in the study area, 95 % confidence bounds are given in parentheses.

Station	Return period						
	2	5	10	20	50	100	200
Hohe Warte	45.4	58.2	69.1	81.3	99.7	115.4	133.0
	(43.3, 47.6)	(54.2, 62.2)	(63.0, 75.2)	(72.3, 90.3)	(85.5, 113.8)	(96.1, 134.8)	(122.6, 196.4)
Gross-Enzersdorf	41.4	51.6	59.28	67.2	78.1	86.8	95.9
	(39.5, 44.3)	(47.6, 55.6)	(53.5, 64.9)	(59.2, 75.1)	(66.5, 89.8)	(71.6, 102.0)	(76.5, 115.2)
Krems	40.6	50.1	57.6	65.3	76.0	84.4	93.1
	(38.2, 43.1)	(45.9, 54.3)	(51.4, 63.7)	(56.7, 74.0)	(63.0, 88.9)	(67.4, 101.3)	(71.5, 114.7)
Mariabrunn	56.1	73.9	89.9	108.5	137.5	163.6	193.7
	(51.4, 60.8)	(65.0, 82.8)	(76.2, 103.7)	(88.0, 128.9)	(104.6, 170.4)	(117.8, 209.4)	(131.2, 256.2)
Unterlaa	39.1	48.5	56.0	64.1	75.4	84.6	94.4
	(36.3, 42.0)	(43.5, 53.4)	(48.7, 63.4)	(53.5, 74.6)	(59.4, 91.5)	(63.4, 105.9)	(66.8, 122.0)
Innere Stadt	45.3	57.8	68.5	80.5	98.3	113.6	130.6
	(40.6, 49.9)	(49.2, 66.5)	(55.3, 81.8)	(61.1, 99.9)	(67.8, 128.8)	(71.9, 155.2)	(75.0, 186.1)
Donaufeld	41.3	50.9	58.5	66.5	77.7	86.6	95.9
	(36.8, 45.8)	(43.0, 58.8)	(46.8, 70.3)	(49.8, 83.2)	(52.5, 102.8)	(53.5, 119.6)	(53.4, 138.3)
Stockerau	43.9	55.4	65.1	75.8	91.6	104.9	119.6
	(38.6, 49.2)	(45.5, 65.3)	(50.1, 80.1)	(53.8, 97.7)	(57.3, 125.8)	(58.6, 151.3)	(58.3, 181.0)
Brunn am Gebirge	45.2	52.9	58.4	63.6	70.1	74.7	79.1
	(39.4, 50.9)	(44.1, 61.6)	(46.5, 70.2)	(48.1, 79.1)	(49.0, 91.2)	(48.9, 100.5)	(48.3, 110.0)
Stammersdorf	43.2	51.7	58.1	64.4	72.7	78.8	84.9
	(37.1, 49.2)	(41.9, 61.6)	(44.2, 72.0)	(45.5, 83.3)	(45.7, 99.7)	(44.7, 112.9)	(42.8, 127.0)

By definition, the POT approach is highly sensitive to the chosen threshold. Initially, the threshold was based on the threshold definition for daily heavy precipitation used in this thesis. However, this is only an averaged value of the 98th percentile of dry and wet days at all stations in the reference period. Another approach would be to calculate the 98th percentile for each station for the whole period where data are available contrary to the first approach where the 98th percentile was calculated only for the reference period 1979-1993 and using individual thresholds for the POT analysis for each station. The 98th percentiles of different stations range from 15.5 mm to 20.0 mm as can be seen in Table 33. As the thresholds computed do not differ substantially the differences of the calculated return periods are also rather marginal (see Table 34).

Table 33: 98th percentile of daily precipitation [mm] for each station calculated considering both dry and wet days since stations were established.

Station	98th percentile
Hohe Warte	17.2
Gross-Enzersdorf	16.3
Krems	15.5
Mariabrunn	20.0
Unterlaa	15.7
Innere Stadt	17.3
Donaufeld	16.1
Stockerau	17.6
Brunn	18.8
Stammersdorf	17.4

Table 34: GP return levels and return periods for the stations in the study area using individual thresholds for each station (u_2 = 98th percentile of each station), 95 % confidence bounds are given in parentheses.

Station	Return period						
	2	5	10	20	50	100	200
Hohe Warte	45.5	58.1	68.8	80.7	98.5	113.6	130.3
	(43.4, 47.6)	(54.2, 62.0)	(62.7, 74.9)	(71.7, 89.8)	(84.1, 112.9)	(93.8, 133.4)	(103.8, 156.9)
Gross-Enzersdorf	42.0	51.6	59.2	67.1	78	86.6	95.6
	(39.6, 44.4)	(47.7, 55.6)	(53.5, 64.9)	(59.2, 75.1)	(66.2, 89.9)	(71.2, 102.1)	(75.9, 115.3)
Krems	40.6	50.2	57.8	65.7	76.6	85.3	94.4
	(38.1, 43.1)	(45.9, 54.5)	(51.5, 64.1)	(56.7, 74.7)	(63.1, 90.2)	(67.5, 103.2)	(71.5, 117.3)
Mariabrunn	56.0	74.6	91.5	111.4	143.3	172.4	206.6
	(51.3, 60.8)	(65.0, 84.2)	(76.0, 107.0)	(87.3, 135.5)	(102.6, 184.0)	(113.9, 230.8)	(124.6, 288.6)
Unterlaa	39.1	48.5	56.1	64.2	75.7	85.1	95.0
	(36.3, 42.0)	(43.5, 53.5)	(48.6, 63.6)	(53.4, 75.0)	(59.2, 92.3)	(63.0, 107.2)	(66.2, 123.8)
Innere Stadt	45.3	58.1	69.1	81.5	100.1	116.2	134.3
	(40.6, 50.0)	(49.1, 67.1)	(54.9, 83.3)	(60.1, 102.9)	(65.5, 134.7)	(68.2, 164.2)	(69.3, 199.3)
Donaufeld	41.4	50.5	57.6	64.9	74.7	82.4	90.2
	(37.0, 45.7)	(43.1, 57.9)	(46.8, 68.5)	(49.6, 80.2)	(52.0, 97.5)	(52.7, 112.0)	(52.5, 127.8)
Stockerau	43.9	56.0	66.5	78.2	95.8	111.1	128.2
	(38.5, 49.4)	(45.1, 66.9)	(49.0, 83.9)	(51.6, 104.8)	(52.4, 139.3)	(50.5, 171.7)	(45.9, 210.5)
Brunn am Gebirge	45.6	52.2	56.5	60.3	64.6	67.4	69.9
	(39.4, 51.8)	(44.1, 60.2)	(46.5, 66.5)	(47.9, 72.6)	(48.7, 80.5)	(48.6, 86.2)	(48.2, 91.6)
Stammersdorf	43.3	51.3	57.0	62.5	69.3	74.3	79.0
	(37.4, 49.2)	(42.3, 60.3)	(44.6, 79.2)	(45.8, 79.2)	(45.9, 92.8)	(45.0, 103.6)	(43.3, 114.8)

6 Summary and Conclusions

This thesis investigated changes in heavy precipitation in the Greater Vienna region from 2006-2020 using daily as well as 10-minute precipitation data provided by ZAMG. The focus was on 10 stations in and around Vienna. Aside from investigating changes in frequency, mean rain rate, and seasonality, different temporal classifications of heavy precipitation were considered. First, changes in heavy precipitation were examined on a daily basis, i.e., 24h precipitation. This was followed by an analysis of 1h-precipitation on clock time. Furthermore, the approach of calculating rolling hourly totals from 10-minute data and using these for the analysis of 1h heavy precipitation was introduced. This made it possible to identify larger heavy precipitation than with hourly totals based on clock time. Lastly, the method of separating precipitation into events was applied. An event was defined as precipitation with no more than 10 continuous minutes of rainless episodes.

To identify heavy precipitation a threshold was set using the 98th percentile of dry and wet days/hours/events in the reference period (1979-1993 for daily analyses and 1991-2005 for hourly and event-based analyses). This threshold was then used to find heavy precipitation in the main study period. The calculations of the 98th percentile showed that in the Greater Vienna region days exceeding 15 mm of precipitation can be classified as heavy, which is higher than Seibert et al. (2007) calculated for the North-Eastern region of Austria. Furthermore, hourly precipitation exceeding 5.9 mm and event precipitation exceeding 3.1 mm constitutes a heavy hour/event in the study area. Moreover, a correlation analysis of annual, spring and summer precipitation was carried out and 2- to 200-year return levels of daily heavy precipitation were calculated.

The quantitative analysis of precipitation data of the last 30 to 40 years clearly showed an increase in frequency and mean rain rate of heavy precipitation in the last 15 years although results varied for different temporal frameworks for which heavy precipitation has been computed. Although there has not been a change in the number of wet days in the study area, the frequency of heavy precipitation days did increase by 43 % meaning that there are now three heavy precipitation days more per year compared to the reference period (from 7.5 to 10.7 HPDs). In contrast to the increase in frequency, the mean rain rate of heavy precipitation increased only by 7 %, with pronounced increases at station Innere Stadt. Although increases in mean rain rate can be observed in all percentiles of heavy precipitation days at all stations except station Krems, this rate of increase does not apply for the absolute strongest days. In fact, the record precipitation day (120 mm/d) recorded at station Mariabrunn in the reference period was not exceeded at any station in recent years. This predominant increase in frequency rather than mean rain rate coincides with the findings of Myhre et al. (2019) and might be related to the fact that changes in mean rain rate might be constrained by available moisture (Ban, et al., 2015). However, a warming climate might increase moisture in the atmosphere, especially as calculations show that all seasons except winter became wetter in the study area. Overall, changes in seasonal mean daily precipitation in the study area were found to be similar to changes in all of Austria (Blöschl, et al., 2017), except summer (+24 %) and spring (+16 %) precipitation which increased considerably more. Naturally, most heavy precipitation days occurred in summer and the least in winter but increases in the frequency were observed in all seasons except spring, with the biggest increase in autumn. Although mean precipitation in spring increased, the intensity of the individual precipitation days appears to be insufficient to classify them as heavy precipitation. Nevertheless, the question arises if a wetter spring serves as a prerequisite for heavy precipitation later in the year. Indeed, spring precipitation (JFMA) and annual heavy precipitation were found to be moderately correlated for the study area. Although for individual stations correlation was non-significant. Furthermore, spring precipitation and summer (MJJA) heavy precipitation were found to be only weakly correlated for the study area with non-significant correlation for individual stations. Naturally,

annual precipitation and annual heavy precipitation as well as annual summer precipitation and heavy summer precipitation were strongly correlated.

In contrast to heavy precipitation days, the frequency of heavy precipitation hours has increased by 25 %. In absolute terms, however, the increase is similar, namely on average 2 more hours of heavy precipitation per year (from 9.1 to 11.4 HPH). While the number of wet hours remained approximately the same in both periods, mean hourly precipitation increased by 10 % suggesting that some moderate precipitation hours increased in magnitude and are now classified as heavy. Like daily heavy precipitation, mean rain rate of hourly heavy precipitation increased only slightly, namely 6 % which is smaller than could be expected for Vienna according to the calculations of Formayer & Fritz (2017). Although a new record was set for hourly precipitation (50.9 mm/h) at station Gross-Enzersdorf in the main study period, there were only small changes within the percentiles of heavy precipitation and even decreases were observed at some stations. Considerably more hourly heavy precipitation occurred in summer than in other seasons and differences are much more pronounced between seasons than for daily heavy precipitation. Nevertheless, increases in frequency were observed in every season. An exception is station Krems which experienced a decrease in summer heavy precipitation. The largest increase in mean rain rate of hourly heavy precipitation was observed in spring (+15 %). This increase leads to the mean rain rate of spring heavy precipitation being almost as strong as the mean rain rate of summer heavy precipitation and could also explain the increase in mean precipitation in spring (+12 %). Mean precipitation increased similarly in autumn; however, the mean rain rate of hourly heavy precipitation in autumn decreased by 10 %, thus, suggesting that there was an increase in the mean rain rate of weak and moderate precipitation hours. While the mean rain rate of heavy precipitation in autumn has decreased, the number of heavy precipitation hours has increased substantially suggesting that the magnitude of heavy precipitation hours in autumn has decreased.

Further, precipitation was analysed separating it into events. Using the above-mentioned definition of events, 400 precipitation events per year were identified. An increase in the mean rain rate (+11 %) was observed while frequency of precipitation events decreased (-11 %) indicating that the magnitude of event precipitation has increased (mean event rain depth +23 %, mean event duration +12 %). A similar increase of mean event duration was observed for heavy precipitation events while mean rain depth of heavy events increased by 13 %. While the increase in frequency of heavy precipitation events was the smallest in relative terms (+10 %) compared to daily and hourly precipitation, it is a similar increase in absolute terms, namely 2.5 heavy events more (from 22.0 to 24.5 heavy events). While the increase in frequency seems to be the smallest for heavy precipitation events, mean rain rate increased the most for this temporal framework (+12 %). The record event in the reference period (58.2 mm/h at station Gross-Enzersdorf) was far exceeded by an event at station Brunn am Gebirge (91.8 mm/h) in the main period. However, no other such extraordinary event was recorded, and most heavy precipitation events have less than 8 mm/h of precipitation. Nevertheless, mean rain rate increased in all percentiles for most stations. Although the strongest 25 % of events at station Krems got weaker the station is still among those with the highest mean rain rates among the stations analysed.

Lastly, return periods of daily heavy precipitation were calculated using the Peak-over-Threshold approach. Results show that maxima of daily precipitation found in the main study period correspond to a return level with a return period of 10-to-20 years at most stations while most maxima found in the reference period correspond to return levels with return periods of 20-to-50 years. Naturally, confidence is high for stations with longer precipitation records as well as for return levels with shorter return periods.

The results illustrate the importance of considering both frequency and mean rainfall rate when analysing changes in heavy precipitation. The largest increase in heavy precipitation frequency

was found for heavy precipitation days and the smallest for heavy precipitation events. Generally, heavy precipitation frequency increased considerably more than the mean rain rate except for heavy precipitation events where increases were similar but slightly stronger for the mean rain rate. While the reference and main study period of hourly analyses fall within phases of decreased and increased convective activity in Austria (Blöschl, et al., 2017), increases in mean rain rate are similar to daily heavy precipitation where both periods are within phases of increased convective activity. This suggests that these phases may not have been so prominent in the Greater Vienna region or may not have had as much influence on the changes in mean rainfall rates. Furthermore, it was noticeable that station Krems often had opposite tendencies (increases/decreases) compared to other stations. This suggests that this station cannot be considered fully representative for the Greater Vienna region.

Although it is common to analyse heavy precipitation on a daily basis, sometimes also on an hourly basis, this thesis has shown that the classification as an event can combine both time units. Certainly, there are some disadvantages to using an event-based approach such as the dependence of results on the definition used to identify events and therefore less comparability across studies. But there are many advantages to it as well. For instance, the definition of an event can be adapted to the study region/ -subject. Moreover, sub-hourly, sub-daily, and multi-day precipitation is combined into one analysis and events of different time length are made comparable through the calculation of the mean rain rate by dividing event rain depth by event duration. Contrary to the approach used for the hourly analysis in this thesis, all 10-minute precipitation measurements are included while at the same time picturing the true mean rain rate of precipitation. Moreover, using 10-minute data also made it possible to identify heavy precipitation events that lasted less than an hour.

Even though hourly precipitation measurements, that are available for longer periods, exist, it has been shown that the use of rolling sums formed with 10-minute values for hourly analyses illustrates higher precipitation intensities better than hourly precipitation that is oriented according to the clock time. Nevertheless, the analysis of hourly heavy precipitation with rolling totals also shows limitations. To avoid overlapping of rolling totals, only the maximum sum per day was selected to calculate thresholds resulting in a rather high threshold for heavy precipitation hours. This becomes particularly clear in comparison with the threshold for heavy precipitation events, which is only half as large, although events last less than two hours on average. In the future, rolling totals could be used for the analysis of heavy precipitation hours while hourly precipitation based on clock time could be used for the calculation of thresholds. A further limitation in this thesis is that 10-minute data sometimes miss measurements thus not allowing to include all heavy precipitation that was identified with daily precipitation measurements. While it is not clear for hourly and event heavy precipitation if increases are due to the reference period falling within a phase of reduced convective activity while the main study period is partly within a phase of high convective activity, using an earlier reference period was only possible for daily analyses. Mainly because daily precipitation measurements are available for longer periods, while 10-minute data are only available for a relatively short period of time.

This thesis was mainly concerned with the question of the extent to which heavy precipitation has increased in the Greater Vienna region. The potentially detrimental effects of this increase on the metropolis of Vienna and the neighbouring Marchfeld, which has high agricultural importance for Austria, could be a potential direction for future research. While this thesis used a short MIT to define events, future studies could explore the impact of different and longer MITs, especially as several studies found that longer events produce higher mean rain rates (Dunkerley, 2008b). Also, it was assumed that the fraction of rainless periods within an event was small, and, thus, a short MIT was used. As the intra-event rainfall intermittency is an indication of intensity, i.e., the higher the percentage of rainless periods within an event the higher the intensity when it rains, future studies could explore if intra-event rainfall intermittency of events with short MITs is indeed low and hence mean rainfall rates are characterising the

intensity of events appropriately. Further, differences between the main study period and the reference period have been partially established as mean across the study region, which complicates the testing for significant differences. Therefore, for future work also an analysis focussing on time-binned information on station basis is suggested to explore the significance of changes in (heavy) precipitation.

References

- Ali, K. S. & Said, M. H., 2009. *Determination of Radar Z-R Relationship For Libya – Tripoli City*. London, UK, World Congress on Engineering.
- Allen, M. R. & Ingram, W. J., 2002. Constraints on future changes in climate and the hydrologic cycle. *NATURE*, Volume 419, p. 224–232.
- AMS, 2012. *Glossary of Meteorology - equivalent reflectivity factor*. [Online] Available at: https://glossary.ametsoc.org/wiki/Equivalent_reflectivity_factor [Accessed 21 07 2021].
- AMS, 2017. *Glossary of Meteorologie - radar reflectivity factor*. [Online] Available at: https://glossary.ametsoc.org/wiki/Radar_reflectivity_factor [Accessed 14 07 2021].
- Ban, N., Schmidli, J. & Schär, C., 2015. Heavy precipitation in a changing climate: Does short term summer precipitation increase faster?. *Geophysical Research Letters*, Volume 42, pp. 1165-1172.
- Beniston, M. et al., 2007. Future extreme events in European climate: an exploration of regional climate model projections. *Climatic Change*, pp. 71-95.
- Blöschl, G. et al., 2018. Auswirkungen der Klimaänderung auf Österreichs Wasserwirtschaft – ein aktualisierter Statusbericht. *Österr Wasser- und Abfallw*, Volume 70, p. 462–473.
- Blöschl, G. et al., 2017. *Klimawandel in der Wasserwirtschaft - Follow up zur ZAMG/TU-Wien Studie (2011) Anpassungsstrategien an den Klimawandel für Österreichs Wasserwirtschaft im Auftrag von Bund und Ländern*, Vienna: Bundesministerium für Land- und Forstwirtschaft, Umwelt und Wasserwirtschaft.
- Breugem, A., Wesseling, J., Oostindie, K. & Ritsema, C., 2020. Meteorological aspects of heavy precipitation in relation to floods – An overview. *Earth-Science Reviews*, Volume 204, p. 103171.
- Bührke, T., 2004. *Satellitendaten für den täglichen Einsatz*. Bonn: Deutsches Zentrum für Luft- und Raumfahrt e.V..
- Český hydrometeorologický ústav, 2003. *Návod pro pozorovatele meteorologických stanic (instructions for observers at the meteorological stations)*. Ostrava, Czech Republic: Český hydrometeorologický ústav.
- Charras-Garrido, M. & Lezaud, P., 2013. Extreme Value Analysis: an Introduction. *Journal de la Société Française de Statistique*, 154(2), pp. 66-97.
- Chimani, B. et al., 2016. *ÖKS15 – Klimaszenarien für Österreich. Daten, Methoden und Klimaanalyse.*, Vienna: s.n.
- Copernicus, 2021. *Widespread European flooding, July 2021*. [Online] Available at: <https://www.efas.eu/en/news/widespread-european-flooding-july-2021> [Accessed 13 12 2021].

- Dankers, R. & Hiederer, R., 2008. *Extreme Temperatures and Precipitation in Europe: Analysis of a High-Resolution Climate Change Scenario*, Luxembourg: Office for Official Publications of the European Communities.
- Davison, A. C., 2005. Extreme Values. In: P. Armitage & T. Colton, eds. *Encyclopedia of Biostatistics*. Chichester: John Wiley & Sons, Ltd, pp. 1877-1882.
- Dhiram, K. & Wang, Z., 2016. Evaluation on Radar Reflectivity-Rainfall Rate (Z-R) Relation-ships for Guyana. *Atmospheric and Climate Sciences*, Volume 6, pp. 489-499.
- Dr. Alfred Müller Meteorologische Instrumente KG , 2020. *Dr.A.Müller - Meteorologische Instrumente KG - R.Fuess* -. [Online]
Available at: <http://www.rfuess-mueller.de/221-0E.pdf>
[Accessed 23 06 2021].
- Dunkerley, D., 2008a. Identifying individual rain events from pluviograph records: A review with analysis of data from an Australian dryland site. *Hydrological Processes*, 22(26), p. 5024–5036.
- Dunkerley, D., 2008b. Rain event properties in nature and in rainfall simulation experiments: A comparative review with recommendations for increasingly systematic study and reporting. *Hydrological Processes*, 22(22), p. 4415–4435.
- Dunkerley, D., 2015. Intra-event intermittency of rainfall: an analysis of the metrics. *Hydrological Processes*, 29(15), p. 3294–3305.
- DWD, n.d. a. *Messinstrumente der Meteorologie - Weterradar in Deutschland*. Offenbach: Deutscher Wetterdienst (DWD).
- DWD, n.d. b. *Wetter- und Klimalexikon*. [Online]
Available at:
<https://www.dwd.de/DE/service/lexikon/Functions/glossar.html?nn=103346&lv2=102134&lv3=714506>
[Accessed 12 07 2021].
- Eddy, M., Ewing, J., Specia, M. & Erlanger, S., 2021. European Floods Are Latest Sign of a Global Warming Crisis. *The New York Times*, 16 July.
- Eggert, B. et al., 2015. Temporal and spatial scaling impacts on extreme precipitation. *Atmospheric Chemistry and Physics*, 15(10), p. 5957–5971.
- Formayer, H. & Fritz, A., 2017. Temperature dependency of hourly precipitation. *International journal of climatology*, 37(1), p. 1–10.
- Formayer, H. & Kromp-Kolb, H., 2009. *Hochwasser und Klimawandel. Auswirkungen des Klimawandels auf Hochwasserereignisse in Österreich.*, Vienna: World Wide Nature Fund.
- Frei, C. et al., 2006. Future change of precipitation extremes in Europe: Intercomparison of scenarios from regional climate models. *Journal of Geophysical Research*, Volume 111, p. D06105.
- Gandini, A. et al., 2020. A holistic and multi-stakeholder methodology for vulnerability assessment of cities to flooding and extreme precipitation events. *Sustainable Cities and Society*, Volume 63, p. 102437.

- Gilli, M. & K llezi, E., 2006. An Application of Extreme Value Theory for Measuring Financial Risk. *Computational Economics*, 27(1), pp. 1-23.
- Gomes, M. I. & Guillou, A., 2015. Extreme Value Theory and Statistics of Univariate Extremes: A Review. *International Statistical Review*, 83(2), pp. 263-292.
- Groenemeijer, P. et al., 2015. *Past Cases of Extreme Weather Impact on Critical Infrastructure in Europe*, Wessling, Germany: European Severe Storms Laboratory e.V..
- Hajat, S., Menne, B., Ebl, K. & Edwards, S., 2003. The human health consequences of flooding in Europe and the implications for public health: a review of the evidence. *Applied Environmental Science and Public Health*, 1(1), pp. 13-21.
- Halmova, D. et al., 2015. Precipitation Regime and Temporal Changes in the Central Danubian Lowland Region. *Advances in Meteorology*.
- H ssler-Kiefhaber, D. & Lorig, R., 2018. Hochwasservorsorgekonzept f r starkregengesch digte Gemeinden. In: S. Heimerl, ed. *Vorsorgender und nachsorgender Hochwasserschutz*. Wiesbaden: Springer Vieweg, pp. 37-43.
- Hiebl, J. & Frei, C., 2018. Daily precipitation grids for Austria since 1961—development and evaluation of a spatial dataset for hydroclimatic monitoring and modelling. *Theor Appl Climatol*, Volume 132, p. 327–345.
- Hofst tter, M. & Matulla, C., 2010. *Prisk-Change. Ver nderung des Risikos extremer Niederschlagsereignisse als Folge des Klimawandels.*, Vienna: ZAMG.
- Hoft tter, M. & Chimani, B., 2012. Van Bebb r’s cyclone tracks at 700 hPa in the Eastern Alps or 1961–2002 and their comparison to Circulation Type Classifications. *Meteorologische Zeitschrift*, 21(5), pp. 459-473.
- IPCC, 2007. *Climate Change 2007: The Physical Science Basis. Contribution of Working Group I to the Fourth Assessment Report of the Intergovernmental Panel on Climate Change*, Cambridge, United Kingdom and New York, NY, USA,: [Solomon, S., D. Qin, M. Manning, Z. Chen, M. Marquis, K.B. Averyt, M. Tignor and H.L. Miller (eds.)].
- IPCC, 2013. *Climate Change 2013: The Physical Science Basis. Contribution of Working Group I to the Fifth Assessment Report of the Intergovernmental Panel on Climate Change*, Cambridge, United Kingdom and New York, NY, USA: Stocker, T.F., D. Qin, G.-K. Plattner, M. Tignor, S.K. Allen, J. Boschung, A. Nauels, Y. Xia, V. Bex and P.M. Midgley (eds.).
- IPCC, 2014. *Climate Change 2014: Synthesis Report. Contribution of Working Groups I, II and III to the Fifth Assessment Report of the Intergovernmental Panel on Climate Change*, Geneva, Switzerland: [Core Writing Team, R.K. Pachauri and L.A. Meyer (eds.)].
- IPCC, 2021. *Climate Change 2021: The Physical Science Basis. Contribution of Working Group I to the Sixth Assessment Report of the Intergovernmental Panel on Climate Change*, Cambridge University Press: Masson-Delmotte, V., P. Zhai, A. Pirani, S.L. Connors, C. P  an, S. Berger, N. Caud, Y. Chen, L. Goldfarb, M.I. Gomis, M. Huang, K. Leitzell, E. Lonnoy, J.B.R. Matthews, T.K. Maycock, T. Waterfield, O. Yelek i, R. Yu, and B. Zhou.

- Isotta, F. A. et al., 2014. The climate of daily precipitation in the Alps: development and analysis of a high-resolution grid dataset from pan-Alpine rain-gauge data. *International journal of climatology*, 34(5), p. 1657–1675.
- Junghändel, T. et al., 2021. *Hydro-klimatologische Einordnung der Stark- und Dauerniederschläge in Teilen Deutschlands im Zusammenhang mit dem Tiefdruckgebiet „Bernd“ am 12. bis 19. Juli 2021*, s.l.: Deutscher Wetterdienst.
- Knapp, A. K. et al., 2008. Consequences of more extreme precipitation regimes for terrestrial ecosystems. *Bioscience*, 58(9), p. 811.
- Kuleshov, Y. et al., 2020. WMO Space-based Weather and Climate Extremes Monitoring Demonstration Project for East Asia and Western Pacific. *Bulletin*, 69(1).
- Lake, I. R. & Barker, G. C., 2018. Climate Change, Foodborne Pathogens and Illness in Higher-Income Countries. *Current Environmental Health Reports*, Volume 5, pp. 187-196.
- Lehmann, J., Coumou, D. & Frieler, K., 2015. Increased record-breaking precipitation events under global warming. *Climatic Change Letters*, 132(4), pp. 501-515.
- Lenderink, G. & van Meijgaard, E., 2010. Linking increases in hourly precipitation extremes to atmospheric temperature and moisture changes. *Environmental Research Letters*, Volume 5, p. 025208.
- Lopez, J. C. B. & Villaruz, H. M., 2015. *Low-Cost Weather Monitoring System with Online Logging and Data Visualization*. Cebu, Philippines, School of Computer Studies, MSU-Iligan Institute of Technology.
- Mapiam, P. P. & Sriwongsit, N., 2008. Climatological Z-R relationship for radar rainfall estimation in the upper Ping river basin. *ScienceAsia*, Volume 34, p. 215–222.
- Mason, B. J. et al., n.d. *Climate*. *Encyclopedia Britannica*. [Online]
Available at: <https://www.britannica.com/science/climate-meteorology/Precipitation>
[Accessed 23 3 2021].
- Messmer, M., Gómez-Navarro, J. J. & Raible, C. C., 2015. Climatology of Vb cyclones, physical mechanisms and their impact on extreme precipitation over Central Europe. *Earth System Dynamics*, Volume 6, p. 541–553.
- Müller, E., Müller, U., Schmidt, W. & Nitzsche, O., 2018. Gute landwirtschaftliche Praxis für die Hochwasservorsorge. In: S. Heimerl, ed. *Vorsorgender und nachsorgender Hochwasserschutz*. Wiesbaden: Springer Vieweg, pp. 225-230.
- Myhre, G. et al., 2019. Frequency of extreme precipitation increases extensively with event rareness under global warming. *Scientific Reports*, 9(1), pp. 16063-10.
- O'Dwyer, J., Dowling, A. & Adley, C., 2016. The Impact of Climate Change on the Incidence of Infectious Waterborne Disease. In: S. Eslamian, ed. *The Urban Water Reuse Handbook*. Boca Raton: Taylor & Francis, pp. 1017-1026.
- Pehsl, C., 2021. *Wetterlexikon | Gewitter: Faszination und Gefahr*. [Online]
Available at: <https://www.zamg.ac.at/cms/de/aktuell/schon->

[gewusst/wetterlexikon/wetterphaenomen-als-nachricht](#)

[Accessed 26 07 2021].

Piroth, K., 2018. Starkniederschläge: Umsetzungs aspekte in der praktischen Planung. In: S. Heimerl, ed. *Vorsorgender und nachsorgender Hochwasserschutz*. Wiesbaden: Springer Vieweg, pp. 303-308.

Pröbstl-Haider, U., Lund-Durlacher, D., Olefs, M. & Prettenthaler, F., 2020. *Tourismus und Klimawandel; Österreichischer Special Report Tourismus und Klimawandel*. Heidelberg: Springer Verlag Berlin.

Puca, S. et al., 2021. *Devastating floods in western Europe*. [Online]
Available at: <https://www.eumetsat.int/devastating-floods-western-europe>
[Accessed 13 12 2021].

Ramli, S. & Tahir, W., 2011. Radar Hydrology: New Z/R Relationships for Quantitative Precipitation Estimation in Klang River Basin, Malaysia. *International Journal of Environmental Science and Development*, Volume 2, pp. 223 -227.

Rosenzweig, C. et al., 2002. Increased crop damage in the US from excess precipitation under climate change. *Global Environmental Change*, Volume 2, pp. 197-202.

Schöll, E. M. & Hille, M., 2020. Heavy and persistent rainfall leads to brood reduction and nest failure in a passerine bird. *Journal of Avian Biology*, 51(7).

Seibert, P., Frank, A. & Formayer, H., 2007. Synoptic and regional patterns of heavy precipitation in Austria. *Theoretical and Applied Climatology*, 87(1-4), p. 139–153.

Seidel, P., 2014. Extremwetterlagen und Auswirkungen auf Schaderreger – extreme Wissenslücken. Weizen, Gerste, Mais, Raps, Kartoffel, Zuckerrübe, Ackerfutterpflanzen und Grünland. *Gesunde Pflanzen*, Volume 66, pp. 83-92.

Stadt Krems, 2021. *Krems in Zahlen*. [Online]
Available at: <https://www.krems.at/wirtschaft/wirtschaft/krems-in-zahlen>
[Accessed 30 11 2021].

Stadt Wien, 2019. *Wiener Stadtgebiet 2019 - Geografische Eckdaten*. [Online]
Available at: <https://www.wien.gv.at/statistik/lebensraum/tabellen/stadtgebiet-eckdaten.html>
[Accessed 29 12 2020].

Stadt Wien, 2021a. *10-jährliches Hochwasser: Wiener Donauinsel sorgt für Hochwasserschutz der Millionenstadt*. [Online]
Available at: <https://www.wien.gv.at/presse/2021/07/21/10-jaehrliches-hochwasser-wiener-donauinsel-sorgt-fuer-hochwasserschutz-der-millionenstadt>
[Accessed 15 12 2021].

Stadt Wien, 2021b. *Überschwemmungen*. [Online]
Available at: <https://www.geschichtewiki.wien.gv.at/index.php?title=%C3%9Cberschwemmungen>
[Accessed 15 12 2021].

Stadt Wien, s.a. a. *Wie der Donau-Hochwasserschutz funktioniert*. [Online]
Available at: <https://www.wien.gv.at/umwelt/gewaesser/hochwasserschutz/donau/funktion.html>
[Accessed 15 12 2021].

Stadt Wien, s.a. b. *"Schwammstadt" macht Bäume für den Klimawandel fit*. [Online]
Available at: <https://www.wien.gv.at/umwelt/cooleswien/schwammstadt.html>
[Accessed 29 11 2021].

Stadt Wien, s.a. c. *Sustainable rainwater management for the Smart City*. [Online]
Available at: <https://smartcity.wien.gv.at/en/viennas-dual-infiltration-model/>
[Accessed 29 11 2021].

Stadtgemeinde Stockerau, s.a. *Services*. [Online]
Available at:
<https://www.stockerau.at/system/web/fakten.aspx?detailonr=172953087&menuonr=225680210&noseo=1>
[Accessed 30 11 2021].

Statistik Austria, 2020. *Endgültige Bevölkerungszahl für das finanzjahr 2021 je Gemeinde (Gebietsstand 2020)*. [Online]
Available at:
http://www.statistik.at/wcm/idc/idcplg?IdcService=GET_PDF_FILE&RevisionSelectionMethod=LatestReleased&dDocName=124329
[Accessed 01 12 2021].

Statistik Austria, 2021. *Datenbank: Bevölkerung zu Jahresbeginn ab 2002 (einheitlicher Gebietsstand 2020)*. [Online]
Available at: <https://statcube.at/statistik.at/ext/statcube/jsf/tableView/tableView.xhtml>
[Accessed 17 12 2021].

Strangeways, I., 2006. *Precipitation: Theory, Measurement and Distribution*. Cambridge: Cambridge University Press.

Tagesschau, 2021. *Mehr als 29 Milliarden Euro Schaden*. [Online]
Available at: <https://www.tagesschau.de/inland/flutkatastrophe-107.html>
[Accessed 14 12 2021].

Tataw, J. T. et al., 2016. Climate change induced rainfall patterns affect wheat productivity and agroecosystem functioning dependent on soil types. *Ecological Research*, 31(2), pp. 203-212.

Tataw, T. J. et al., 2014. Soil types will alter the response of arable agroecosystems to future rainfall patterns. *Annals of Applied Biology*, 164(1), pp. 35-45.

Teschl, F., Randeu, W. L. & Schönhuber, M., 2005. *Z to R relationships for snowfall-events in Austria, determined by modelling winterly precipitation particles realistically*. Albuquerque, 32nd Conference on Radar Meteorology - American Meteorological Society .

The R foundation, s.a.. *The R Project for Statistical Computing*. [Online]
Available at: <https://www.r-project.org/>
[Accessed 07 01 2022].

Trenberth, K. E., 1999. Conceptual Framework for changes of extremes of the hydrological cycle with climate change. *Climatic Change*, Volume 42, pp. 327-339.

UN, 2016. *Report: Inequalities exacerbate climate impacts on poor*. [Online]
Available at: <https://www.un.org/sustainabledevelopment/blog/2016/10/report-inequalities->

exacerbate-climate-impacts-on-poor/

[Accessed 12 11 2021].

UNFCCC, 2007. *Climate Change: Impacts, vulnerabilities and adaptation in developing countries*. Bonn, Germany: UNFCCC.

Villarini, G., Smith, J. A., Ntelekos, A. A. & Schwarz, U., 2011. Annual maximum and peaks-over-threshold analyses of daily rainfall accumulations for Austria. *Journal of Geophysical Research*, Volume 116.

Weilhammer, V. et al., 2021. Extreme weather events in Europe and their health consequences – A systematic review. *International Journal of Hygiene and Environmental Health*, Volume 223, p. 113688.

Westra, S., Alexander, L. V. & Zwiers, F. W., 2013. Global Increasing Trends in Annual Maximum Daily Precipitation. *Journal of Climate*, 26(11), pp. 3904-3918.

WKO, 2021. *Bedeutung der Forst- und Holzwirtschaft für Österreichs Wirtschaft*. [Online]
Available at: <https://news.wko.at/news/oesterreich/Bedeutung-der-Forst--und-Holzwirtschaft-fuer-Oesterreichs.html>

[Accessed 03 08 2021].

WMO, 2011. *Manual on Codes*. 2019 ed. Geneva, Switzerland: World Meteorological Organization.

WMO, 2017. *Glossary*. [Online]

Available at: <https://cloudatlas.wmo.int/en/glossary.html>

[Accessed 07 01 2022].

WMO, 2018a. *Guide to Instruments and Methods of Observation. Volume I – Measurement of Meteorological Variables*. Switzerland: World Meteorological Organization (WMO).

WMO, 2018b. *Guide to Instruments and Methods of Observation - Volume IV – Space-based Observations*. Geneva, Switzerland: World Meteorological Organization.

WMO, 2018c. *Guide to Instruments and Methods of Observation - Volume II – Measurement of Cryospheric Variables*. Geneva, Switzerland: World Meteorological Organization.

WMO, 2020. *Aviation | Hazards | Precipitation*. [Online]

Available at: <https://community.wmo.int/activity-areas/aviation/hazards/precipitation>

[Accessed 8 3 2021].

Woollings, T. et al., 2018. Blocking and its Response to Climate Change. *Current Climate Change Reports*, Volume 4, p. 287–300.

World Health Organization, n.d.. *Flooding and communicable diseases fact sheet*. [Online]

Available at:

<https://www.who.int/hac/techguidance/ems/FloodingandCommunicableDiseasesfactsheet.pdf>

[Accessed 12 10 2021].

ZAMG, 2019. *Welttag der Meteorologie: Österreich sehr aktiver Teil der meteorologischen Weltgemeinschaft*. [Online]

Available at: <https://www.zamg.ac.at/cms/de/aktuell/news/welttag-der-meteorologie-oesterreich->

sehr-aktiver-teil-der-meteorologischen-weltgemeinschaft

[Accessed 26 07 2021].

ZAMG, s.a. a. *Klimamittel*. [Online]

Available at: <https://www.zamg.ac.at/cms/de/klima/informationsportal-klimawandel/daten-download/klimamittel>

[Accessed 01 12 2021].

ZAMG, s.a. b. *Wetterstationen*. [Online]

Available at: <https://www.zamg.ac.at/cms/de/klima/messnetze/wetterstationen>

[Accessed 18 12 2020].

ZAMG, s.a. c. *Datenprüfung*. [Online]

Available at: <https://www.zamg.ac.at/cms/de/klima/messnetze/datenpruefung>

[Accessed 01 12 2021].

ZDF, 2021. *Hochwasser-Katastrophe - Ahrtal: Flut-Opferzahl nach unten korrigiert*. [Online]

Available at: <https://www.zdf.de/nachrichten/panorama/ahrtal-tote-fluten-hochwasser-100.html>

[Accessed 14 12 2021].

Zeder, J. & Fischer, E. M., 2020. Observed extreme precipitation trends and scaling in Central Europe. *Weather and Climate Extremes*, Volume 29, p. 100266.

Zevenberger, C., Fu, D. & Pathirana, A., 2018. Transitioning to Sponge Cities: Challenges and Opportunities to Address Urban Water Problems in China. *Water*, Volume 10, p. 1230.

Table of Figures

FIGURE 1: REGIONS IN AUSTRIA WITH SIMILAR DAILY PRECIPITATION IDENTIFIED THROUGH CLUSTERING BY SEIBERT ET AL. (2007) FOR A) THE WHOLE YEAR, B) THE SUMMER HALF-YEAR AND C) THE WINTER HALF-YEAR. DIFFERENT PRECIPITATION REGIONS INDICATED BY GREY SHADING; WHITE LINES MARK THE FEDERAL STATES OF AUSTRIA. CORRELATION OF STATIONS WITH OTHERS OF THEIR CLUSTERS IS REPRESENTED BY CROSSES.	6
FIGURE 2: SCHEMATIC REPRESENTATION OF A TYPICAL MANUAL NON-RECORDING RAIN GAUGE AND ITS COMPONENTS (ČESKÝ HYDROMETEOROLOGICKÝ ÚSTAV, 2003, MODIFIED).....	15
FIGURE 3: SCHEMATIC REPRESENTATION OF A FLOAT-OPERATING MECHANICAL RECORDING RAIN GAUGE. (A) APERTURE RING, (B) FLOAT VESSEL, (C) FLOAT, (D) CONTAINER, (H) SIPHON, (K) COLLECTING VESSEL, (Z) PEN ARM (DR. ALFRED MÜLLER METEOROLOGISCHE INSTRUMENTE KG, 2020).	16
FIGURE 4: SCHEMATIC REPRESENTATION OF A WEIGHT-OPERATED MECHANICAL RECORDING RAIN GAUGE (STRANGEWAYS, 2006). .	16
FIGURE 5: SCHEMATIC REPRESENTATION OF A TIPPING BUCKET TYPE RAIN GAUGE (LOPEZ & VILLARUZ, 2015, MODIFIED).	17
FIGURE 6: SCHEMATIC REPRESENTATION OF THE OPERATING PRINCIPLE OF A WEATHER RADAR. OUTGOING RADAR SIGNALS ARE REFLECTED BY PRECIPITATION AND RETURNED TO THE RADAR DISH (OWN ILLUSTRATION).	19
FIGURE 7: PASSIVE MICROWAVE EMISSIONS FROM LAND, SEA AND HYDROMETEORS BEING EMITTED, SCATTERED OR ABSORBED AND EVENTUALLY RECEIVED BY THE SATELLITE. EMISSIVITY DESCRIBES HOW EFFECTIVELY A SURFACE CAN EMIT RADIATION (STRANGEWAYS, 2006, MODIFIED).	21
FIGURE 8: THE OPERATING PRINCIPLE OF A PRECIPITATION SATELLITE RADAR ACTIVELY EMITTING MICROWAVES, WHICH PRODUCES THREE ECHOS: REFLECTED FROM (A) PRECIPITATION, (B) THE GROUND, AND (C) SCATTERED BY PRECIPITATION AND REFLECTED FROM THE GROUND (MIRROR-IMAGE ECHO). (D) REPRESENTS THE STRENGTH OF THE ECHO THROUGH A PRECIPITATION FREE ATMOSPHERE AND IS FOR COMPARISON WITH (B) TO ESTIMATE HOW MUCH THE SIGNAL IS ATTENUATED BY TRAVELLING THROUGH PRECIPITATION (STRANGEWAYS, 2006, MODIFIED).....	21
FIGURE 9: METEOROLOGICAL MEASUREMENT NETWORK OF THE ZAMG IN AUSTRIA, RED RECTANGLE REPRESENTING THE STUDY AREA (ZAMG S.A. B, MODIFIED).	24
FIGURE 10: STATIONS USED IN THESIS MARKED WITH RED CROSSES (ZAMG S.A. B, MODIFIED).	24
FIGURE 11: OCCURRENCE OF HEAVY PRECIPITATION DAYS (>15MM/D) ACROSS ALL STATIONS FOR 2006-2020.	38
FIGURE 12: STRONGEST TWENTY HEAVY PRECIPITATION DAYS AT EACH STATION FROM 2006 - 2020, BRUNN AM GEBIRGE AND STAMMERSDORF FROM 2008-2020.	38
FIGURE 13: OCCURRENCE OF HEAVY PRECIPITATION DAYS (>15MM/D) ACROSS ALL STATIONS FOR 1979-1993.	39
FIGURE 14: STRONGEST TWENTY HEAVY PRECIPITATION DAYS AT EACH STATION IN THE REFERENCE PERIOD FROM 1979-1993, INNERE STADT FROM 1985-1993.	39
FIGURE 15: SEASONAL FRACTION OF HEAVY PRECIPITATION DAYS PER YEAR IN 2006-2020. NOTE, THAT STATION BRUNN WAS ONLY ESTABLISHED AT THE END OF 2008.	42
FIGURE 16: CORRELATION OF TOTAL ANNUAL PRECIPITATION AND ANNUAL HEAVY PRECIPITATION IN MM IN THE STUDY AREA. SIGNIFICANCE ACCEPTED AT ALPHA = 0.05.	43
FIGURE 17: CORRELATION OF TOTAL ANNUAL PRECIPITATION [MM] AND ANNUAL NUMBER OF HEAVY PRECIPITATION DAYS IN THE STUDY AREA. SIGNIFICANCE ACCEPTED AT ALPHA = 0.05.	44
FIGURE 18: CORRELATION OF SPRING PRECIPITATION AND ANNUAL HEAVY PRECIPITATION IN MM IN THE STUDY AREA. SIGNIFICANCE ACCEPTED AT ALPHA = 0.05.	45
FIGURE 19: CORRELATION OF SPRING PRECIPITATION [MM] AND ANNUAL NUMBER OF HEAVY PRECIPITATION DAYS IN THE STUDY AREA. SIGNIFICANCE ACCEPTED AT ALPHA = 0.05.	45
FIGURE 20: CORRELATION OF SPRING PRECIPITATION AND ANNUAL HEAVY SUMMER PRECIPITATION IN MM IN THE STUDY AREA. SIGNIFICANCE ACCEPTED AT ALPHA = 0.05.	46
FIGURE 21: CORRELATION OF SPRING PRECIPITATION [MM] AND ANNUAL NUMBER OF HEAVY PRECIPITATION DAYS IN SUMMER IN THE STUDY AREA. SIGNIFICANCE ACCEPTED AT ALPHA = 0.05.	46
FIGURE 22: CORRELATION OF SUMMER PRECIPITATION AND ANNUAL HEAVY PRECIPITATION IN SUMMER IN MM IN THE STUDY AREA. SIGNIFICANCE ACCEPTED AT ALPHA = 0.05.	47
FIGURE 23: CORRELATION OF SUMMER PRECIPITATION [MM] AND ANNUAL NUMBER OF HEAVY PRECIPITATION DAYS IN SUMMER IN THE STUDY AREA. SIGNIFICANCE ACCEPTED AT ALPHA = 0.05.	47

FIGURE 24: OCCURRENCE OF HEAVY PRECIPITATION HOURS, 2006-2020. NOTE, STATIONS BRUNN AM GEBIRGE AND STAMMERSDORF RECORDED DATA ONLY SINCE LATE 2008.	53
FIGURE 25: STRONGEST TWENTY HEAVY PRECIPITATION HOURS AT EACH STATION 2006-2020. NOTE, STATIONS BRUNN AM GEBIRGE AND STAMMERSDORF RECORDED DATA ONLY SINCE LATE 2008.	53
FIGURE 26: OCCURRENCE OF HEAVY PRECIPITATION HOURS 1991-2005. NOTE, NOT ALL STATIONS RECORDED DATA SINCE 1991 (REFER TO CHAPTER 4.1 FOR MORE DETAILS).	54
FIGURE 27: STRONGEST TWENTY HEAVY PRECIPITATION HOURS AT EACH STATION 1991-2005. NOTE, NOT ALL STATIONS RECORDED DATA SINCE 1991 (REFER TO CHAPTER 4.1 FOR MORE DETAILS).	55
FIGURE 28: SEASONAL FRACTION OF HEAVY PRECIPITATION HOURS PER YEAR FOR THE REFERENCE (1991-2005) AND MAIN STUDY PERIOD (2006-2020). NOTE, STATIONS BRUNN AM GEBIRGE, HOHE WARTE AND UNTERLAA HAVE NOT DATA FOR EVERY SEASON IN THEIR FIRST YEAR OF ESTABLISHMENT.	57
FIGURE 29: OCCURRENCE OF HEAVY PRECIPITATION EVENTS, 2006-2020. NOTE, STATIONS BRUNN AM GEBIRGE AND STAMMERSDORF RECORDED DATA ONLY SINCE LATE 2008. ALSO, THE HEAVIEST EVENT WITH 91.8MM/H AT STATION BRUNN AM GEBIRGE IS EXCLUDED IN THIS ILLUSTRATION TO ALLOW FOR A BETTER ANALYSIS AND COMPARISON OF THE REMAINING HEAVY PRECIPITATION EVENTS.	62
FIGURE 30: STRONGEST TWENTY EVENTS FOR EACH STATION, 2006-2020. NOTE, THE HEAVIEST EVENT WITH 91.8MM/H AT STATION BRUNN AM GEBIRGE IS EXCLUDED IN THIS ILLUSTRATION TO ALLOW FOR A BETTER ANALYSIS AND COMPARISON OF THE REMAINING HEAVY PRECIPITATION EVENTS.	62
FIGURE 31: OCCURRENCE OF HEAVY PRECIPITATION EVENTS, 1991-2005. NOTE, NOT ALL STATIONS RECORDED DATA SINCE 1991 (REFER TO CHAPTER 4.1 FOR MORE DETAILS).	63
FIGURE 32: STRONGEST TWENTY HEAVY PRECIPITATION HOURS AT EACH STATION 1991-2005. NOTE, NOT ALL STATION RECORDED DATA SINCE 1991 (REFER TO CHAPTER 4.1 FOR MORE DETAILS).	63
FIGURE 33: SEASONAL FRACTION OF HEAVY PRECIPITATION HOURS PER YEAR FOR THE REFERENCE (1991-2005) AND MAIN STUDY PERIOD (2006-2020). NOTE, STATIONS BRUNN AM GEBIRGE, HOHE WARTE AND UNTERLAA HAVE NOT DATA FOR EVERY SEASON IN THEIR FIRST YEAR OF ESTABLISHMENT.	65
FIGURE 34: PROBABILITY DENSITY FUNCTION (PDF) OF THE GENERALIZED PARETO DISTRIBUTION OF DAILY HEAVY PRECIPITATION AT STATION HOHE WARTE. BLACK SOLID LINE REPRESENTS THE PROBABILITIES OF EXCESSES RELATED TO THE THRESHOLD $U = 15\text{MM}$, BLUE DASHED LINE REPRESENTS THE MODEL DISTRIBUTION THAT WAS CALCULATED BASED ON THOSE EXCESSES.	68
FIGURE 35: PROBABILITY DENSITY FUNCTION (PDF) OF THE GENERALIZED PARETO DISTRIBUTION OF DAILY HEAVY PRECIPITATION AT STATION STAMMERSDORF. BLACK SOLID LINE REPRESENTS THE PROBABILITIES OF EXCESSES RELATED TO THE THRESHOLD $U = 15\text{MM}$, BLUE DASHED LINE REPRESENTS THE PDF THAT WAS CALCULATED BASED ON THOSE EXCESSES.	69
FIGURE 36: CALCULATED RETURN LEVELS FOR DIFFERENT RETURN PERIODS AT STATION HOHE WARTE. CONFIDENCE BOUNDS ARE CALCULATED FOR RETURN PERIODS > 1 YEAR.	69
FIGURE 37: CALCULATED RETURN LEVELS FOR DIFFERENT RETURN PERIODS AT STATION STAMMERSDORF. CONFIDENCE BOUNDS ARE CALCULATED FOR RETURN PERIODS > 1 YEAR.	70

List of Tables

TABLE 1: STATIONS IN THE STUDY AREA AND THEIR GEOGRAPHICAL CHARACTERISTICS.	24
TABLE 2: AVAILABILITY OF 10-MINUTE RAINFALL DATA FOR THE DIFFERENT STATIONS IN THE STUDY AREA. STATIONS ARE LISTED IN TIME CHRONOLOGICAL ORDER OF THE START OF THEIR RECORDS.	28
TABLE 3: AVAILABILITY OF DAILY RAINFALL DATA FOR THE DIFFERENT STATIONS IN THE STUDY AREA. STATIONS ARE LISTED IN TIME CHRONOLOGICAL ORDER OF THE START OF THEIR RECORDS.	28
TABLE 4: 98TH PERCENTILE VALUES IN [MM/D] OF DAILY PRECIPITATION AT EACH OF THE 10 STATIONS FOR THE MAIN STUDY PERIOD (2006-2020) AS WELL AS FOR THE REFERENCE PERIOD USED BY SEIBERT ET AL. (2007). NOTE THAT (*) INDICATES STATIONS WHERE DATA ARE NOT AVAILABLE THROUGHOUT THE PERIOD. VALUE FOR THE STUDY AREA IN PARENTHESES SHOWS THE MEAN CALCULATED WITH ALL STATIONS INCLUDING THOSE THAT WERE NOT ESTABLISHED IN THE REFERENCE PERIOD.	33
TABLE 5: SEASONAL MEAN PRECIPITATION (RR IN [MM/D]) IN THE STUDY AREA FOR THE TIME PERIODS USED IN BLÖSCHL ET AL. (2018). NOTE THAT THE MEAN VALUE WAS CALCULATED ONLY WITH STATIONS IN THE STUDY AREA THAT EXISTED IN THE REFERENCE PERIOD.	34
TABLE 6: SEASONAL MEAN PRECIPITATION (RR IN [MM/D]) IN THE STUDY AREA FOR THE STUDY PERIOD AND REFERENCE PERIOD USED IN THE FREQUENCY ANALYSIS. NOTE THAT THE MEAN VALUE IN COLUMN THREE WAS CALCULATED ONLY WITH STATIONS THAT EXISTED IN REFERENCE PERIOD.	34
TABLE 7: MEAN DAILY PRECIPITATION [MM], CALCULATED INCLUDING WET AND DRY DAYS, FOR THE REFERENCE (1979-1993) AND MAIN STUDY PERIOD (2006-2020). NOTE THAT (*) INDICATES STATIONS WHERE DATA ARE NOT AVAILABLE THROUGHOUT THE ENTIRE PERIOD. VALUE FOR THE STUDY AREA IN PARENTHESES SHOWS THE MEAN CALCULATED WITH ALL STATIONS INCLUDING THOSE THAT WERE NOT ESTABLISHED IN THE REFERENCE PERIOD.	35
TABLE 8: MEAN PRECIPITATION OF RAINY DAYS [MM] FOR THE REFERENCE AND MAIN PERIOD AT EACH STATION. NOTE THAT (*) INDICATES STATIONS WHERE DATA ARE NOT AVAILABLE THROUGHOUT THE ENTIRE PERIOD. VALUE FOR THE STUDY AREA IN PARENTHESES SHOWS THE MEAN CALCULATED WITH ALL STATIONS INCLUDING THOSE THAT WERE NOT ESTABLISHED IN THE REFERENCE PERIOD.	35
TABLE 9: AVERAGE NUMBER OF DAYS PER YEAR WITH PRECIPITATION >15MM FOR THE REFERENCE PERIOD AND MAIN STUDY PERIOD, AS WELL AS THE INCREASE EXPRESSED AS A PERCENTAGE. NOTE THAT (*) INDICATES STATIONS WHERE DATA ARE NOT AVAILABLE THROUGHOUT THE ENTIRE PERIOD. VALUE FOR THE STUDY AREA IN PARENTHESES SHOWS THE MEAN CALCULATED WITH ALL STATIONS INCLUDING THOSE THAT WERE NOT ESTABLISHED IN THE REFERENCE PERIOD.	36
TABLE 10: 25TH, 50TH AND 75TH PERCENTILE OF PRECIPITATION (RR) IN [MM/D] OF HEAVY PRECIPITATION DAYS (RR > 15MM/D) FOR THE REFERENCE AND MAIN PERIOD OF ANALYSIS. NOTE THAT (*) INDICATES STATIONS WHERE COMPLETE DATA ARE NOT AVAILABLE THROUGHOUT THE PERIOD.	40
TABLE 11: SEASONAL MEAN HEAVY PRECIPITATION (RR > 15MM/D) IN [MM/D] IN THE STUDY AREA. NOTE THAT THE MEAN VALUE IN COLUMN THREE WAS CALCULATED ONLY WITH STATIONS THAT EXISTED IN REFERENCE PERIOD.	42
TABLE 12: MEAN PRECIPITATION OF CTHS (DRY AND WET HOURS) [MM/H] FOR THE REFERENCE PERIOD (1991-2005) AND MAIN STUDY PERIOD (2006-2020) AT EACH STATION IN THE STUDY AREA. NOTE THAT (*) INDICATES STATIONS WHERE DATA ARE NOT AVAILABLE THROUGHOUT THE ENTIRE PERIOD. VALUE FOR THE STUDY AREA IN PARENTHESES SHOWS THE MEAN CALCULATED WITH ALL STATIONS INCLUDING THOSE THAT WERE NOT ESTABLISHED IN THE REFERENCE PERIOD.	48
TABLE 13: MEAN HOURLY PRECIPITATION OF CTHS >0MM/H (WET HOURS ONLY) FOR THE REFERENCE PERIOD (1991-2005) AND MAIN STUDY PERIOD (2006-2020) AT EACH STATION IN THE STUDY AREA. NOTE THAT (*) INDICATES STATIONS WHERE DATA ARE NOT AVAILABLE THROUGHOUT THE ENTIRE PERIOD. VALUE FOR THE STUDY AREA IN PARENTHESES SHOWS THE MEAN CALCULATED WITH ALL STATIONS INCLUDING THOSE THAT WERE NOT ESTABLISHED IN THE REFERENCE PERIOD.	49
TABLE 14: MAXIMUM RECORDED HOURLY PRECIPITATION [MM/H] FOR THE CTHS AND MRSD CALCULATION METHOD FOR THE REFERENCE AND MAIN STUDY PERIOD. THE NUMBERS IN BOLD SHOW AN INCREASE IN THE MAXIMUM RECORDED RAINFALL TOTAL FOR EACH RESPECTIVE PERIOD. THE TREND COLUMN IS SHOWING THE CHANGE OF MAXIMUM HOURLY SUMS BETWEEN PERIODS FOR BOTH CALCULATION METHODS. NOTE THAT (*) INDICATES STATIONS WHERE DATA ARE NOT AVAILABLE THROUGHOUT THE ENTIRE PERIOD. VALUE FOR THE STUDY AREA IN PARENTHESES SHOWS THE MEAN CALCULATED WITH ALL STATIONS INCLUDING THOSE WHICH WERE NOT ESTABLISHED IN THE REFERENCE PERIOD.	49
TABLE 15: 98TH PERCENTILE OF HOURLY PRECIPITATION [MM/H] CALCULATED WITH MRSD FOR THE REFERENCE PERIOD (1991-2005) AND MAIN STUDY PERIOD (2006-2020) AT EACH STATION IN THE STUDY AREA. NOTE THAT (*) INDICATES STATIONS	

WHERE DATA ARE NOT AVAILABLE THROUGHOUT THE ENTIRE PERIOD. VALUE FOR THE STUDY AREA IN PARENTHESES SHOWS THE MEAN CALCULATED WITH ALL STATIONS INCLUDING THOSE THAT WERE NOT ESTABLISHED IN THE REFERENCE PERIOD.	50
TABLE 16: AVERAGE NUMBER OF HEAVY PRECIPITATION HOURS PER YEAR IN EACH RESPECTIVE PERIOD AT EACH STATION IN THE STUDY AREA USING THS. NUMBERS ARE AVERAGED OVER YEARS IN EACH PERIOD AND AT EACH STATION. NOTE THAT (*) INDICATES STATIONS WHERE DATA ARE NOT AVAILABLE THROUGHOUT THE ENTIRE PERIOD. VALUE FOR THE STUDY AREA IN PARENTHESES SHOWS THE MEAN CALCULATED WITH ALL STATIONS INCLUDING THOSE THAT WERE NOT ESTABLISHED IN THE REFERENCE PERIOD.	51
TABLE 17: MINIMUM AND MAXIMUM NUMBER OF HEAVY PRECIPITATION HOURS IN A YEAR IN EACH RESPECTIVE PERIOD FOR EACH STATION IN THE STUDY AREA. NOTE THAT (*) INDICATES STATIONS WHERE DATA ARE NOT AVAILABLE THROUGHOUT THE ENTIRE PERIOD. VALUE FOR THE STUDY AREA IN PARENTHESES SHOWS THE MEAN CALCULATED WITH ALL STATIONS INCLUDING THOSE THAT WERE NOT ESTABLISHED IN THE REFERENCE PERIOD.	52
TABLE 18: 25TH, 50TH AND 75TH PERCENTILE OF PRECIPITATION (RR) IN [MM/H] OF HEAVY PRECIPITATION HOURS (RR > 6MM/H) FOR THE REFERENCE AND MAIN STUDY PERIOD. NOTE THAT (*) INDICATES STATIONS WHERE COMPLETE DATA ARE NOT AVAILABLE THROUGHOUT THE ENTIRE PERIOD.	56
TABLE 19: MEAN HOURLY HEAVY PRECIPITATION [MM/H] PER SEASON FOR THE REFERENCE AND THE MAIN STUDY PERIOD.	57
TABLE 20: MEAN HOURLY PRECIPITATION [MM/H] PER SEASON IN THE STUDY AREA FOR REFERENCE AND THE MAIN STUDY PERIOD, USING CTHS.	58
TABLE 21: NUMBER OF HEAVY PRECIPITATION HOURS PER YEAR AND SEASON FOR THE STUDY AREA; CALCULATED WITH AVERAGES PER STATION.	58
TABLE 22: 98TH PERCENTILE OF MEAN EVENT RAIN RATE [MM/H] CALCULATED WITH DRY AND WET EVENTS FOR THE REFERENCE PERIOD (1991-2005) AND MAIN STUDY PERIOD (2006-2020) AT EACH STATION IN THE STUDY AREA. NOTE THAT (*) INDICATES STATIONS WHERE DATA ARE NOT AVAILABLE THROUGHOUT THE ENTIRE PERIOD. VALUE FOR THE STUDY AREA IN PARENTHESES SHOWS THE MEAN CALCULATED WITH ALL STATIONS INCLUDING THOSE THAT WERE NOT ESTABLISHED IN THE REFERENCE PERIOD.	59
TABLE 23: AVERAGE NUMBER OF HEAVY PRECIPITATION EVENTS (RR > 3.1 MM/H) PER YEAR IN EACH RESPECTIVE PERIOD AT EACH STATION IN THE STUDY AREA. NUMBERS ARE AVERAGED OVER AVAILABLE YEARS IN THE RESPECTIVE PERIOD. NOTE THAT (*) INDICATES STATIONS WHERE DATA ARE NOT AVAILABLE THROUGHOUT THE ENTIRE PERIOD. VALUE FOR THE STUDY AREA IN PARENTHESES SHOWS THE MEAN CALCULATED WITH ALL STATIONS INCLUDING THOSE THAT WERE NOT ESTABLISHED IN THE REFERENCE PERIOD.	60
TABLE 24: MINIMUM AND MAXIMUM NUMBER OF HEAVY PRECIPITATION HOURS IN A YEAR IN EACH RESPECTIVE PERIOD FOR EACH STATION IN THE STUDY AREA. NOTE THAT (*) INDICATES STATIONS WHERE DATA ARE NOT AVAILABLE THROUGHOUT THE ENTIRE PERIOD. VALUE FOR THE STUDY AREA IN PARENTHESES SHOWS THE MEAN CALCULATED WITH ALL STATIONS INCLUDING THOSE THAT WERE NOT ESTABLISHED IN THE REFERENCE PERIOD.	61
TABLE 25: 25TH, 50TH AND 75TH PERCENTILE OF MEAN RAIN RATE [MM/H] OF HEAVY PRECIPITATION EVENTS (RR > 3.1 MM/H) FOR THE REFERENCE AND MAIN STUDY PERIOD. NOTE THAT (*) INDICATES STATIONS WHERE COMPLETE DATA ARE NOT AVAILABLE THROUGHOUT THE ENTIRE PERIOD.	64
TABLE 26: MEAN RAIN RATE IN [MM/H] OF HEAVY PRECIPITATION EVENTS (RR > 3.1 MM/H) PER SEASON IN THE STUDY AREA FOR THE REFERENCE AND MAIN STUDY PERIOD.	66
TABLE 27: MEAN RAIN RATE [MM/H] OF EVENTS (INCLUDING DRY AND WET EVENTS) FOR THE REFERENCE AND MAIN STUDY PERIOD.	67
TABLE 28: MEAN RAIN DEPTH [MM] OF EVENTS (INCLUDING DRY AND WET EVENTS) FOR THE REFERENCE AND MAIN STUDY PERIOD.	67
TABLE 29: MEAN RAIN DEPTH [MM] OF WEAK AND MODERATE EVENTS (0 MM/H < RR < 3.1 MM/H) FOR BOTH PERIODS.	67
TABLE 30: NUMBER OF ALL PRECIPITATION EVENTS (RR > 0MM/H) IN THE STUDY AREA FOR THE REFERENCE AND MAIN STUDY PERIOD.	67
TABLE 31: AVERAGE ANNUAL NUMBER OF HEAVY PRECIPITATION EVENTS (RR > 3.1 MM/H) PER SEASON IN THE STUDY AREA.	67
TABLE 32: GP ($U_1 = 15\text{MM}$) RETURN LEVELS AND RETURN PERIODS FOR THE STATIONS IN THE STUDY AREA, 95 % CONFIDENCE BOUNDS ARE GIVEN IN PARENTHESES.	71
TABLE 33: 98TH PERCENTILE OF DAILY PRECIPITATION [MM] FOR EACH STATION CALCULATED CONSIDERING BOTH DRY AND WET DAYS SINCE STATIONS WERE ESTABLISHED.	72
TABLE 34: GP RETURN LEVELS AND RETURN PERIODS FOR THE STATIONS IN THE STUDY AREA USING INDIVIDUAL THRESHOLDS FOR EACH STATION ($U_2 = 98^{\text{TH}}$ PERCENTILE OF EACH STATION), 95 % CONFIDENCE BOUNDS ARE GIVEN IN PARENTHESES.	73

List of Abbreviations

Abbreviation	Meaning
AQUAS	Austria Quality Service
cdf	Cumulative distribution function
CTHS	Clock-time based hour sum
ENSO	El Niño Southern Oscillation
GEV	Generalized extreme value
GPD	Generalized Pareto distribution
HPD	Heavy precipitation day
HPH	Heavy precipitation hour
IERI	Intra-event rainfall intermittency
IET	Inter-event time
MIT	Minimum inter-event time
MRSD	Maximum 1h value per day of rolling sums
NAO	North Atlantic Oscillation
POT	Peak-over-threshold
THS	Total heavy hour sum
ZAMG	Austrian National Weather Service

Appendix

List of appendices

Appendix A – Daily heavy precipitation analysis	A-1
Appendix A.1: Frequency plots of daily heavy precipitation.....	A-1
Appendix A.2: Seasonality plots of daily heavy precipitation	A-3
Appendix A.3: Correlation plots of seasonal and annual heavy precipitation per station	A-5
Appendix B – Hourly precipitation analysis.....	B-10
Appendix B.1: General precipitation change.....	B-10
Appendix B.2: Frequency plots of hourly precipitation.....	B-11
Appendix B.3: Seasonality plots of hourly precipitation	B-12
Appendix C – Event analysis	C-13
Appendix C.1: General precipitation change.....	C-13
Appendix C.2: Frequency plots of event precipitation.....	C-14
Appendix C.3: Seasonality plots of event precipitation	C-15

Appendix A – Daily heavy precipitation analysis

Appendix A.1: Frequency plots of daily heavy precipitation

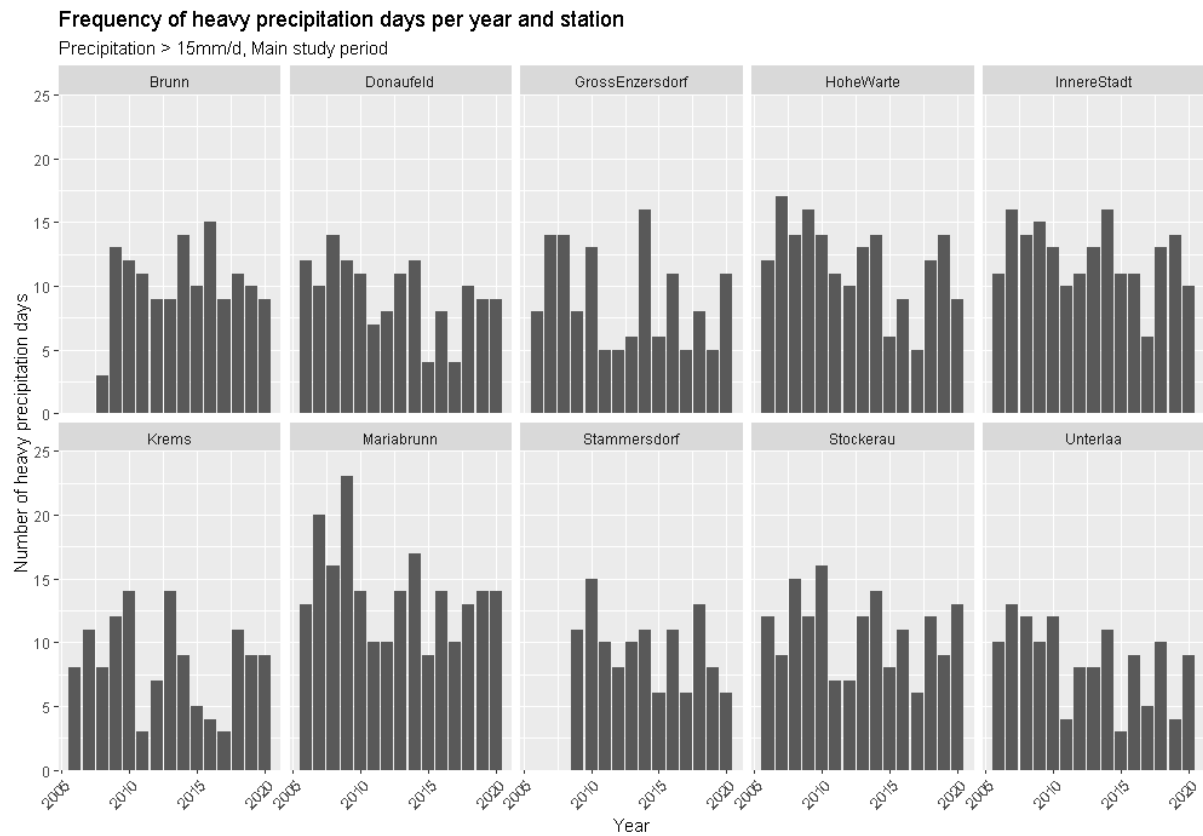


Figure A 1: Number of heavy precipitation days per year and station with precipitation >15mm for the period 2006-2020, Brunn am Gebirge 2008-2020 and Stammersdorf 2009-2020.

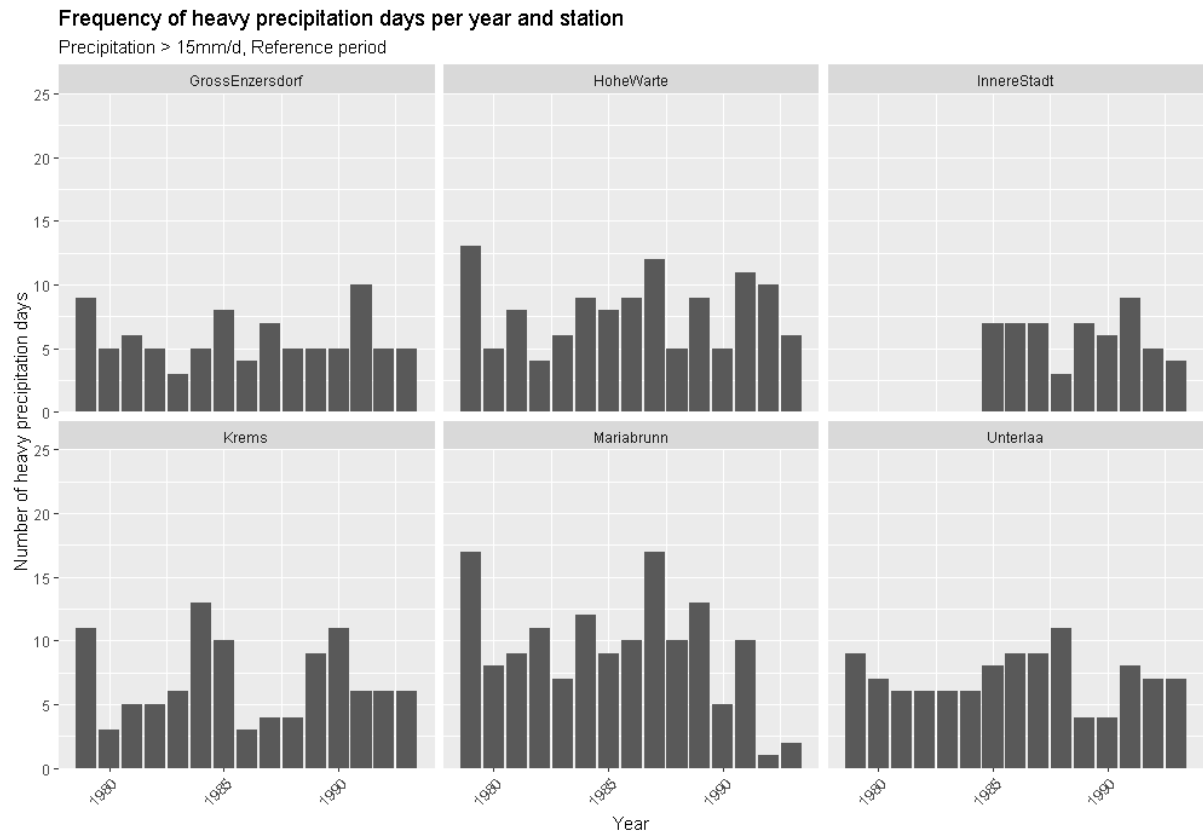


Figure A 2: Number of heavy precipitation days per year and station with precipitation >15mm for the reference period. Note that station Innere Stadt has no data available before 1985, station Mariabrunn has missing data from 1990-1993.

Appendix A.2: Seasonality plots of daily heavy precipitation

Number of heavy precipitation days per season, 2006-2020

Number of days averaged over years in period

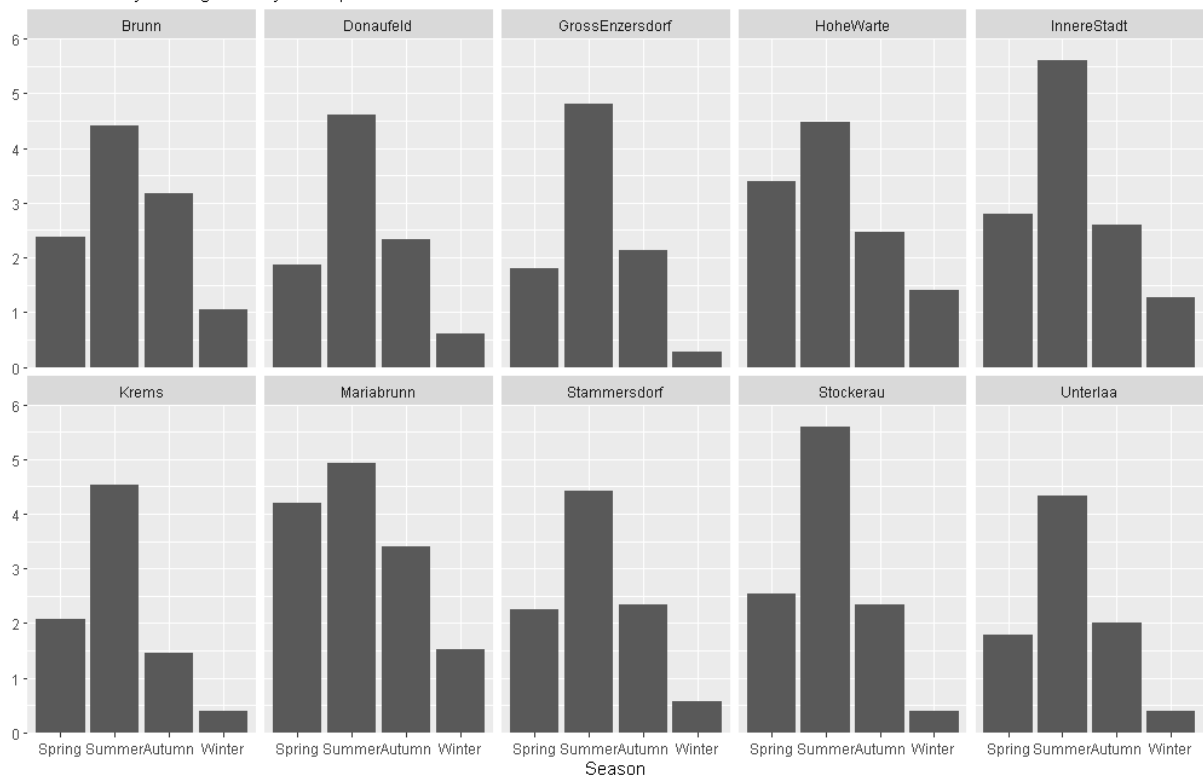


Figure A 3: Number of heavy precipitation days per season and station in the main study period. Total number of heavy precipitation days was averaged over 12.25 years at Brunn station, 12 years at Stammersdorf station and 15 years at any other station.

Number of heavy precipitation days per season, 1979-1993

Number of hours averaged over years in period

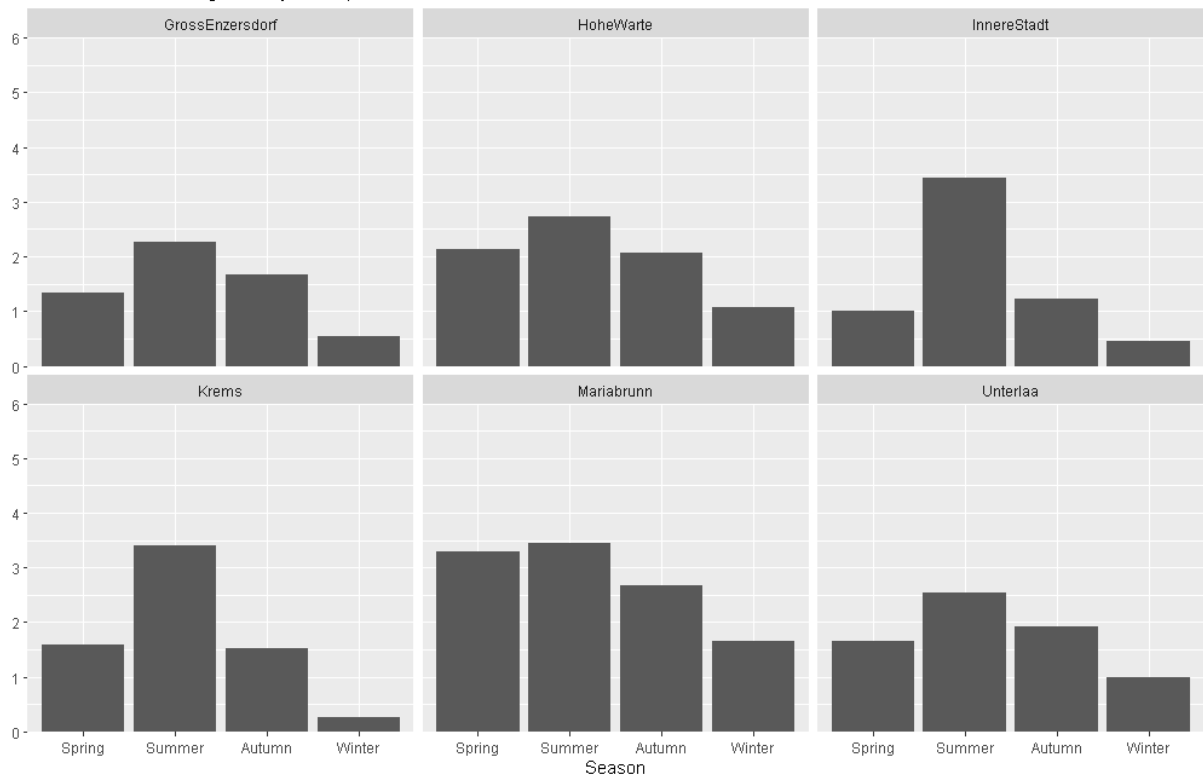


Figure A 4: Number of heavy precipitation days per season and station in the reference period. Total number of heavy precipitation days was averaged over 9 years at Innere Stadt station, 12.74 years at Mariabrunn station and 15 years at any other station.

Distribution of autumn heavy precipitation days in September

in 2006-2020

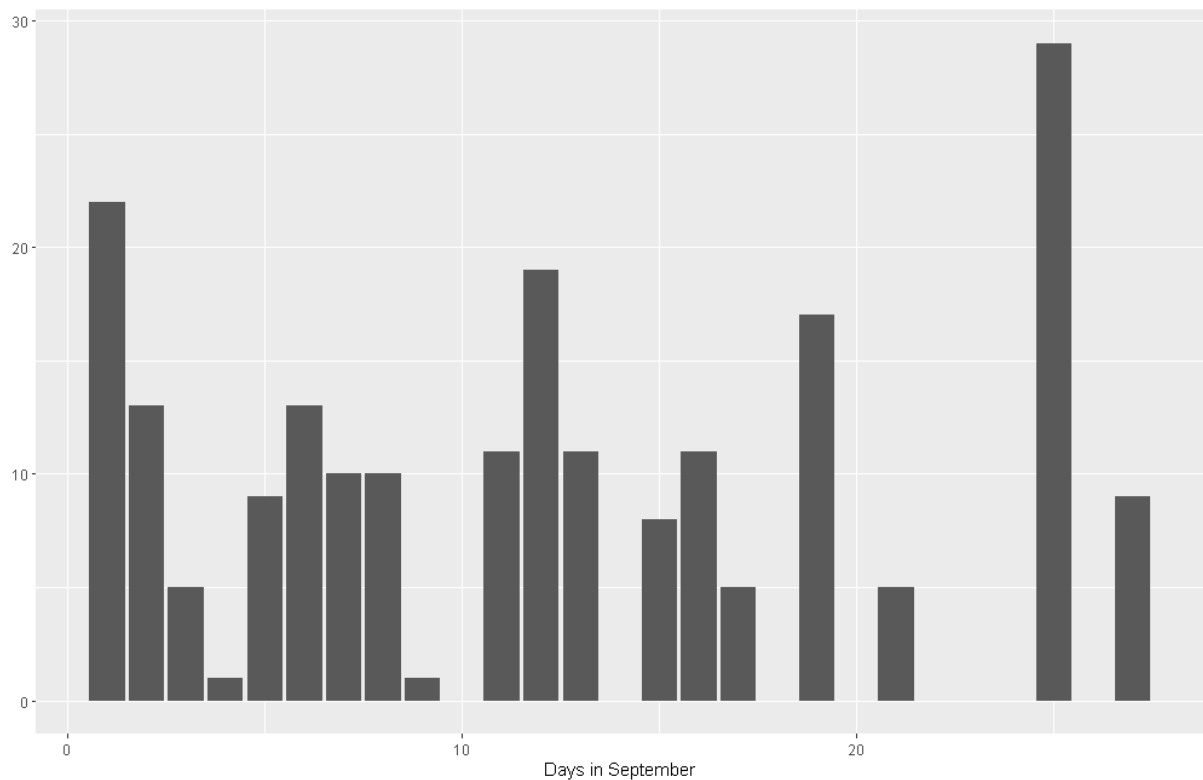


Figure A 5: Distribution of September heavy precipitation days in the study area for the main study period.

Appendix A.3: Correlation plots of seasonal and annual heavy precipitation per station

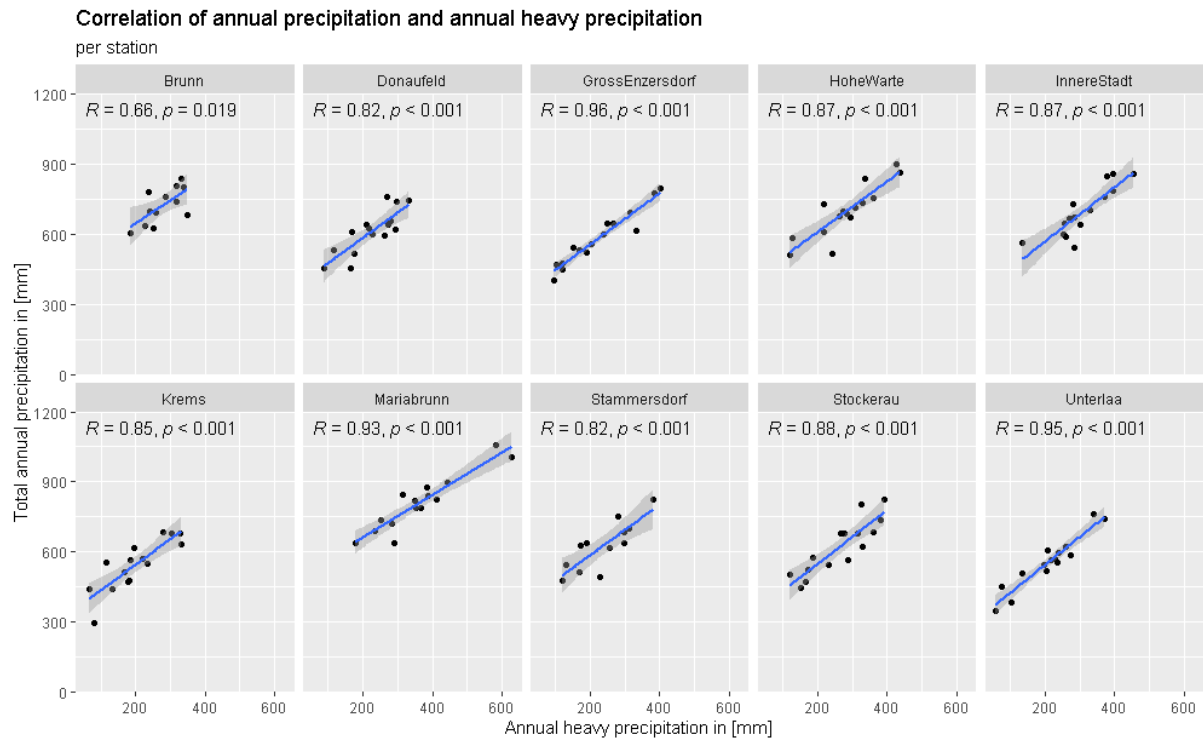


Figure A 6: Correlation of total annual precipitation and annual heavy precipitation in mm per station. Significance accepted at $\alpha = 0.05$.

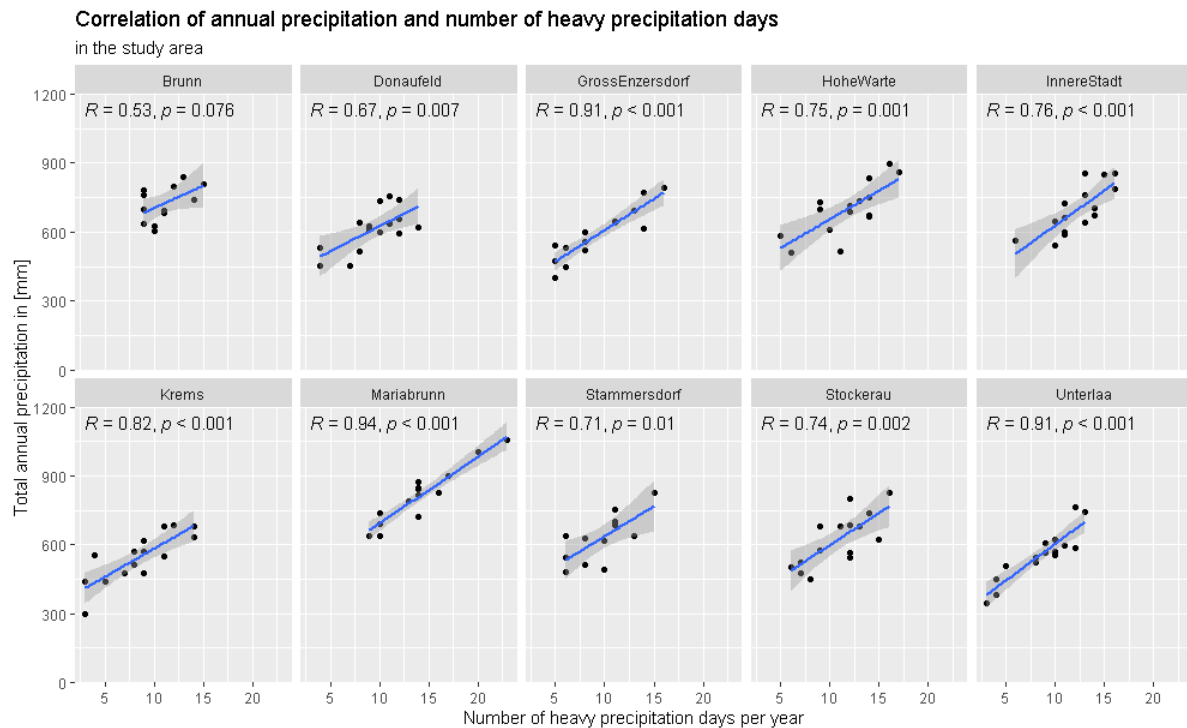


Figure A 7: Correlation of total annual precipitation [mm] and annual number of heavy precipitation days per station. Significance accepted at $\alpha = 0.05$.

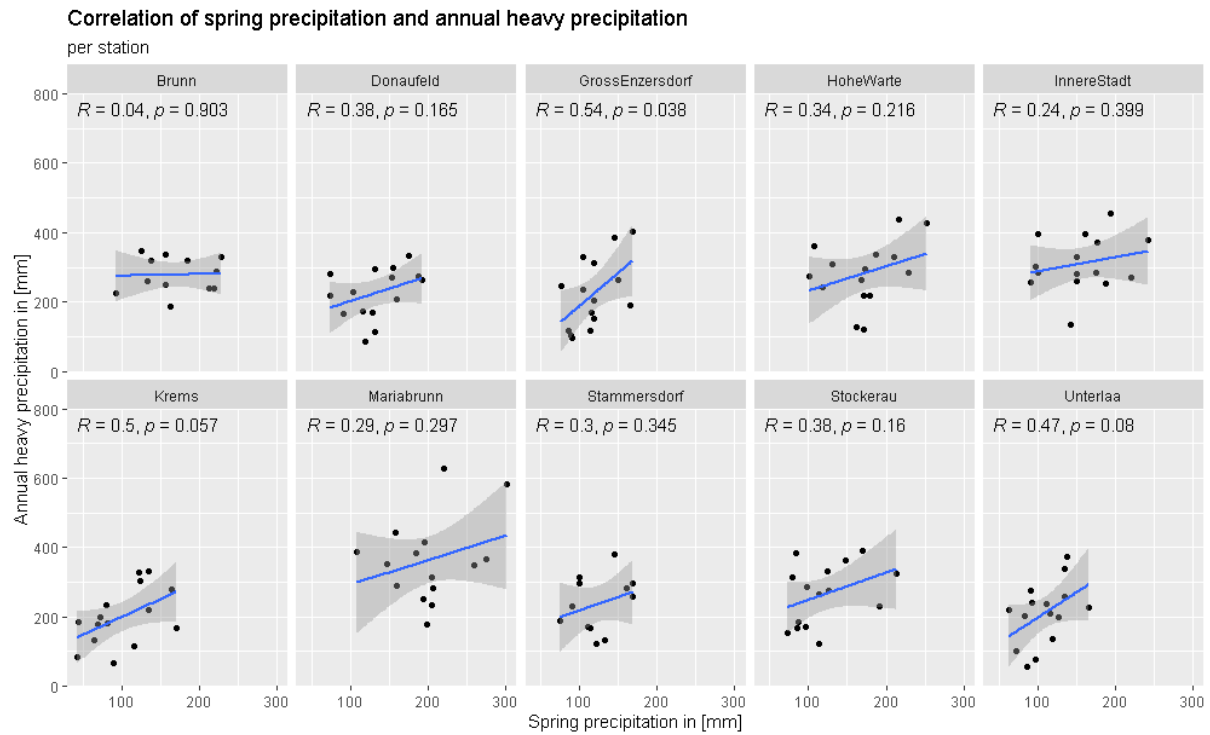


Figure A 8: Correlation of spring precipitation and annual heavy precipitation in mm per station. Significance accepted at $\alpha = 0.05$.

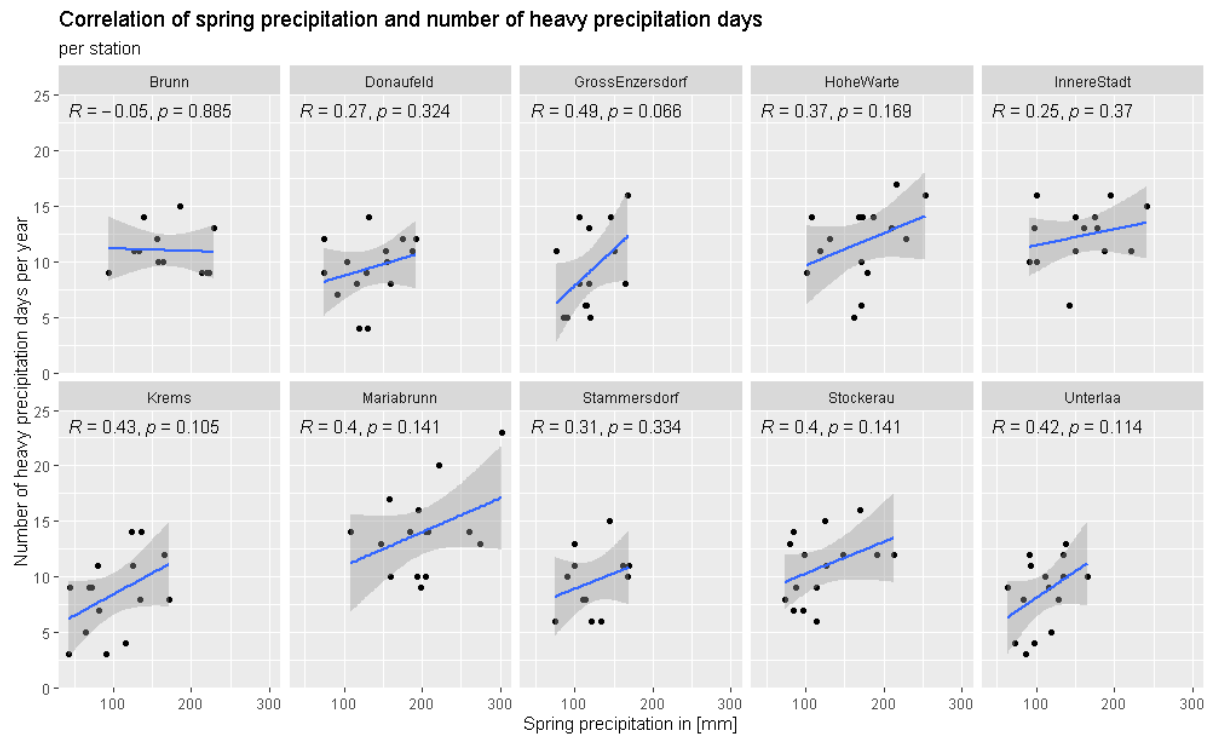


Figure A 9: Correlation of spring precipitation [mm] and annual number of heavy precipitation days per station. Significance accepted at $\alpha = 0.05$.

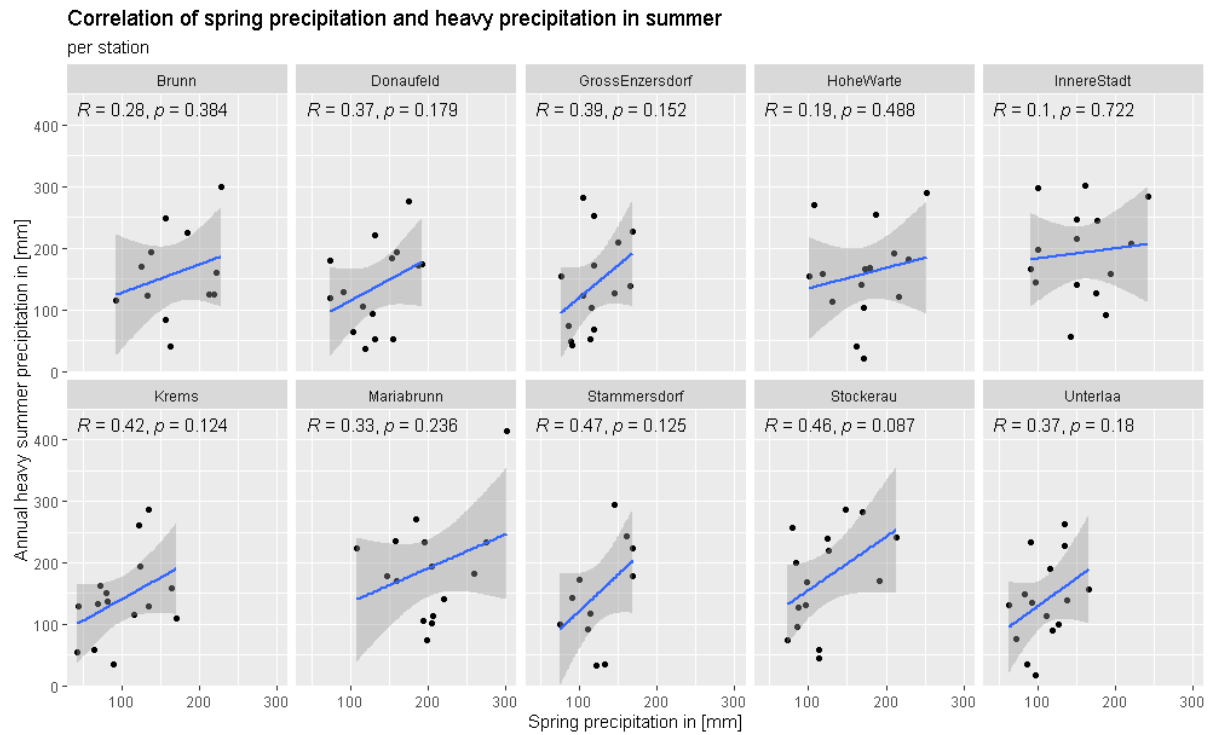


Figure A 10: Correlation of spring precipitation and annual heavy summer precipitation in mm per station. Significance accepted at $\alpha = 0.05$.

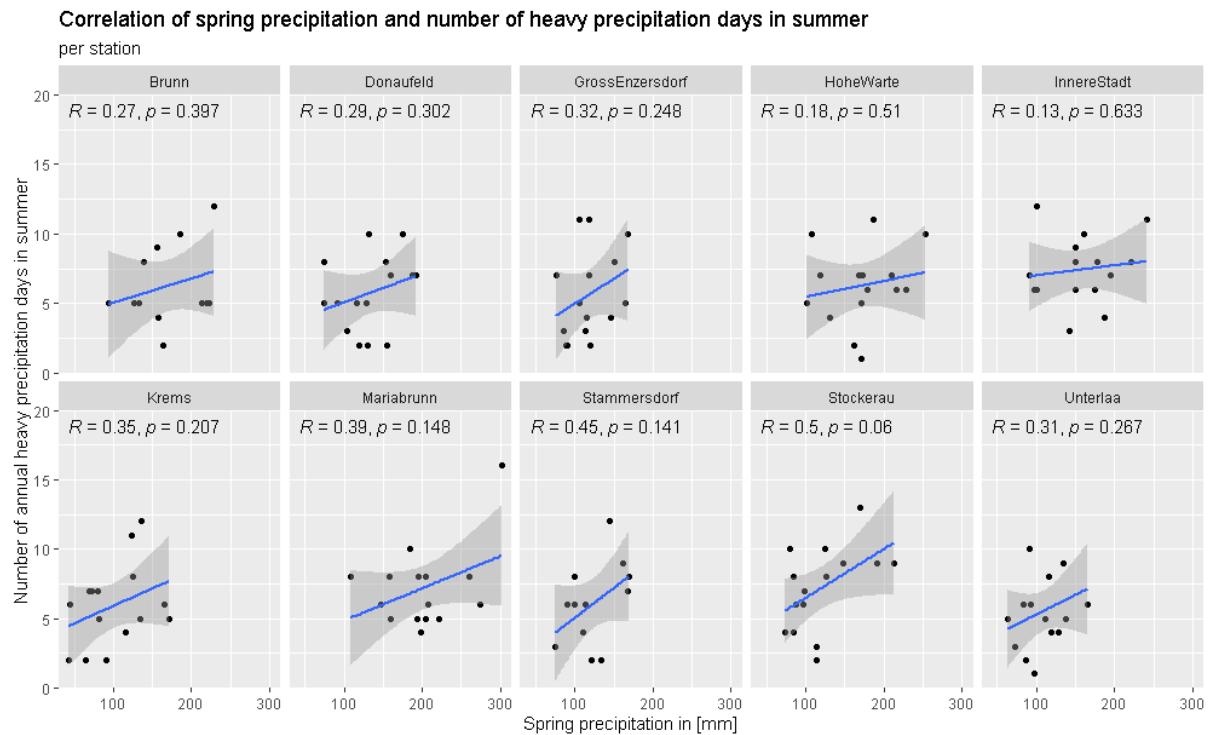


Figure A 11: Correlation of spring precipitation [mm] and annual number of heavy precipitation days in summer per station. Significance accepted at $\alpha = 0.05$.

Table A 1: Number of heavy precipitation days and rain depth of heavy precipitation days per season. In absolute numbers and as a fraction.

Season	Type of precipitation	Number of days	% of all days	RR in mm	% of total precipitation
Spring	heavy	363	7	8488	37
	not heavy	4726	93	14443.2	63
Summer	heavy	690	13	17247	51
	not heavy	4599	87	16523.9	49
Autumn	heavy	348	7	9327.4	43
	not heavy	4354	93	12608.4	57
Winter	heavy	114	2	2330.5	16
	not heavy	5009	98	12235.1	84

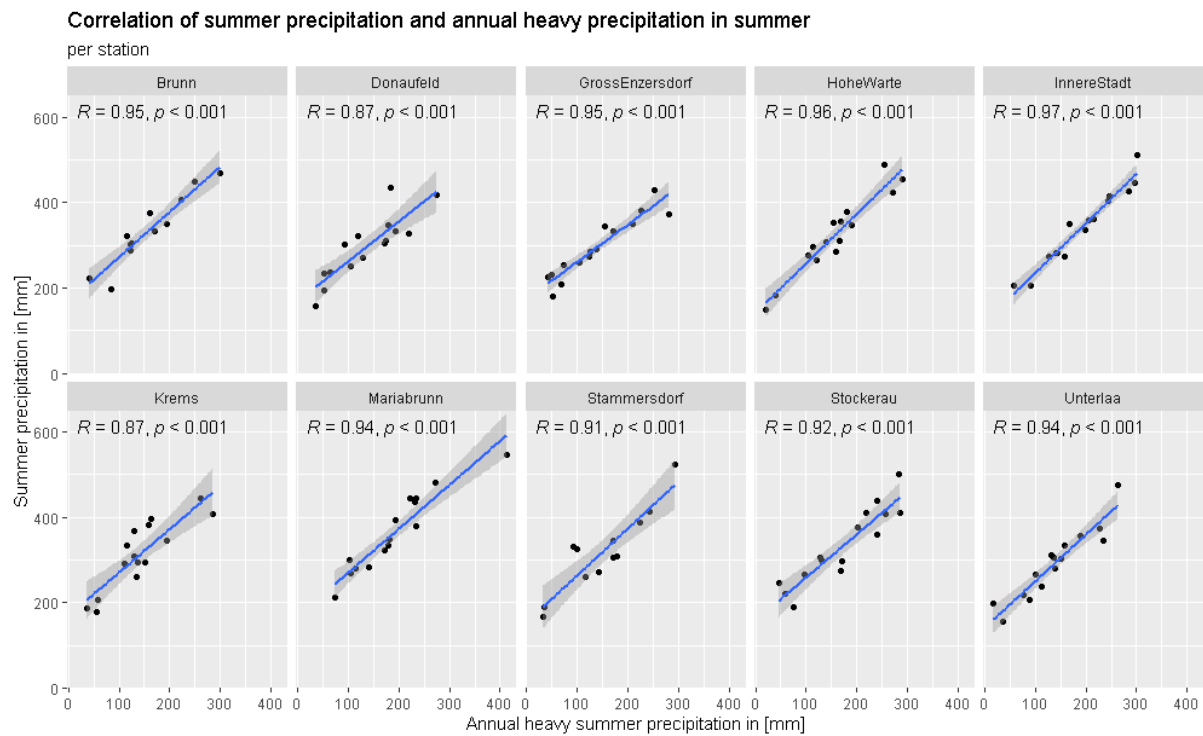


Figure A 12: Correlation of summer precipitation and annual heavy precipitation in summer in mm per station. Significance tested at $\alpha = 0.05$.

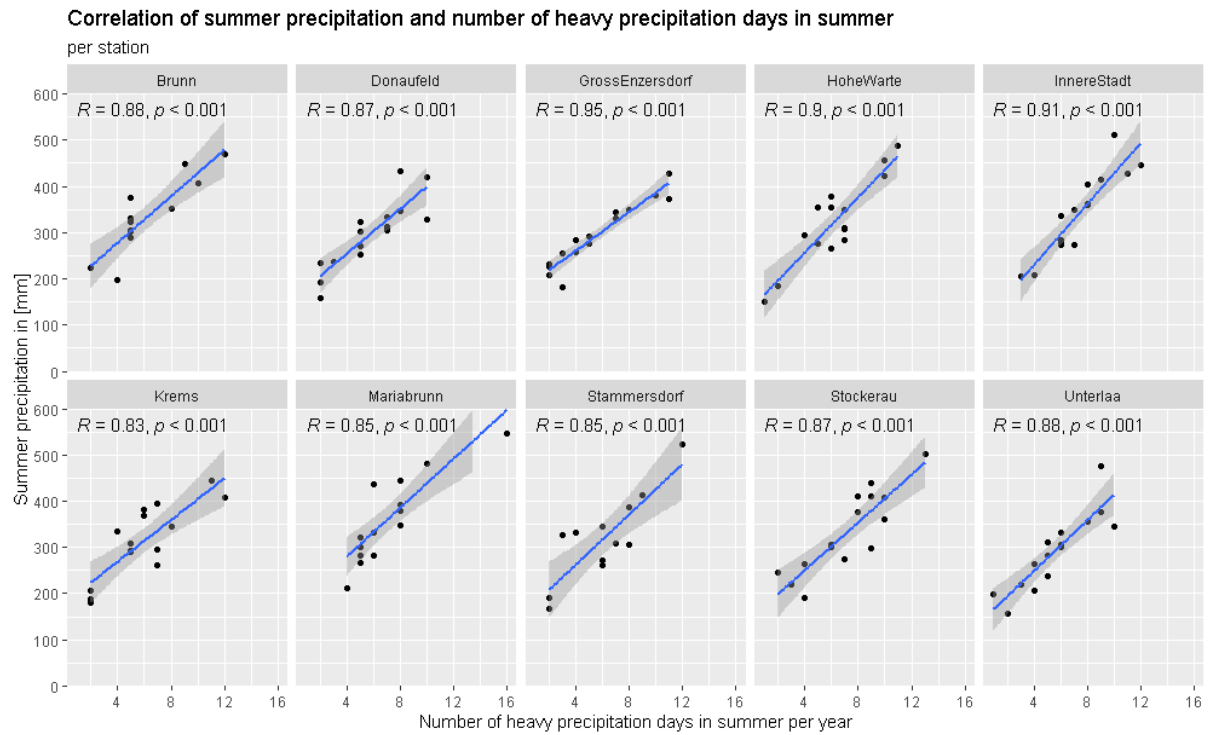


Figure A 13: Correlation of summer precipitation [mm] and annual number of heavy precipitation days in summer per station. Significance tested at $\alpha = 0.05$.

Appendix B – Hourly precipitation analysis

Appendix B.1: General precipitation change

Table B 1: Mean precipitation of MHSD (dry and wet hours) [mm/h]. Note that () indicates stations where data are not available throughout the entire period. Value for the study area in parentheses shows the mean calculated with all stations including those that were not established in the reference period.*

Station	1991-2005	2006-2020	Change in %
Innere Stadt	0.61	0.83	36
Hohe Warte	0.74*	0.83	11
Gross-Enzersdorf	0.58*	0.72	25
Krems	0.71*	0.70	-2
Donaufeld	0.62*	0.72	17
Mariabrunn	0.79*	0.88	11
Stockerau	0.59*	0.72	23
Unterlaa	0.57*	0.68	20
Brunn am Gebirge	NA	(0.80*)	NA
Stammersdorf	NA	(0.77*)	NA
Across all stations	0.65	0.76 (0.76)	17

Table B 2: Mean hourly precipitation of MHSD > 0mm/h (wet hours only). Note that () indicates stations where data are not available throughout the entire period. Value for the study area in parentheses shows the mean calculated with all stations including those that were not established in the reference period.*

Station	1991-2005	2006-2020	Change in %
Innere Stadt	1.81	2.24	24
Hohe Warte	1.68*	2.07	23
Gross-Enzersdorf	1.81*	2.05	13
Krems	1.82*	1.95	7
Donaufeld	1.61*	1.96	22
Mariabrunn	1.72*	2.15	25
Stockerau	1.53*	1.98	29
Unterlaa	1.58*	1.94	23
Brunn am Gebirge	NA	(2.04*)	NA
Stammersdorf	NA	(2.03*)	NA
Across all stations	1.70	2.04 (2.04)	21

Appendix B.2: Frequency plots of hourly precipitation

Frequency of heavy precipitation hours per year and station

Precipitation > 5.9 mm/h, Reference Period

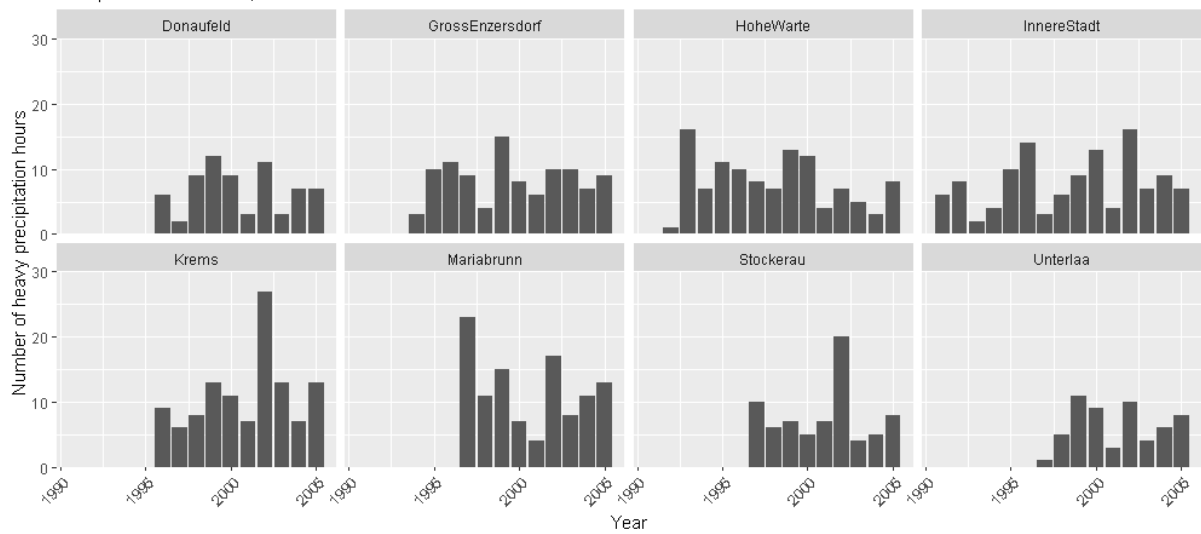


Figure B 1: Number of heavy precipitation hours per year in the reference period (1991-2005) for each station. Note, most stations have been established after 1991; stations that did not exist before 2005 are not included. Also, the years 1992 at station Hohe Warte and 1997 at station Unterlaa are not representing a full year of data.

Frequency of heavy precipitation hours per year and station

Precipitation > 5.9 mm/h, Main study period

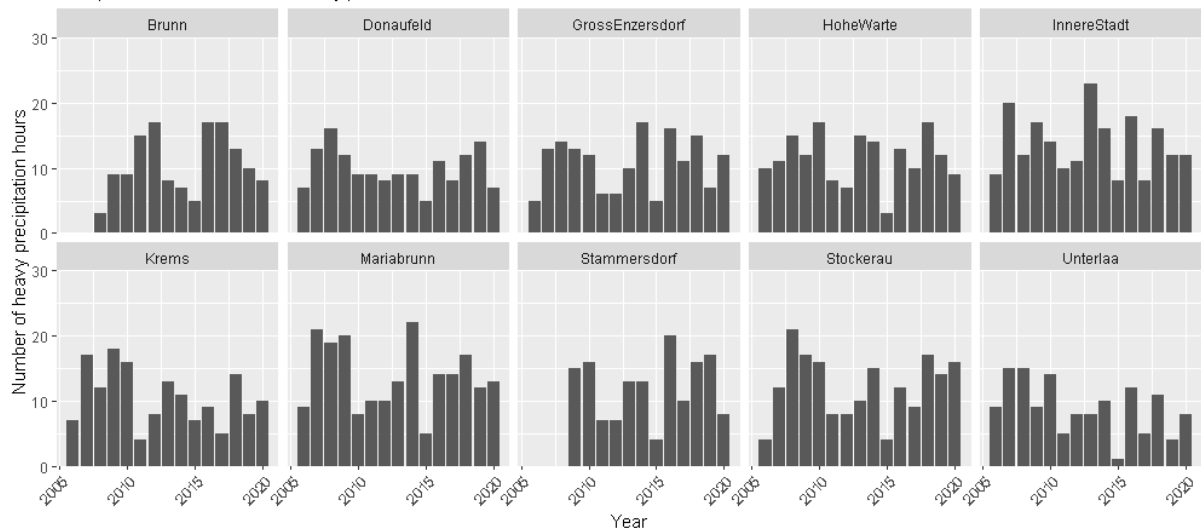


Figure B 2: Number of heavy precipitation hours per year in the main study period (2006-2020). Note, station Brunn established late 2008; thus, 2008 is not representing a full year of data; Station Stammersdorf 2009-2020.

Appendix B.3: Seasonality plots of hourly precipitation

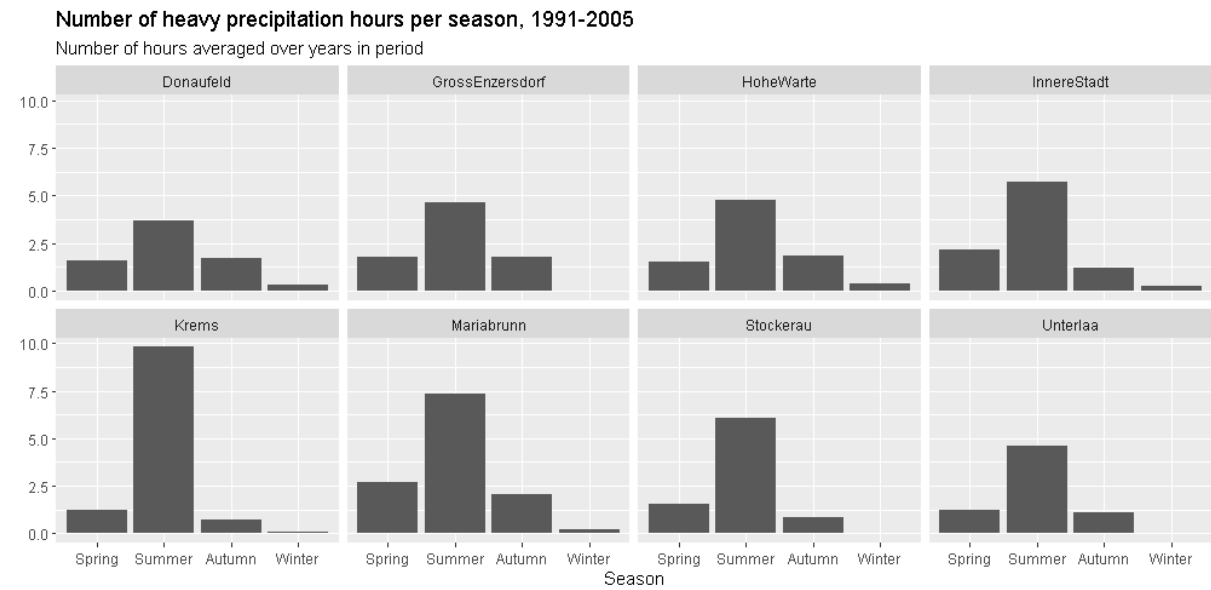


Figure B 3: Number of heavy precipitation hours per season and station in the reference period. Total number of heavy precipitation hours was averaged over years in period (refer to chapter 4.1).

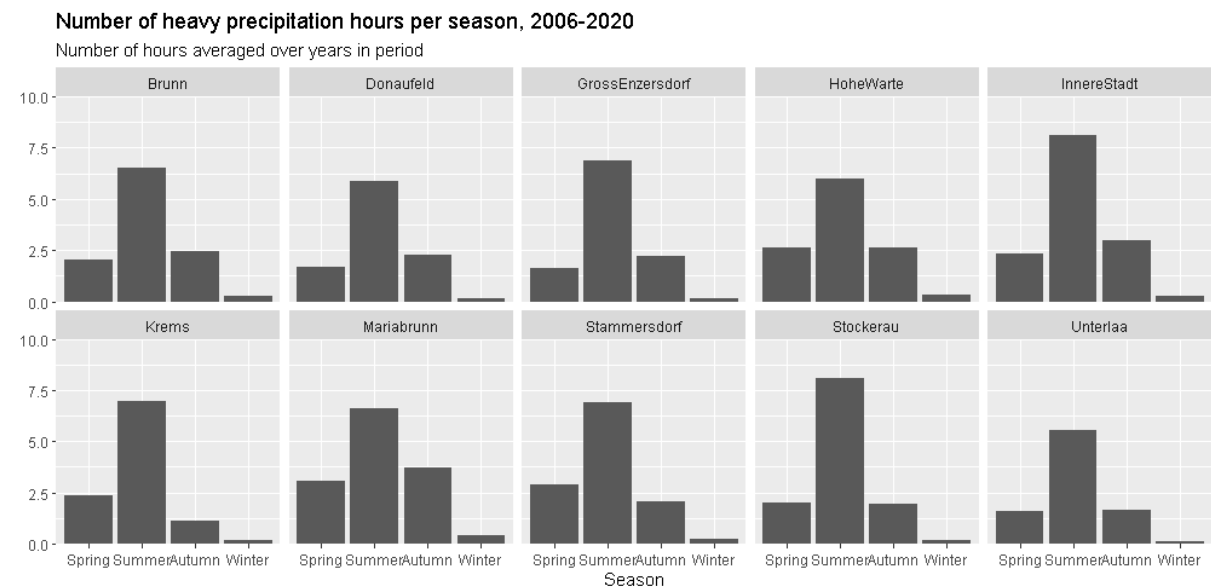


Figure B 4: Number of heavy precipitation hours per season and station in the main study period. Total number of heavy precipitation days was averaged over 12.25 years at Brunn station, 12 years at Stammersdorf station and 15 years at any other station.

Appendix C – Event analysis

Appendix C.1: General precipitation change

Table C 1: Number of precipitation events (RR > 0 mm/h) per year in period using a minimum interevent time of 20 minutes.

Station	1991-2005	2006-2020	Change in %
Innere Stadt	454.0	407.5	-10
Hohe Warte	555.9	453.3	-19
Gross Enzersdorf	435.3	384.8	-12
Krems	431.8	393.3	-9
Donaufeld	437.5	403.8	-8
Mariabrunn	553.6	472.1	-15
Stockerau	429.6	393.9	-8
Unterlaa	401.5	379.9	-5
Brunn	NA	471.4	NA
Stammersdorf	NA	427.0	NA
Across study area	462.4	411.1	-11

Table C 2: Mean event rain rate of precipitation events (RR > 0 mm/h) at each station in the reference and main study period.

Station	1991-2005	2006-2020	Change in %
Innere Stadt	1.07	1.25	17
Hohe Warte	1.01	1.20	19
Gross Enzersdorf	1.13	1.22	8
Krems	1.18	1.20	2
Donaufeld	1.03	1.17	14
Mariabrunn	1.05	1.16	11
Stockerau	1.06	1.18	11
Unterlaa	1.07	1.18	10
Brunn	NA	1.13	NA
Stammersdorf	NA	1.19	NA
Across study area	1.10	1.20	11

Appendix C.2: Frequency plots of event precipitation

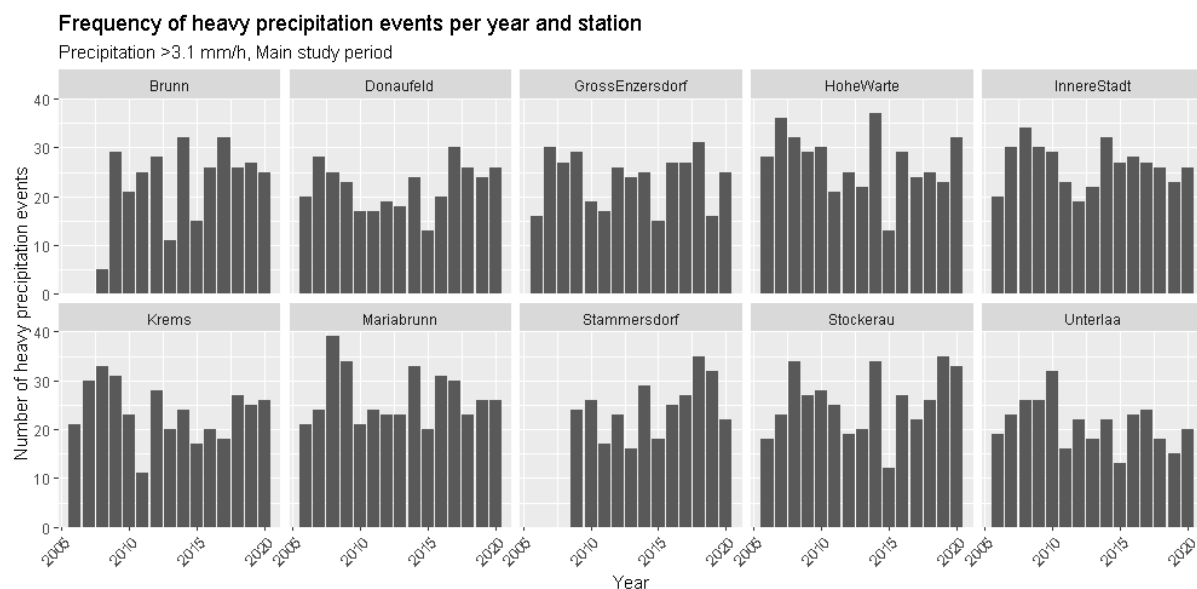


Figure C 1: Number of heavy precipitation events per year in the main study period (2006-2020). Station Brunn established end of 2008; thus 2008 is not representing a full year of data; Station Stammersdorf 2009-2020.

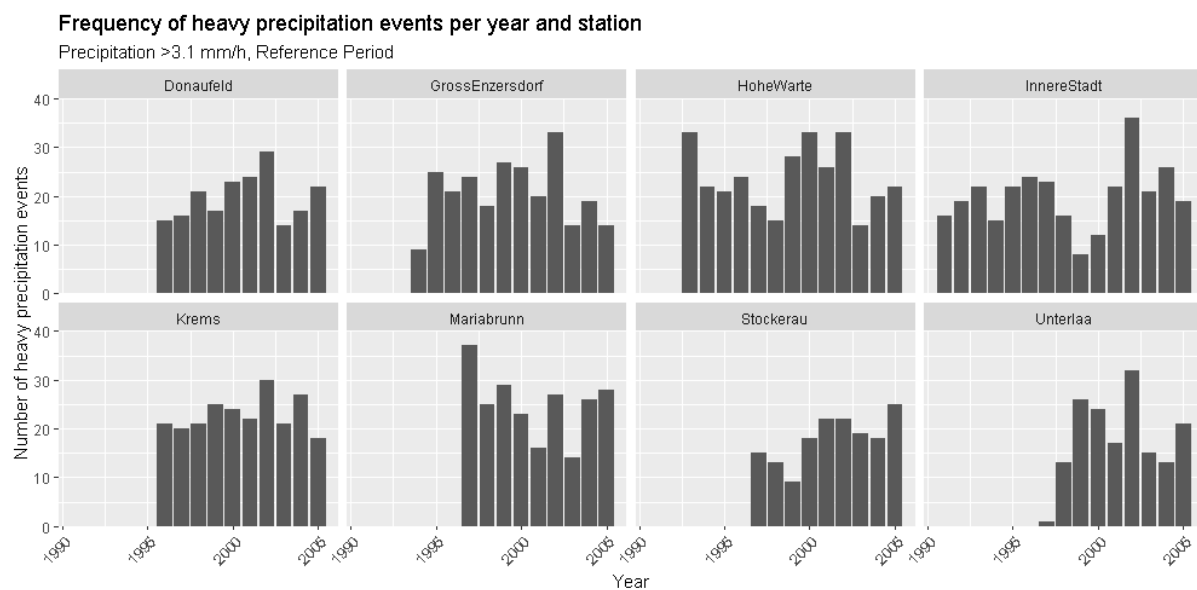


Figure C 2: Number of heavy precipitation events per year in the reference period (1991-2005) for each station. Most stations established after 1991; stations that did not exist before 2005 are not included. Note, the years 1992 at station Hohe Warte and 1997 at station Unterlaa are not representing a full year of data.

Appendix C.3: Seasonality plots of event precipitation

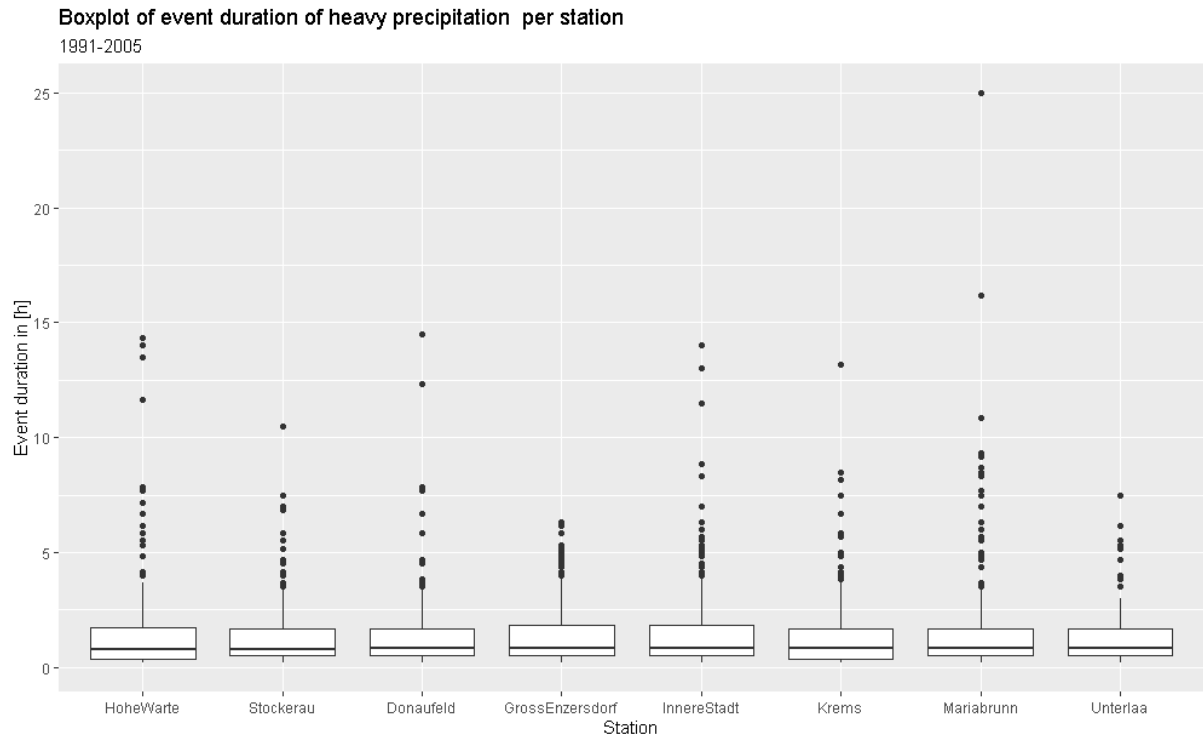


Figure C 3: Boxplot of event duration of heavy precipitation events in the reference period for every station in the study area. Stations are plotted in ascending order of size of the median.

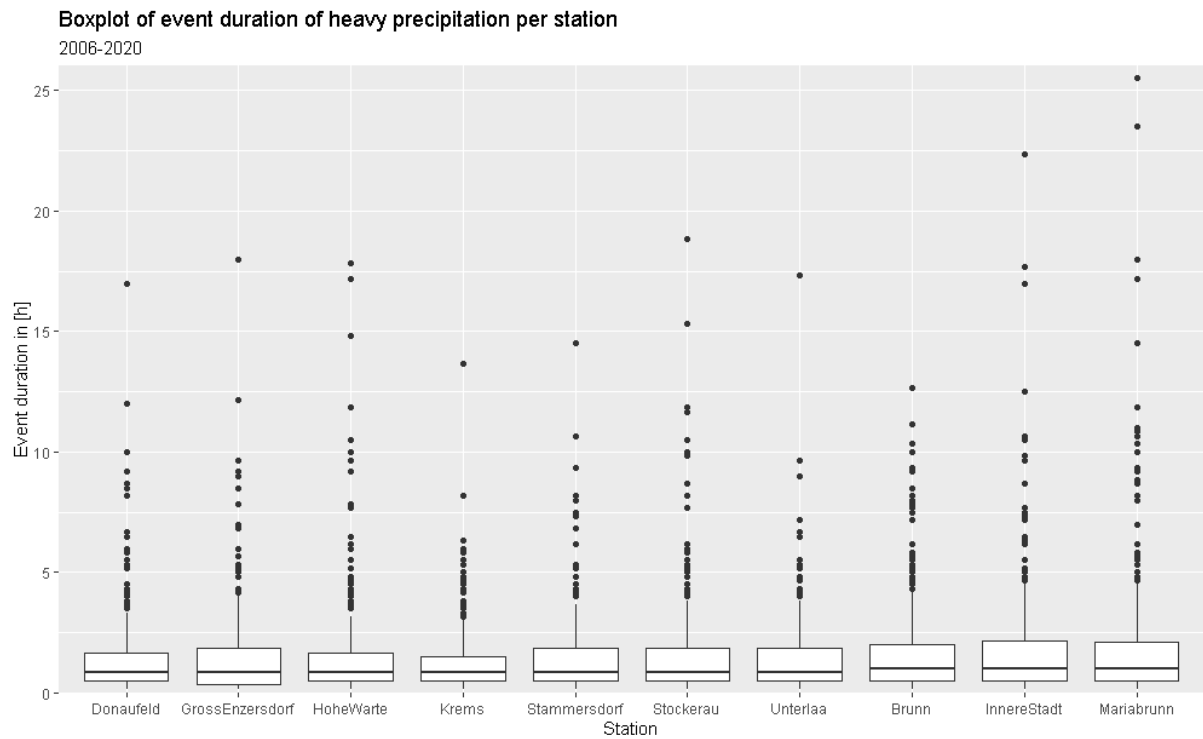


Figure C 4: Boxplot of event duration of heavy precipitation events in the main study period for every station in the study area. Stations are plotted in ascending order of size of the median.

Number of heavy precipitation events per season, 1991-2005

Number of events averaged over years in period

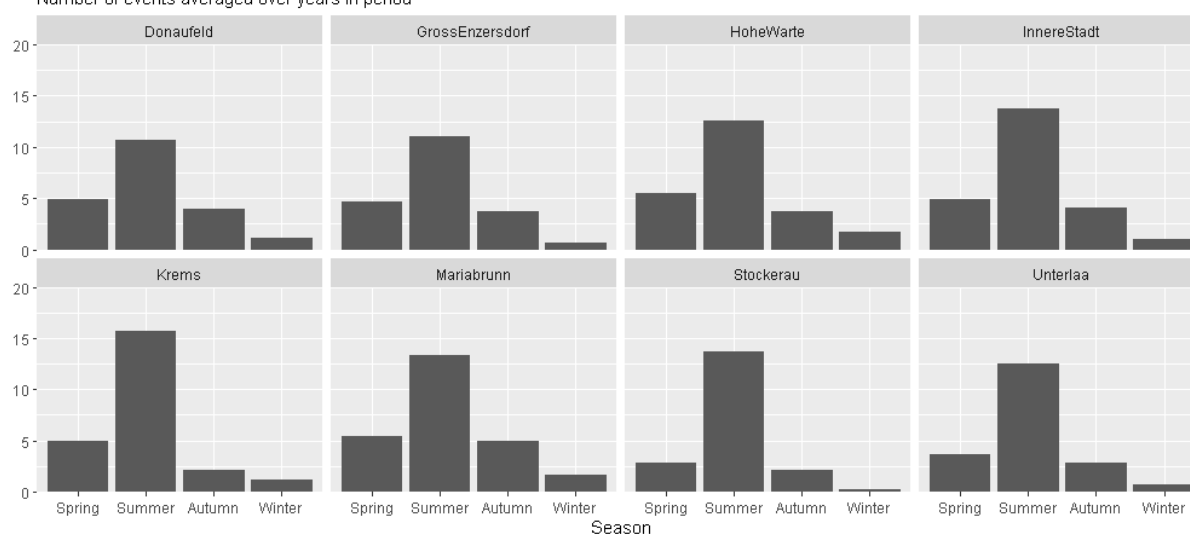


Figure C 5: Number of heavy precipitation events ($RR > 3.1$ mm/h) per season and station in the reference period. Total number of heavy precipitation events was averaged over years in period (refer to chapter 4.1).

Number of heavy precipitation events per season, 2006-2020

Number of events averaged over years in period

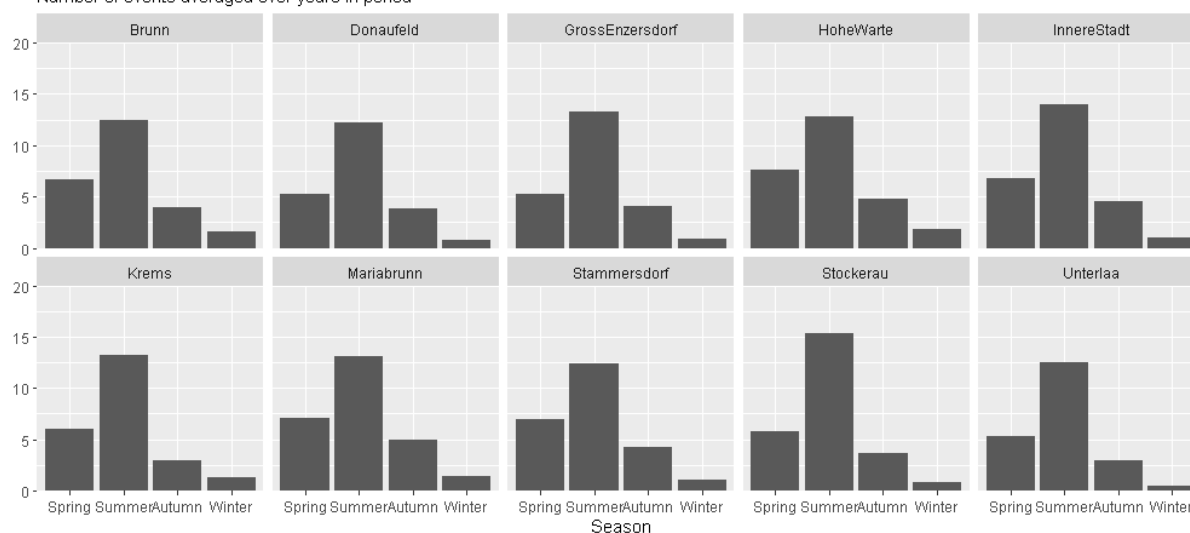


Figure C 6: Number of heavy precipitation events ($RR > 3.1$ mm/h) per season and station in the main study period. Total number of heavy precipitation days was averaged over 12.25 years at Brunn station, 12 years at Stammersdorf station and 15 years at any other station.

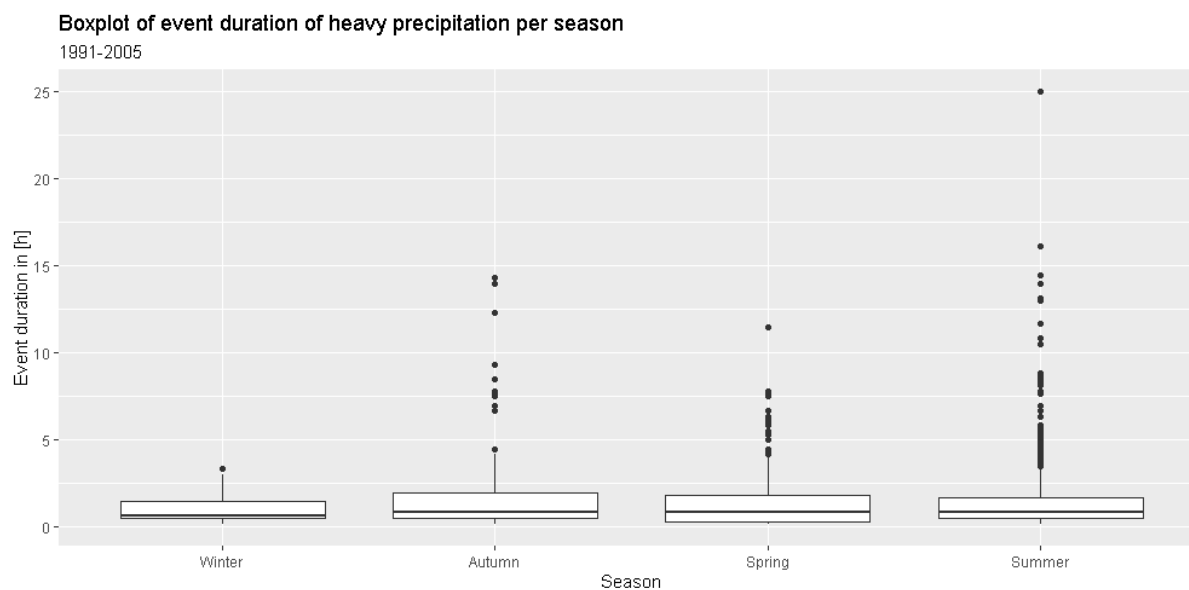


Figure C 7: Boxplot of event duration of heavy precipitation events ($RR > 3.1 \text{ mm/h}$) in the reference period per season. Seasons are plotted in ascending order of size of the median.

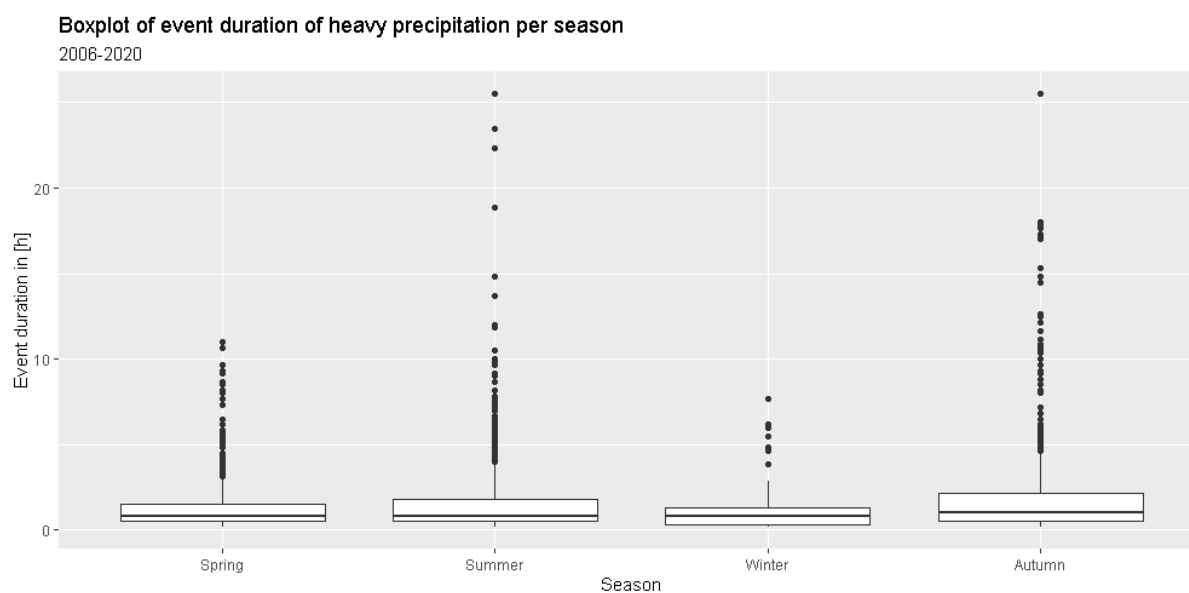


Figure C 8: Boxplot of event duration of heavy precipitation events ($RR > 3.1 \text{ mm/h}$) in the main study period per season. Seasons are plotted in ascending order of size of the median.

Table C 3: Mean rain depth of heavy precipitation events ($RR > 3.1 \text{ mm/h}$) in the reference and main study period.

Season	1991-2005	2006-2020	Change in %
Spring	7.0	7.2	2
Summer	8.0	9.1	14
Autumn	7.8	9.9	28
Winter	3.9	4.7	22

Table C 4: Mean duration of heavy precipitation events ($RR > 3.1$ mm/h) in the reference and main study period.

Season	1991-2005	2006-2020	Change in %
Spring	1.42	1.34	-6
Summer	1.38	1.50	9
Autumn	1.53	2.13	39
Winter	0.9	1.18	28